THE NSS BULLETIN

Journal of Caves and Karst Studies

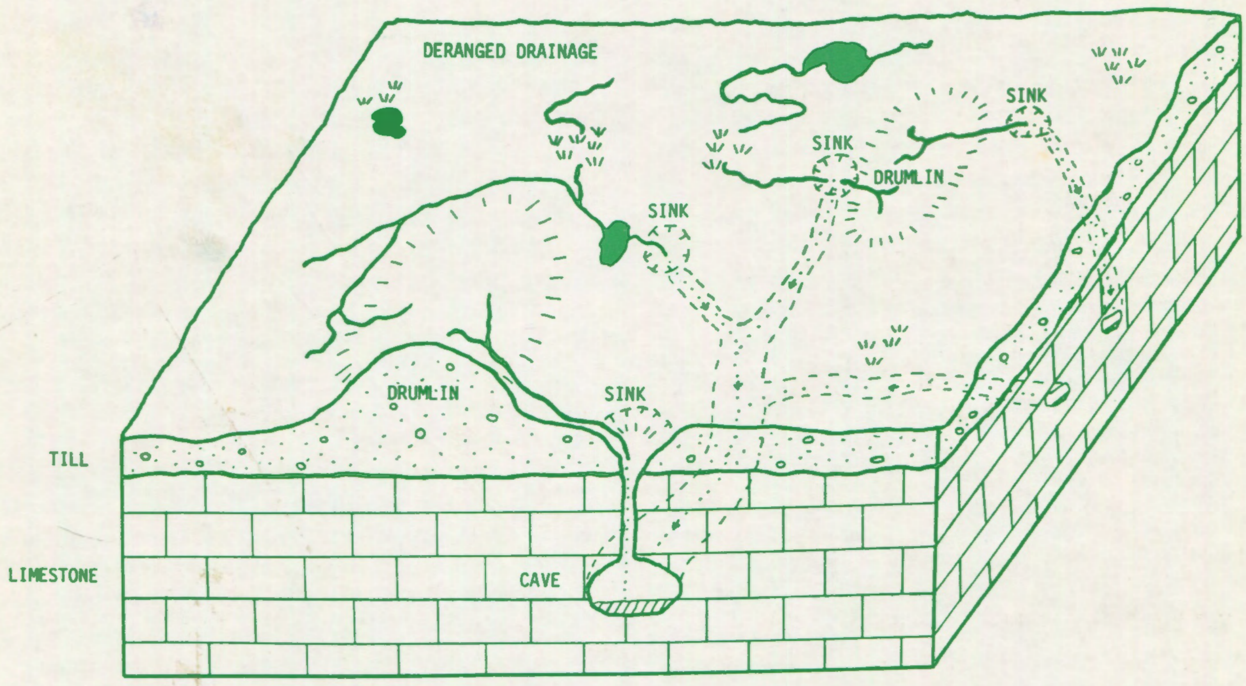

SPECIAL ISSUE:
SPELEOGENESIS

Volume 49 December, 1987 Number 2

Published by

The National Speleological Society

ISSN 0146-9517

Material to be included in a given number must be received at least 90 days prior to the first of the month in which publication is desired. No submission will be accepted for publication unless and until one of the three options in our printed "Copyright Agreement" form has been selected by the author(s) and the form has been properly dated, signed, and returned to the Editor.

Discussion of papers published in *The Bulletin* is invited. Discussions should be 2000 words or less in length, with not more than 3 illustrations; they should be forwarded to the appropriate editor within 3 months of publication of the original paper.

A voluntary contribution of $25.00 per page is solicited from authors after their manuscripts have reached page-proof stage. This represents about one-quarter of the cost of publication.

A catalog of issues still in print and their cost can be obtained from our Business Office at no charge; facsimile copies of out-of-print issues can be supplied for a nominal fee.

The NSS Bulletin (ISSN 0146-9517) is published semiannually by the National Speleological Society, Inc., Cave Avenue, Huntsville, Alabama 35810. The annual subscription fee, worldwide, by surface mail, is $18 U.S. Airmail delivery outside the United States of both *The NSS NEWS* and *The NSS Bulletin* is available for an additional fee of $40 (total: $55); *The NSS Bulletin* is not available alone by airmail. POSTMASTER: send address changes to *The NSS Bulletin,* Cave Avenue, Huntsville, Alabama 35810.

Graphic Publishing Co., Inc.
Lake Mills, IA 50450

Cover: See Mylroie, page 67.

INTRODUCTION TO SPELEOGENESIS

Caves, particularly large solution caves developed in limestone, dolomite, and gypsum have aroused curiosity since the dawn of history. From the beginnings of modern geology in the mid and late 17th century many explanations for the existence of caves were put forth. Attempts in the United States to explain the occurrence of caves peaked out with the classic papers of Davis, Swinnerton, Gardner, and Bretz in the 1930's and early 1940's. The problem was that these early studies mostly relegated caves to the role of geological trivia. They were interesting features of the landscape and therefore must be provided with some manner of explanation but they had no obvious connection with other matters of interest in early to mid 20th century geology.

The classic papers of the 1930's, and the massive writings of William Morris Davis and J. Harlan Bretz in particular, are characterized by three curious features. All caves are recognized to be the result of dissolution of soluble rock by moving water. However, the interpretation of cave origins is totally innocent of the chemistry of limestone solution and the physics of fluid flow (although A. C. Swinnerton is a notable exception). Second, very little attention was given to the geologic setting, e.g., the thickness of beds, geologic structure, and their mineralogic and lithologic character. It was somehow thought possible to write down a general theory of cave origin that would account for specific caves with no consideration of their geologic setting. Third, Davis, the grand master of early geomorphology, was convinced that caves are very old. He claimed that caves were dissolved by slow, randomly percolating waters beneath old peneplains which were later uplifted, dissected, the caves drained, and entrances formed to give access to human exploration. As such, caves would be relicts, having no relationship to contemporary drainage basins and the behavior of contemporary surface and ground water. These conceptual difficulties brought the theorizing of the classic period into what was essentially an intellectual dead end (Watson and White, 1985).

The early theorists were also preoccupied with the role of the water table and with the question of whether caves formed deep below, near, or above the water table. This preoccupation with the water table caused many otherwise interesting studies to degenerate into a sterile debate about whether some specific cave was of vadose or phreatic origin. It may also have been responsible for the general loss of interest in caves among the geological community at large who through the 1940's and 1950's had many other interesting things to occupy their attention. Caves were boring, as many contemporary cave researchers discovered when they submitted manuscripts to the mainstreams geological journals and had them promptly rejected. The responsibility for worrying about caves was transferred, perhaps by diffusion or osmosis, from the professional geologists to the National Speleological Society during the hiatus between the classic period which ended in 1942 and the onset of modern cave research which dates from 1957.

The Society's first major expression on the subject of cave origins was a symposium held in cooperation with the AAAS in December of 1959 and published in the *NSS Bulletin* in 1960. That symposium was, in a sense, a passage from the older way of looking at the cave origin problem to what we might consider to be the modern period of karst hydrogeological research of which cave origin theory is merely one of a number of interesting topics.

Some aspects of current work were already apparent in the 1959 symposium. The modern research on the origin of caves has evolved along three lines. The first, and perhaps most obvious, was to supply the missing geology. Caves do not occur in isolation. They occur in specific geologic settings and the geology places important bounds on the pathways and mechanisms of groundwater flow and on the chemistry of bedrock dissolution. The beginnings of this trend, which follows most directly from the classic period, was represented in the 1959 symposium by William E. Davies who showed semi-quantitative relationships between the levels of cave passages and terrace levels in the upper Potomac River Basin, a theme that reappears in the present *Bulletin* in A. N. Palmer's paper. Detailed studies of the geologic setting of Breathing Cave, Virginia, Fulford Cave, Colorado, and a set of caves in central Pennsylvania are also indicative of this trend. The geologic interpretation of cave development is perhaps best exemplified by the present day work of Derek Ford and his colleagues, particularly what might be called the "Ford-Ewers Model" (Ford and Ewers, 1978) which combines a careful interpretation of cave patterns in terms of recharge areas, flow paths, and fracture frequency in the bedrock. Indeed, the Ford-Ewers classification has gone a long way towards resolving the ancient water table controversy and answering most of the questions posed by the geologists of the classic period.

The second approach has been to attempt to model the process of bedrock removal in terms of the chemistry of limestone dissolution, both equillibrium and kinetics, and the mechanics of fluid flow in conduits and in fractured media. This is a reductionist approach to cave origin problems in which one attempts to simplify the problem sufficiently to be able to deal with the mathematics. This approach is seen in W. Dreybrodt's contribution to the present *Bulletin*.

The third direction is to take the patterns of cave lengths, number of entrances, and cave passage plans, and other descriptive parameters simply as data and then attempt to interpret these geometrical pieces of information with statistical or other mathematical models. The beginning of this was seen in the 1959 symposium in Rane Curl's paper on the distribution of cave lengths in relation to the number of cave entrances. This work has continued down to Curl's most recent contribution (Curl, 1986) in which populations of caves are shown to follow a fractal geometry and have a range of self-similarity found in many other seemingly stochastic phenomena.

This issue of the *NSS Bulletin* is intended to bring together some examples of contemporary research dealing with the origins of caves. Some things have changed since the 1959 symposium. The data base is orders of magnitude larger and spans more diverse geologic settings. The scientific sophistication of the researchers is much greater. No longer is geology a refuge for those with no taste for physics, chemistry, or mathematics. Cave geology is more integrated with the larger body of earth sciences. No longer are caves considered isolated objects of little interest to the serious geologist. New methods of age dating cave deposits and a new appreciation for the relationship of caves to late Tertiary and Pleistocene climatic changes and geomorphic history makes cave data a valuable resource. After many years cave research has been reunited with mainstream geology. These papers are a celebration of that accomplishment.

William B. White
Department of Geosciences and Materials Research Laboratory
The Pennsylvania State University
University Park, PA 16802

REFERENCES

Curl, R. L., 1986. Fractal dimensions and geometries of caves: Mathematical Geology, v. **18**, p. 765–783.

Ford, D. C. and Ewers, R. O., 1978. The development of limestone cave systems in the dimensions of length and depth: Canadian Journal of the Earth Sciences, v. **15**, p. 1783–1798.

Watson, R. A. and White, W. B., 1985. The history of American theories of cave origin: Geological Society of America Centennial Special Volume 1, p. 109–123.

Dreybrodt, Wolfgang—The Kinetics of Calcite Dissolution and Its Consequences to Karst Evolution from the Initial to the Mature State: *NSS Bulletin* **49**: 31-49.

THE KINETICS OF CALCITE DISSOLUTION AND ITS CONSEQUENCES TO KARST EVOLUTION FROM THE INITIAL TO THE MATURE STATE

WOLFGANG DREYBRODT
Fachbereich 1—Physik, Universität Bremen, D 2800 Bremen 33
Federal Republic of Germany

The dissolution rates of calcite in the system $CaCO_3$-H_2O-CO_2 are determined by three processes: a) surface controlled dissolution at the solid-liquid interface, b) diffusion of the molecular and ionic species, and c) slow conversion of CO_2 to H^+ and HCO_3^-. We present a theory, which taking these processes into account, predicts dissolution rates of calcite for a) the case of a water-layer flowing on a plane calcite surface with the other surface in contact to a CO_2-containing atmosphere (open system), and b) for a water layer flowing between two parallel planar calcite surfaces (closed system). Both laminar and turbulent flow conditions have been considered. In the case of turbulent flow, the dissolution rates are higher by a factor of ten compared to laminar flow.

The theoretically calculated dissolution rates have been asserted by experiments, the results of which are in close agreement to the theory.

From the theoretical results penetration lengths are calculated for given cross sectional dimensions of water leading conduits. The distribution of flow and hydraulic gradients in simple karst systems is simulated by an electric analogue resistor network. Combining these two concepts, karst development can be explained in its scales of length and time.

INTRODUCTION

The formation of karst landscapes in limestone areas is almost entirely determined by solutional removal of bedrock. To address problems of karstification processes such as cave genesis from its initial state to mature conduit drainage systems, or surface denudation and development of morphologic features of karst landscapes a detailed knowledge of the dissolution kinetics of calcite is of utmost importance. It is not sufficient to consider only the equilibrium chemistry of karst waters, one has also to regard the solutional rates which determine the evolution of karst systems through time.

These rates are determined by three independent contributions:

a) The kinetics of dissolution at the phase boundary between the aqueous system and the limestone rock depends on the chemical composition of the solution at the phase boundary. Once this composition is known, rates can be derived by empirical rate equations published by Plummer et al. (1978, 1979). These PWP-equations are at present the most recent and most reliable description on dissolution of calcite.

b) The kinetics of conversion of CO_2, dissolved in the aqueous phase into $HCO_3^- + H^+$, which constitute the aggressive agents in the process of calcite-dissolution. This conversion is a slow process, depending on the pH of the solution and has been reviewed in detail by Kern (1960) and Usdowski (1982). This slow process can be rate determining, especially in cases where the ratio of the volume of solution to the surface area of the rock in contact with the solution is small, such as when aggressive water is flowing in narrow joints or partings.

c) Mass transport by diffusion of the dissolved ionic species, i.e. Ca^{++}, HCO_3^-, $CO_3^{=}$ and CO_2 and H_2CO_3 from and to the phase boundaries. This transport mechanism depends on the hydrodynamic flow conditions of the solution. In laminar flow transport is by molecular diffusion quantified by diffusion coefficient D_M. In turbulent flow eddy diffusion is dominant and the related coefficient of diffusion is by at least three orders of magnitude larger than D_M, (Tien, 1959; Bird et al., 1960; Skelland, 1974). Therefore hydrodynamic flow conditions are of great importance and have to be considered in any case.

A rigorous theory of calcite dissolution, taking into account all three processes described above and its experimental verification has recently been published by Buhmann and Dreybrodt (1985a, 1985b). It provides data, from which dissolution rates of limestone can be derived easily for a variety of geological situations.

In this paper we will discuss the consequences of these data to problems of cave genesis and surface denudation in karst areas. In the first part we will define the boundary and flow conditions relevant to karst situations and give a review of the theoretical work of Buhmann and Dreybrodt. Then we will discuss some important concepts in karstification. The first is the saturation length or penetration distance, which gives the travelling distance water can flow until it loses 63.2% of its solutional power. Since this is related to the distribution of the hydraulic gradients in the flow net of the rock formation, we present simple flow net models for different hydrodynamic and geological settings. The penetration distance, which is determined as well by the dissolution kinetics of limestone as by the hydrodynamics of water flow, actually combines these two, and determines the length scale of caves. It is therefore an important key to understand karstification processes.

Finally we present a model for the evolution of karst and cave systems from its initial to the mature state.

THE KINETICS OF CALCITE DISSOLUTION IN GEOLOGICALLY RELEVANT SITUATIONS

Water flow in karst systems takes place either in the unsaturated zone (vadose) or in the saturated zone (phreatic). Vadose flow is either laminar or turbulent with one surface of the solution open to the CO_2-containing atmosphere and the other in contact with the dissolving rock. CO_2 exchange with the atmosphere is possible, thus defining an open system. In the saturated zone all the water is in contact to the dissolving rock and no exchange of CO_2 is possible (closed system). To obtain simple, mathematically treatable conditions, these situations are idealized in Figure 1.

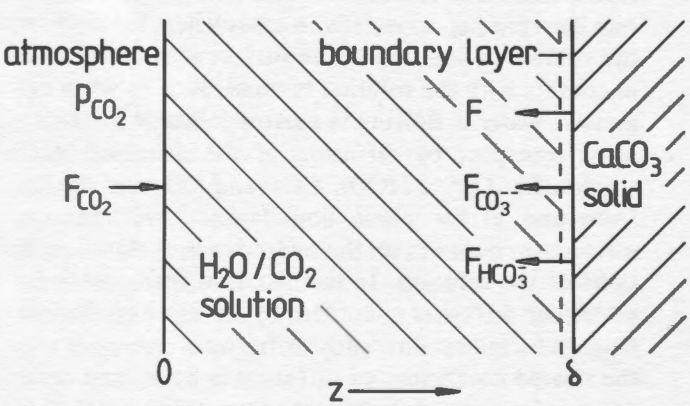

***Figure 1a.* Geometric model of a water layer of thickness δ for the open system. The fluxes of the different species are indicated by arrows.**

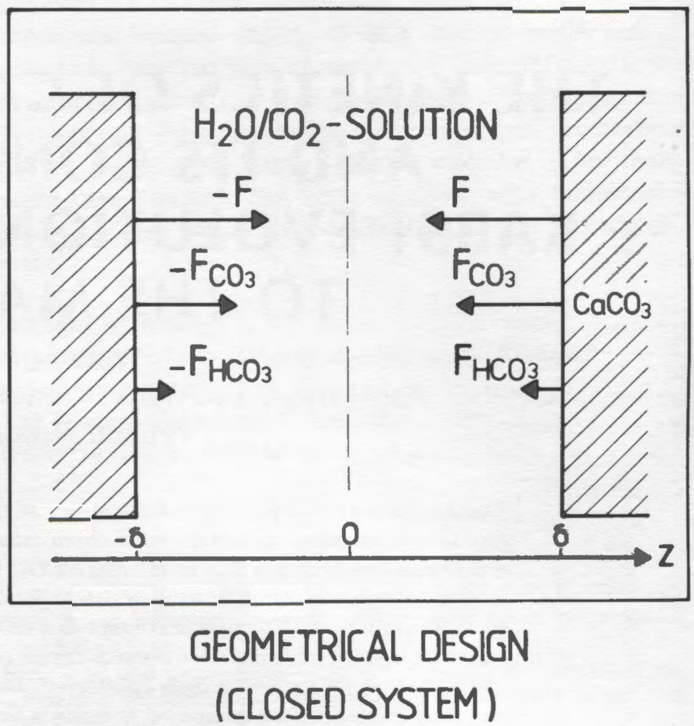

***Figure 1b.* Geometric model of a water layer of thickness 2δ enclosed by two calcite planes (closed system). The fluxes of the different species are indicated by arrows.**

Calcite Dissolution in an Open System

In vadose flow situations, as is the case in waters flowing on bare karst surfaces or in cave conduits, we assume a planar layer of water with thickness δ flowing on a planar calcite surface (Fig. 1a). For a further simplification we assume plug flow, i.e. constant velocity v_y, in flow direction. In this case the evolution of the dissolved calcite concentration is depending only on the time t of contact of the solution with the rock. In other words, the concentration of the solution in the flowing layer after travelling the distance y would be the same, as the concentration of a corresponding stagnant layer in contact with the rock surface for $t = y/v_y$. This equivalence allows us to treat the simple case of a stagnant layer in contact to the calcite surface, since the evolution of its dissolved $CaCO_3$ concentration in time is simply related to the spatial evolution of concentration in a flowing layer. Furthermore, to verify the theory experimentally it is sufficient to measure the time dependence of the Ca^{2+} concentration in stagnant layers.

The boundary conditions for mass transport are shown in Figure 1a. At $z = 0$, the interface atmosphere-water, there is a flux F_{CO_2} into the layer. Simultaneously dissolution of calcite produces a flux F of Ca^{++} ions, $F_{CO_3^-}$ of CO_3^- ions and F_{HCO_3} of HCO_3^- ions from the calcite surface into the bulk solution. For reasons of stochiometry of the chemical reaction $CaCO_3 + H_20 + CO_2 \rightleftharpoons CaCO_3 + H_2CO_3 \rightleftharpoons Ca^{++} + 2HCO_3^-$, the release of each Ca^{++} consumes one molecule of CO_2. Therefore $F_{CO_2} = F$. The flux is determined by the Plummer-Wigley-Parkhurst equation (Plummer et al., 1978, 1979).

$$F = \chi_1 (H^+) + \chi_2 \bullet (H_2CO_3^*) + \chi_3 - \chi_4 \bullet (Ca^{2+}) \bullet (HCO_3^-) \qquad (1)$$

The round brackets represent activities at $z = \delta$, the solid-solution interface $(H_2CO_3{}^*) = (H_2CO_3^0) + (CO_2)_{aq}$. The rate constants, χ_1, χ_3, χ_4 are only slightly dependent on temperature, whereas χ_2 changes by roughly a factor or two, for a change from 10° C to 20° C. Their values can be taken from the work of Plummer et al. The transport of all species is now given by a set of coupled differential transport equations, Bird et al. (1980).

$$-\frac{\partial C_i}{\partial t} + D_i \frac{\partial^2 C_i}{\partial z^2} = \Gamma_i (C_1, C_2, \ldots C_i, \ldots, C_n) \qquad (2)$$

C_i is the concentration of species i, D_i its coefficient of diffusion. Γ_i describes the production rate of species i by chemical reaction with the other species. In our case only the reaction $H_20 + CO_2 \rightleftharpoons HCO_3^- + H^+$ is slow. All other species participate in very fast reactions, which means that they are at equilibrium to each other and the corresponding Γ_i are negligible.

By using the reaction rates of $H_20 + CO_2 \rightarrow H^+ + HCO_3^-$ conversion as given by Kern (1960) the set of transport equations for our system is given by

$$-\frac{\partial [CO_2]}{\partial t} + D_{CO_2} \frac{\partial^2 [CO_2]}{\partial z^2} = (k_1 + k_2 \bullet [OH^-])\,[CO_2] - (k_{-1} \bullet [H^+] + k_{-2})\,[HCO_3^-]$$

$$-\frac{\partial [HCO_3^-]}{\partial t} + D \bullet \frac{\partial^2 [HCO_3^\circ]}{\partial z^2} = -(k_1 + k_2 \bullet [OH^-] \bullet [CO_2] + (k_{-1} [H^+] + k_{-2})\,[HCO_3^\circ]$$

$$-\frac{\partial [CO_3^{2\circ}]}{\partial t} + D \bullet \frac{\partial^2 [CO^{-2}]}{\partial z^2} = 0$$

$$-\frac{\partial [Ca^{2+}]}{\partial t} + D \bullet \frac{\partial^2 [Ca^{2+}]}{\partial z^2} = 0 \qquad (3)$$

The square brackets denote concentrations. The terms on the right side of eqs. (3a, 3b) result from CO_2 conversion and are dependent on the pH of the solution. Since we assume all the other species to be in equilibrium, we can obtain two more equations for $[H^+]$ and $[OH^-]$.

$$\gamma OH\, \gamma H\, [H^+]\,[OH^-] = K_W;\ \gamma CO_3\, \gamma_H\, [H^+]\,[CO_3^{2-}] = K_2 \bullet [HCO_3^-] \bullet \gamma HCO_3$$

where k_w and k_2 are equilibrium constants (4)

The activity coefficients γ are calculated by the Debye-Hückel approximation. Eqs. (2), (3), and (4) constitute a coupled system which has to be solved for the appropriate boundary conditions (Fig. 1a). The details of this calculations are published in detail elsewhere, Buhmann and Dreybrodt (1985a). Here we shall only give the results and discuss the underlying processes.

The dissolution rates F calculated for an open system in equilibrium with an atmosphere of $P_{CO_2} = 5 \bullet 10^{-3}$ atm for various thicknesses δ of the water layer and temperatures are shown in Figure 2.

As the most important result we state that all the curves can be reasonably well approximated by

Table 1. Open system: Calculated values of α in 10^{-5} cm s^{-1} and $[Ca^{++}]_{eq}$ in 10^{-4} mo1/1 for various temperatures, layer thicknesses δ in cm and P_{CO_2} in atm. a) laminar flow, b) turbulent flow, c) $[Ca^{++}]_{eq}$.

	$P_{CO_2} = 3 \bullet 10^{-4}$ atm			$P_{CO_2} = 1 \bullet 10^{-3}$			$P_{CO_2} = 5 \bullet 10^{-3}$ atm		
δ[cm]	5°C	10°C	20°C	5°C	10°C	20°C	5°C	10°C	20°C
(a)									
0.001	0.041	0.0714	0.232	0.0619	0.11	0.358	0.153	0.25	0.679
0.002	0.076	0.135	0.407	0.134	0.233	0.75	0.294	0.467	1.36
0.005	0.197	0.341	1.04	0.33	0.583	1.69	0.647	1.11	2.74
0.01	0.37	0.635	1.84	0.619	1.08	2.76	1.00	1.54	3.13
0.03	0.803	1.29	2.91	0.979	1.61	3.29	0.969	1.47	2.87
0.05	0.915	1.29	2.57	0.907	1.40	2.64	0.926	1.35	2.63
0.1	0.636	0.919	1.60	0.68	1.0	1.63	0.85	1.21	2.0
(b)									
0.1	3.3	5.7	13.5	5.2	8.0	14.7	7.25	8.3	11.0
0.2	5.9	9.5	20.0	8.4	11.5	17.5	7.9	8.8	12.0
0.5	11.5	16.5	26.0	12.0	14.5	18.5	8.0	9.0	12.0
1.0	16.0	20.6	28.5	13.5	15.0	19.0	8.0	9.0	12.0
2.0	20.0	24.0	30.0	13.5	15.0	19.0	8.0	9.0	12.0
(c)									
$[Ca^{2+}]_{eq}$	6.75	6.3	5.6	10.0	9.3	8.3	17.0	16.2	14.3

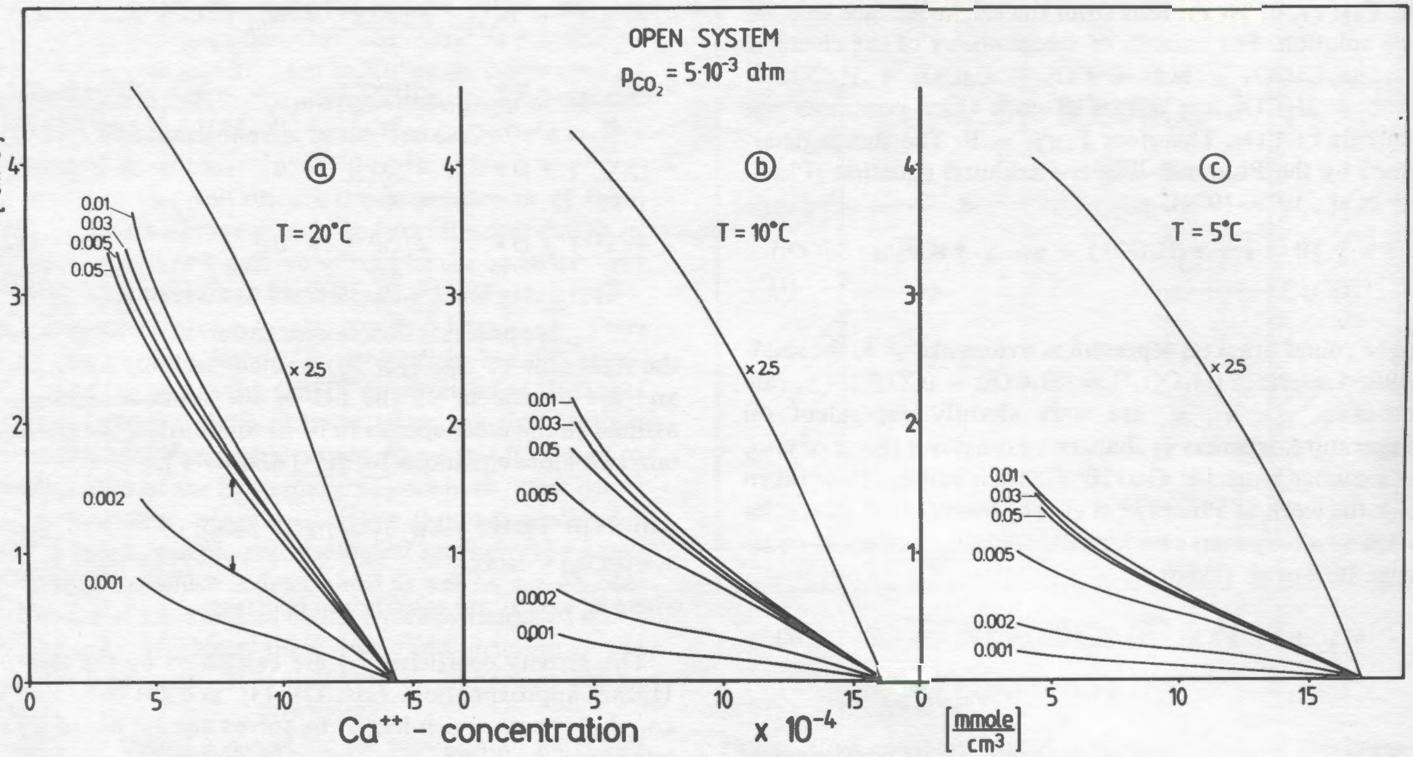

Figure 2: **Open system: Theoretical dissolution rates at P_{CO_2} = $5 \cdot 10^{-3}$ atm for different temperatures and layer thicknesses. The number at the solid lines gives the thickness δ in cm. The upmost curves have to be multiplied by a factor of 2.5 as indicated in the figure. The arrows in figure (a) indicate the situation, for which the concentration profiles in Figure 3 are calculated.**

$$F = \alpha ([Ca^{++}]_{eq} - [Ca^{++}]) \qquad (5)$$

The kinetic coefficient α depends on δ, the temperature and on the coefficient of diffusion. Its numerical value is obtained from the theory. $[Ca^{++}]_{eq}$ is the equilibrium concentration. Values of α and $[Ca^{++}]_{eq}$ are listed in Table 1 for various values of P_{CO_2}, temperature T, and thickness δ of the water layer.

Three different regions can be distinguished in the rate curves (Fig. 2).

a) At small $\delta \leq$ 0.003 cm the dissolution rates for each value of $[Ca^{++}]$ are proportional to δ and there is a significant increase of the rates with increasing temperature. In this region, CO_2 conversion is the slowest process and therefore rate determining. From the stoichiometric condition that for each Ca^{++} dissolved one molecule of CO_2 is consumed we obtain

$$\frac{d[Ca^{++}]}{dt} = S \bullet F = V \frac{d[CO_2]}{dt} \qquad F = \delta \bullet \frac{d[CO_2]}{dt} \qquad (3)$$

S is the surface of the limestone rock and V the volume of solution covering it. Thus, the dissolution rate F is determined by δ and the temperature dependence of CO_2 conversion.

b) With the increasing thickness of the layer, $\delta \geq 0.005$ cm the dissolution rates become almost independent of δ. The rate curves converge towards a limit at $\delta \approx 0.01$ cm.

In this case chemically enhanced diffusion is the limiting process, which is controlled by the diffusion length λ = . K is an effective CO_2-conversion constant, determining the temperature dependence of the process. This interpretation is supported by inspection of the concentration profiles, which are calculated for the conditions marked in Figure 2a by arrows and are shown in Figure 3. At small δ = 0.002 cm practically no concentration gradients build up, showing that diffusion plays only a minor role in the region where CO_2 conversion is rate determining. At δ = 0.05 cm there are large concentration gradients, especially for H^+ and CO_3^-, showing that the conversion of CO_3^- into HCO_3^- by H^+ diffusing towards the calcite surface takes place only in the region of thickness λ, which is the distance CO_3^- can travel by diffusion until it is con-

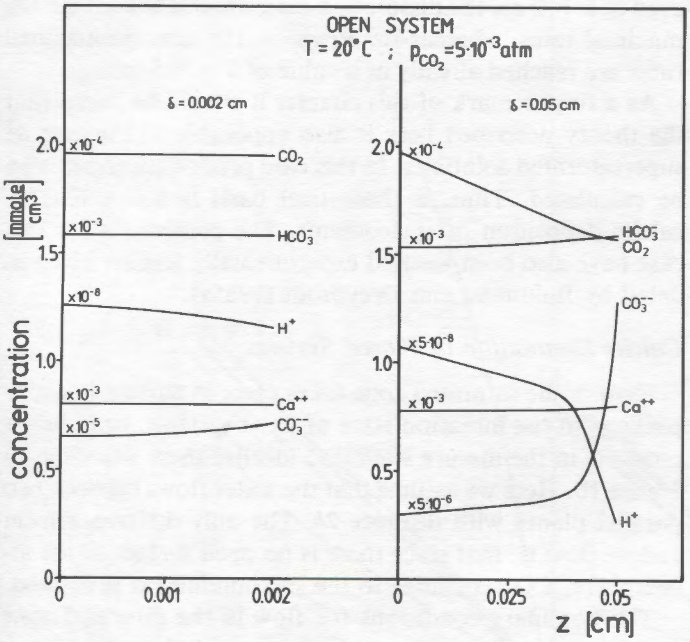

Figure 3. **Open system: Concentration profiles of CO_2 and the four most important ions at $[Ca^{++}]_\delta = 8 \bullet 10^{-4}$ $\frac{mmole}{cm^3}$ across a water film of 0.002 cm and 0.05 cm thickness respectively. The concentration scale for the individual species has to be multiplied by the factor given at the corresponding line.**

verted to HCO_3^-. This determines the dissolution rate, which therefore becomes almost independent of δ.

The dissolution rates in the region a) and b) have been calculated for laminar flow using the coefficient of molecular diffusion. For values of δ > 0.5 cm, in real karst systems, however, usually turbulent flow sets in.

c) Therefore the upmost curves in Figure 2 have been calculated for turbulent flow conditions where eddy diffusivity controls diffusion. In this case the coefficient of diffusion has been increased by a factor of 10^4. The results show that the dissolution rates became practically independent of δ. The process now is entirely controlled by the calcite surface reactions given by the PWP-equation, eq. (1). In turbulent flow diffusion is so fast that practically no concentration gradients build up and all species are in equilibrium with each other. CO_2 is also in equilibrium, since the volume is large and therefore sufficient supply of H_2CO_3 is always available. Therefore the reaction rate at the calcite surface is controlled by the composition of the bulk solution. Calculating this composition by equilibrium theory, assuming only the Ca^{++} and $CO_3^=$ ions not to be in equilibrium with calcite, and inserting the activities into eq. (1) leads to exactly the same results.

In comparison to the regions a) and b) where the temperature dependence of the rates is given by the rate constants of CO_2 conversion, dissolution rates in turbulent flow for δ > 0.5 cm show only a very weak dependence on temperature reflecting the properties of the rate constants χ in the PWP-equation.

Note that the upmost curves in Figure 2 are scaled down by a factor of 2.5. Compared to laminar flow the dissolution rates are higher by a factor of 10 under turbulent flow conditions. This proves for the first time the postulate of the "hydraulic jump" proposed by White and Longyear (1962) as an important feature in cave genesis.

To provide further data we have calculated the dissolution rates for atmospheric $P_{CO_2} = 3 \bullet 10^{-4}$ atm. This situation controls dissolution of water flowing on bare karst surfaces and is therefore important for denudation rates.

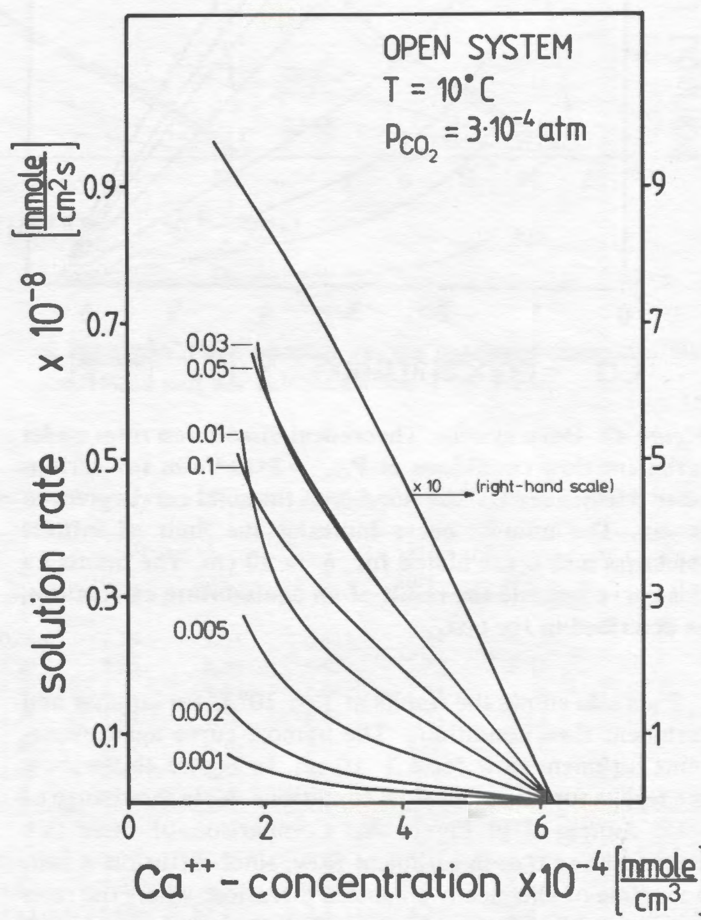

Figure 4a. **Open system: Theoretical dissolution rates for laminar flow at $P_{CO_2} = 3 \bullet 10^{-4}$ atm and T = 10° C for various layer thicknesses. The number at the solid curves gives the thickness δ in cm. The upmost curve has to be multiplied by a factor of 10 or to be read by the right-hand scale.**

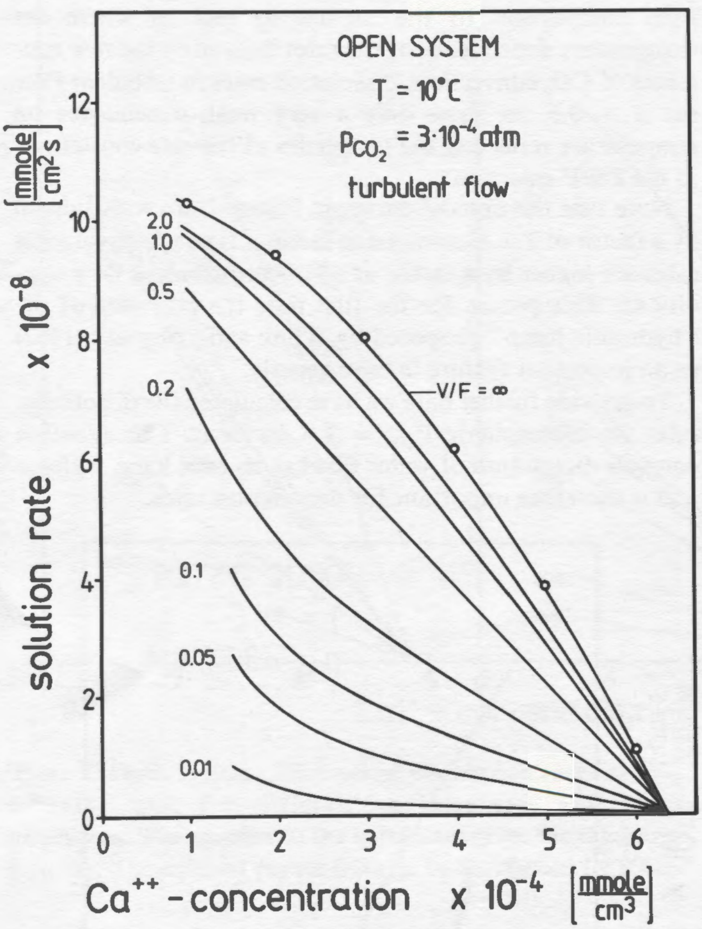

***Figure 4b*. Open system: Theoretical dissolution rates under turbulent flow conditions at $P_{CO_2} = 3 \cdot 10^{-4}$ atm for various layer thicknesses δ. The number at the solid curves gives δ in cm. The upmost curve indicates the limit of infinite thickness and is calculated for $\delta = 10$ cm. The points on this curve indicate the result of an equillibrium calculation, as described in the text.**

Figure 4a shows the results at T = 10° C for laminar and turbulent flow conditions. The upmost curve again represents turbulent flow for $\delta \geq 10$ cm. In Figure 4b we show the results for turbulent flow conditions. Note the change of scale compared to Figure 4a. Comparison of these two figures shows that in turbulent flow, since diffusion is fast, no regime of chemically enhanced diffusion, where the rates become independent on δ, exists. In turbulent flow only two rate limiting processes compete: CO_2-conversion and surface reactions. Therefore, with increasing δ the rates increase until surface reaction control takes over. It should be noted here that the lower the value of P_{CO_2}, the larger is the value of δ where the reaction is still controlled by CO_2-conversion. This is so, since the product $P_{CO} \cdot \delta$ controls the supply of CO_2. Thus, in the case of $P_{CO_2} = 3 \cdot 10^{-4}$ atm even at $\delta = 2$ cm the dissolution rates are still lower than the maximal rates, whereas for $P_{CO_2} = 10^{-3}$ atm the maximal rates are reached already at a value of $\delta = 0.5$ cm.

As a final remark of this chapter it should be stated that the theory described here is also applicable to the case of supersaturated solutions. In this case precipitation rates can be calculated. Thus, a theoretical basis is also given for calcite deposition of speleothems. The predictions for this case have also been verified experimentally and are given in detail by Buhmann and Dreybrodt (1985a).

Calcite Dissolution in Closed Systems

Flow in the saturated zone takes place in narrow joints or partings in the initiation state of karst systems, or in larger conduits in the mature state. We idealize these situations in Figure 1b. Here we assume that the water flows between two parallel planes with distance 2δ. The only difference from vadose flow is, that since there is no open surface to the atmosphere, CO_2-exchange to the surroundings is prevented.

The boundary conditions for flow in the saturated zone are shown by Figure 1b. As in the case of the open system there is a flux of Ca^{++}, HCO_3^- and $CO_3^{=}$ from the calcite surfaces into the bulk solution. For the closed system we define an initial CO_2-pressure $P^i_{CO_2}$. This is the pressure initially in equillibrium with water, which has not yet dissolved calcite, i.e. at $[Ca^{++}] = 0$. In the progress of dissolution the CO_2 necessary for the dissolution of calcite is taken from the bulk solution itself, lowering its CO_2-concentration $[CO_2]$. For all geologically relevant situation, the stochiometric condition leads to the relation

$$[CO_2] = [CO_2]_i - [Ca^{++}] \qquad (7)$$

$[CO_2]_i$ is the initial concentration, related to $P^i_{CO_2}$ by the Henry constant K_H

$$P^i_{CO_2} = \frac{[CO_2]_i}{K_H} \qquad (8)$$

$[CO_2]$ is the concentration in the bulk solution, which is established when concentration of Ca^{++} has reached the value $[Ca^{++}]$.

In the closed system the transport equations (eqs. 3, 4) are valid. The boundary conditions, however, are

$$\left.\frac{\partial [CO_2]}{\partial z}\right|_{z=0} = 0 ; V \cdot \frac{\partial [CO_2]_{ave}}{\partial t} = F \cdot S \qquad (9)$$

The first equation states the fact that, because of symmetry, no mass transport is possible at z = 0. The second equation stands for the stoichiometric condition that each Ca^{++} released into the solution consumes one molecule of CO_2 dissolved in the bulk. With these new conditions the

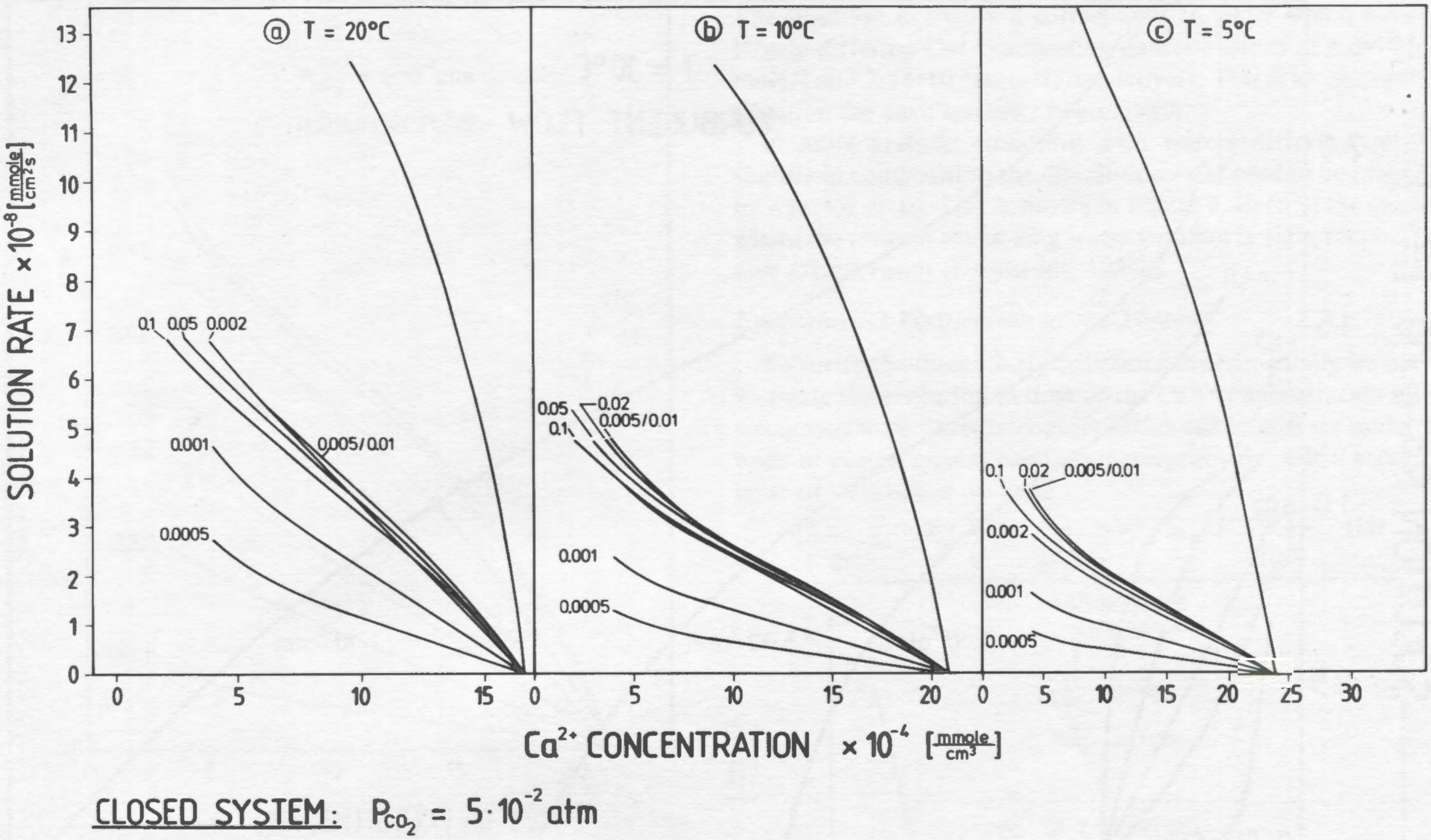

Figure 5. **Closed system: Calculated dissolution rates at $P_{CO_2} = 5\bullet10^{-2}$ atm for various layer thicknesses 2δ and temperatures. The number on the solid lines gives the value of δ in cm. The upmost curves represent turbulent flow conditions and are calculated for $\delta = 1$ cm.**

Table 2. Closed system: Calculated values of α and $[Ca^{++}]_{eq}$ for various temperatures, δ and $P^i_{CO_2}$; units as in Table 1. a) laminar flow, b) turbulent flow, c) $[Ca^{++}]_{eq}$.

	$P_{CO_2} = 1\bullet10^{-2}$ atm			$3\bullet10^{-2}$ atm			$5\bullet10^{-2}$ atm			$1\bullet10^{-1}$ atm		
δ[cm]	5°C	10°C	20°C	5°C	10°C	20°C	5°C	10°C	20°C	5°C	10°C	20°C
(a)												
0.001	0.714	1.6	7.14	0.606	1.1	3.33	0.666	1.19	3.33	0.833	1.39	3.23
0.002	1.3	2.8	13.3	1.18	2.1	6.25	1.25	2.25	5.26	1.05	1.73	3.33
0.005	3.13	6.4	21.7	2.13	3.5	8.93	1.49	2.5	5.0	1.06	1.73	3.33
0.01	5.26	9.6	21.7	2.04	3.5	8.7	1.49	2.47	4.76	1.06	1.73	3.23
0.02	5.13	9.5	18.2	2.0	3.46	6.9	1.46	2.44	4.76	1.05	1.70	3.17
0.05	4.76	8.4	16.1	2.0	3.3	6.5	1.43	2.43	4.67	1.04	1.68	3.07
0.1	4.08	7.7	12.7	1.89	3.25	5.9	1.4	2.29	4.46	1.01	1.61	2.95
(b)												
0.001	1.08	3.3	9.75	0.63	1.08	4.1	0.655	1.17	3.37	0.82	1.37	3.5
0.003	2.9	7.3	22.0	1.8	3.3	9.5	1.97	3.32	8.14	2.28	3.5	6.0
0.005	5.08	10.2	27.5	2.9	5.1	13.0	3.13	5.09	10.4	3.3	4.7	7.8
0.01	8.6	15.1	34.0	5.4	8.75	17.0	5.2	7.3	13.0	4.54	6.05	9.0
0.02	13.2	20.5	45.0	8.2	11.3	19.0	6.9	8.9	13.9	5.5	7.0	10.2
c)												
$[Ca^{2+}]_{eq}$	6.4	5.5	4.1	16.6	14.4	11.0	24.3	21.4	16.9	38.8	35.1	28.0

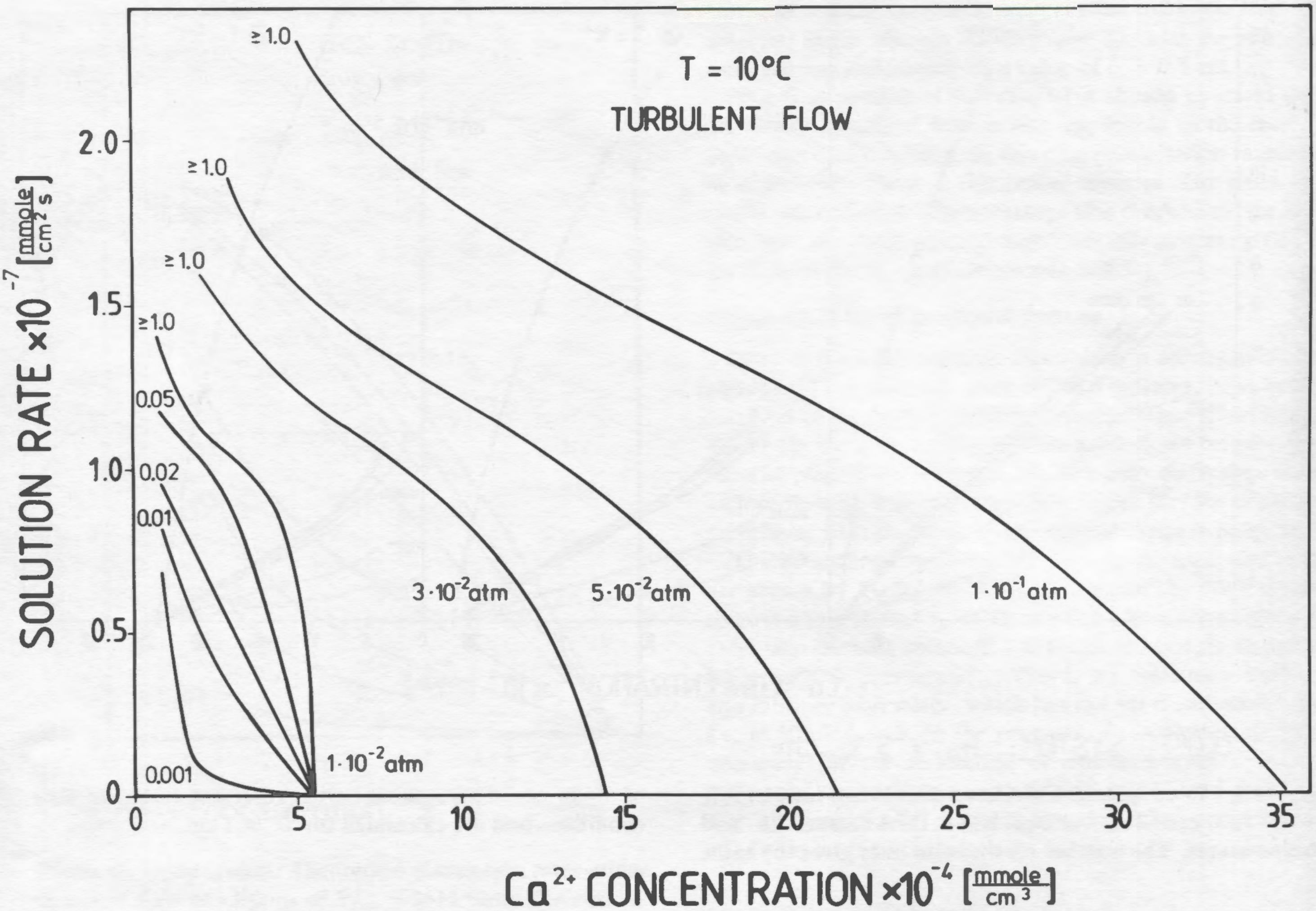

Figure 6. **Closed system: Calculated dissolution rates under turbulent flow conditions for various CO_2 pressures, and also various layer thicknesses 2δ in the case of $P_{CO_2} = 1 \bullet 10^{-2}$ atm. The numbers on the solid lines give δ in cm.**

procedure of the rate calculations is similar as in the case of the open system (Buhmann and Dreybrodt, 1985b).

Figure 5 shows dissolution rates for $P^i_{CO_2} = 5 \bullet 10^{-2}$ atm for various values of δ, and for various temperatures for laminar flow. The upmost curves are for turbulent flow and $\delta \geq 0.1$ cm. The situation is similar as in the open system represented by Figure 2. For values of $\delta \lesssim 0.001$ cm the rates are determined by slow CO_2-conversion. For values $0.002 \leq \delta \leq 0.5$ cm chemically enhanced diffusion is rate limiting. In the turbulent case surface reaction determines the rates. Again an increase of the dissolution rates by a factor of 10 is found on the transition from laminar to turbulent flow.

For values of $\delta \leq 0.1$ cm the rates again can be represented by the linear relation of eq. (5). Values of α and $[Ca^{++}]_{eq}$ for the closed system are listed in Table 2 for the case of laminar and turbulent flow. For values of $\delta \geq 0.1$ cm in turbulent flow the situation is different.

Figure 6 represents dissolution rates for turbulent flow for various initial CO_2-pressures $P^i_{CO_2}$. The results show that in contrast to the open system the rates can be no longer approximated by a simple linear relation as in eq. (5). Instead of this two linear regimes exist.

Figure 7 shows the results for turbulent flow for $P_{CO_2} = 5 \bullet 10^{-2}$ atm at 10° C. Again as in the case of the open system no region due to chemically enhanced diffusion is observed.

Calcite Dissolution in the Case of Mixing Corrosion

A very important situation in karst systems is encountered, when two calcite saturated solutions of differing chemical composition are mixing with each other under closed system conditions. In this case the mixture gains renewed aggressiveness and calcite can be dissolved. This concept was introduced by Bögli (1964) and its equillibrium chemistry is discussed in detail by Wigley and Plummer (1976). It is supposed that this effect plays a most important

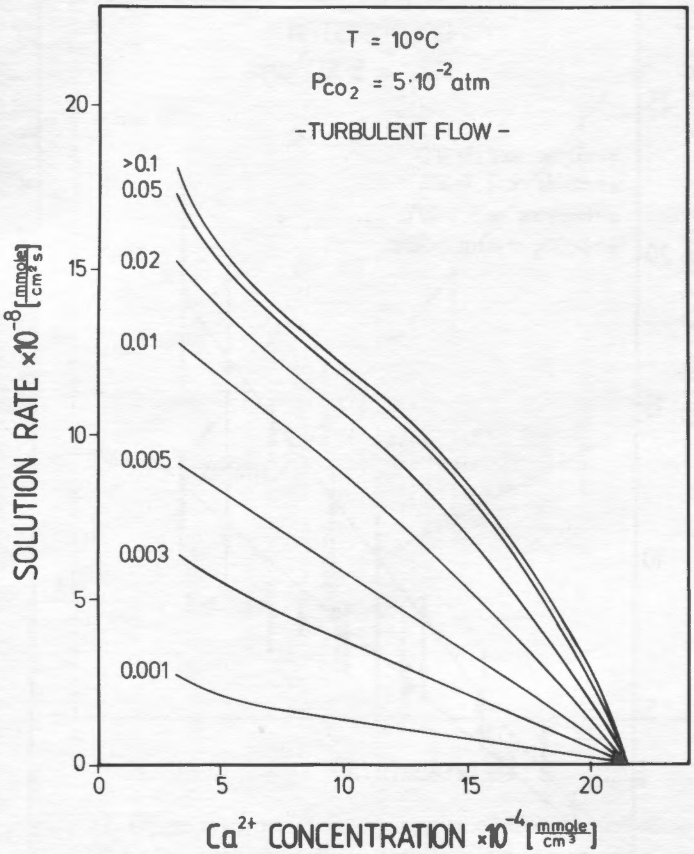

Figure 7. **Closed system: Calculated dissolution rates under turbulent flow conditions for various layer thicknesses 2δ . The upmost curve indicates the limit of infinite film thickness.**

role in the evolution of karstification (Bögli, 1980; Dreybrodt, 1981a,b; Thrailkill, 1968). The dissolution rates can be calculated by applying the theory of closed system dissolution. The Ca^{++} and CO_2 concentrations of the aggressive mixture immediately after mixing can easily be computed, if the volumes and the chemical compositions of the solutions before mixture are known. If the composition of this mixture is $[Ca^{++}]_m$ and $[CO_2]_m$, its behaviour is identical to a solution which initially had the value $P^{im}_{CO_2}$ and which has evolved to a Ca^{++} concentration $[Ca^{++}]_m$, and a CO_2-concentration $[CO_2]_m$. The value of $P^{im}_{CO_2}$ is easily derived from eq (7) and eq. (8). To obtain the dissolution rates and the new equilibrium of the mixture one has to apply closed system theory for $[Ca^{++}]$ $[Ca^{++}]_m$ to a solution with initial $P^i_{CO_2} = P^{im}_{CO_2}$.

Figure 8 shows the results calculated for two solutions with initial values $P^1_{CO_2}$ and $P^2_{CO_2}$ and different volumes V_1 and V_2, Buhmann (1984). Similar calculations, which are correct for turbulent flow are given by Dreybrodt (1981a). The lower curves in Figure 8 are calculated for laminar flow, the upmost ones are for δ = 1 cm and for turbulent flow.

The situation in Figure 8 corresponds to water which have largely differing Ca^{++}-saturation concentrations of $5.5\cdot10^{-4}$ mole/l and $2.14\cdot10^{-3}$ mole/l, respectively. This is an extreme situation for cave systems, Bögli (1980).

In more realistic situations with waters differing only slightly in composition the dissolution rates tend to be lower by a factor of 10. This is shown in Figure 9. Even in the case where the ratio of the mixing water volumes is 1:10, remarkable effects result (Dreybrodt, 1981a).

Experimental Verification of the Theory

To verify the theoretical predictions experimentally we investigate the evolution in time of the Ca^{++} concentration of a stagnant water layer in contact with a calcite surface under open or closed system conditions, respectively. For a water layer of thickness δ we have

$$\frac{d[Ca^{++}]}{dt} = F \cdot \frac{S}{V} = \frac{\alpha}{\delta} \cdot ([Ca^{++}]_{eq} - [Ca^{++}]) \qquad (10)$$

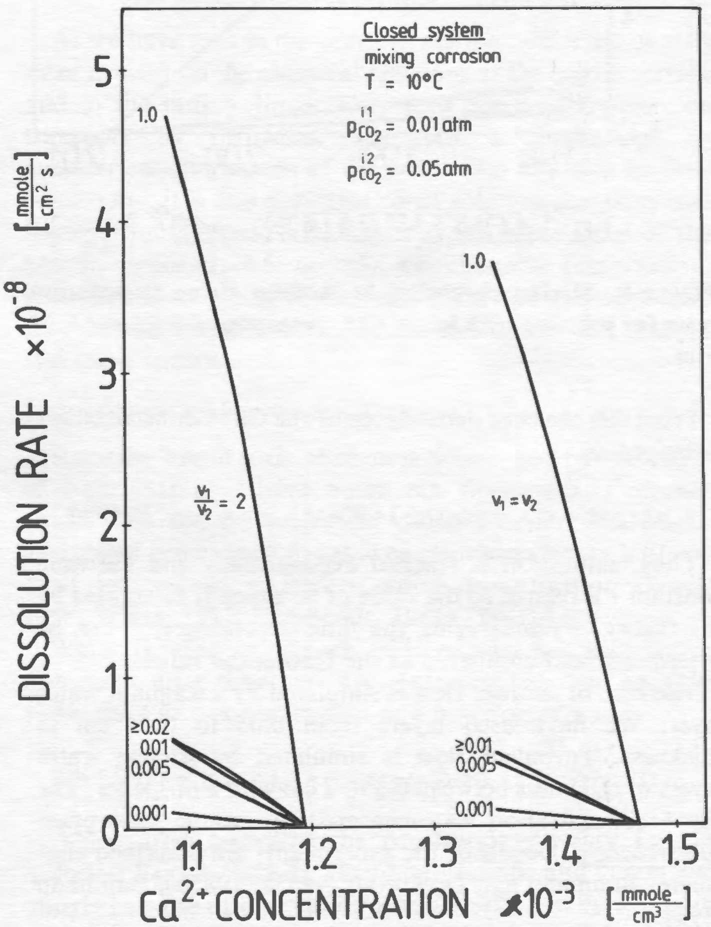

Figure 8. **Mixing corrosion in laminar flow: Dissolution rates for two different ratios $\frac{V_1}{V_2}$ of volume. The numbers on the curves give one half of the layer thickness, i.e., δ . The upmost curve represents turbulent flow. The initial CO_2-pressures are 0.01 atm and 0.05 atm.**

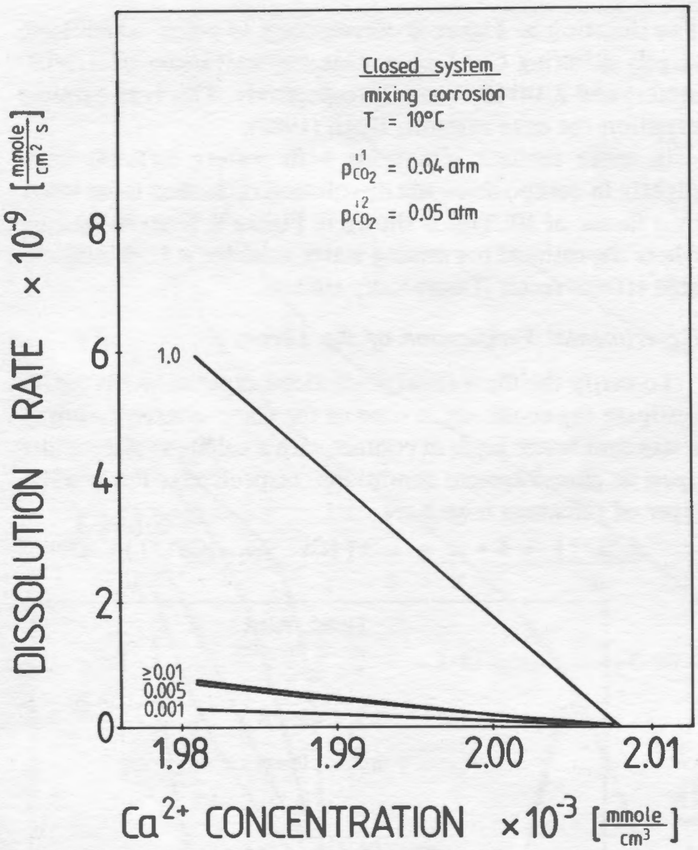

Figure 9. **Mixing corrosion in laminar flow: Dissolution rates for solution with initial CO_2-pressures of 0.04 and 0.05 atm.**

From this the time dependence of the Ca^{++} concentration is derived as

$$[Ca^{++}](t) = (1 - \exp(-t/\tau)) \bullet [Ca^{++}]_{eq}; \tau = \delta/\alpha \qquad (10a)$$

Thus, saturation is reached exponentially and the time constant τ is related to the value of α, which is calculated by the theory. By measuring the time dependence, τ can be determined and compared to the theoretical value.

The case of laminar flow is simulated by a stagnant water layer. We have used layers from 0.05 to 0.15 cm in thickness. Turbulent flow is simulated by stirring water layers of thickness between 0.5 to 2 cm with a propeller. The Ca^{++} concentration was measured by atomic absorption spectroscopy. Details of the experiments are described elsewhere, Buhmann and Dreybrodt (1985a, 1985b), Buhmann (1984).

Figure 10 shows results for the open system of different calcite samples for the laminar region. The solid curves are theoretically calculated values of τ. We have used a large $CaCO_3$ single crystal, a sample of white Carrara marble and a pure natural limestone. The experimental results are in

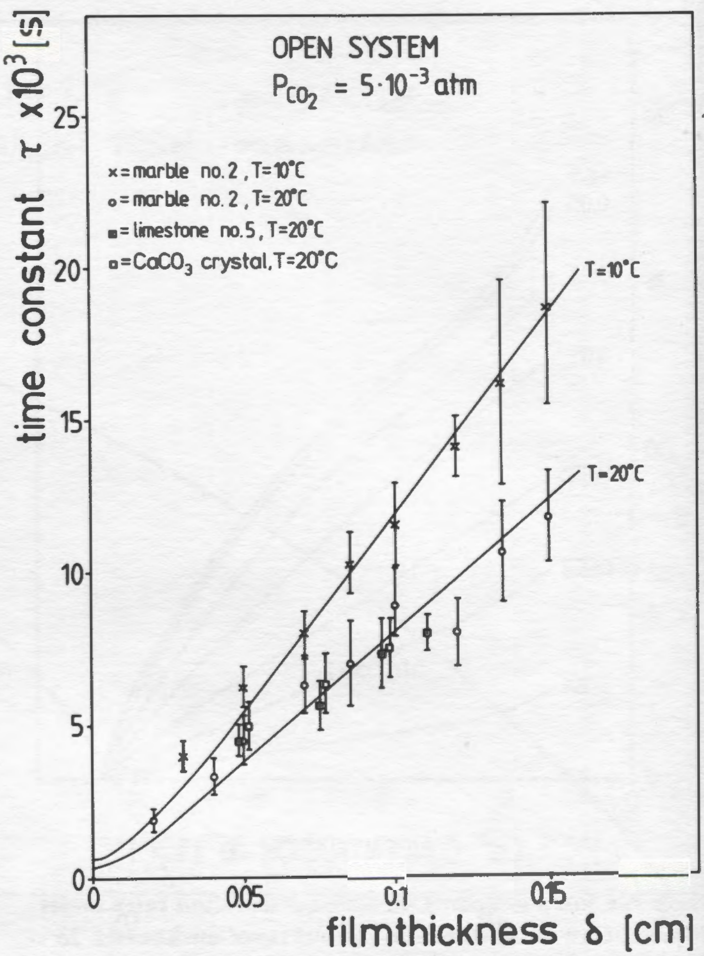

Figure 10. **Open system: Time constants of $CaCO_3$ solution measured under laminar flow conditions for various layer thicknesses at P_{CO_2} = 5•10^{-3} atm and T = 10° C and 20° C. For T = 20° C measurements on limestone and a pure calcite crystal are included. The solid lines are the theoretical curves.**

good agreement with the theory, showing that the dissolution rates are independent of the nature of the samples. Similar results were obtained for P_{CO_2} = 3•10^{-4} atm. Figure 11 shows the results for turbulent flow conditions. Again the agreement between experiment and theory is excellent, proving the hydraulic jump for the first time experimentally. We have also performed experiments under closed system conditions and again found excellent agreement with the theory for both laminar and turbulent conditions (Buhmann and Dreybrodt, 1985b).

At this point the theory is only for the pure H_2O-CO_2-$CaCO_3$ system. The question arises, to what extent dissolution rates may be changed at natural limestone samples, due to differing lithology etc. In this case the surface controlled processes may be altered and much lower dissolution rates

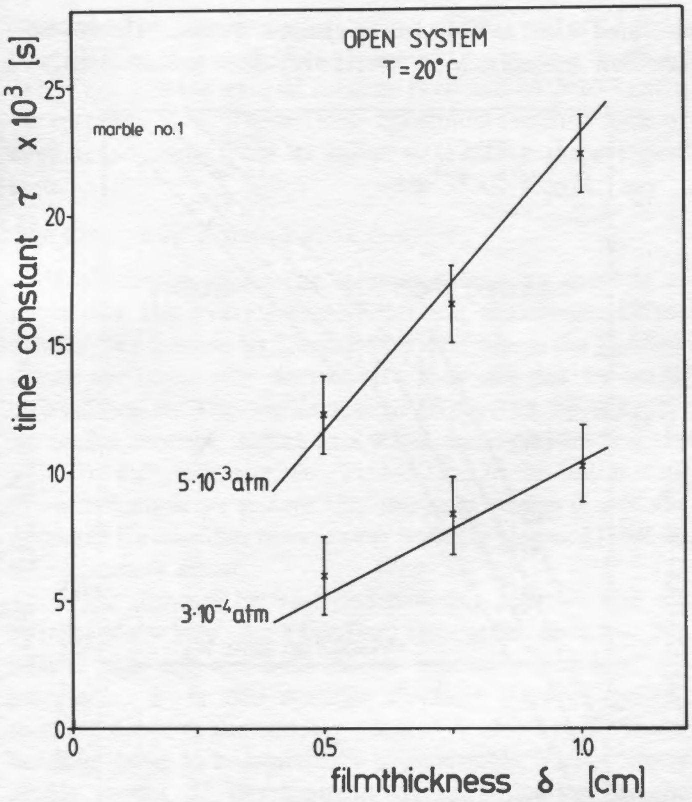

Figure 11. **Open system: Time constants of $CaCO_3$ solution measured under turbulent flow conditions for various film thicknesses and CO_2 pressures at T = 20° C. The speed of rotation of the glass stirrer is 200 rpm, which gives an effective diffusion constant $D_{eff} = 1000\ D_{CO_2}$.**

seem possible. We therefore in the meantime have investigated dissolution rates of pure limestone samples collected from various European karst areas. For turbulent flow conditions, as has been shown above, the dissolution rates are controlled exclusively by surface reactions. We have found only slightly differing dissolution rates indicating that the theory is also applicable to natural samples. This is also in agreement with the work of Rauch and White (1977), who observed dissolution rates on a large variety of limestone samples under turbulent flow conditions by using an experimental set-up much different from what we used. They also found no significant difference in dissolution rates for pure limestone samples with MgO weight percentages between 0.15 to 2.5% and for petrologically greatly different samples. Furthermore, the rates they measured are in close agreement with our theoretical prediction.

Since in karst systems most natural waters contain ions other than Ca^{++}, HCO_3^- as e.g. Na^+, K^+, Mg^{++}, $SO_4^=$, and Cl^- one may also question for the influence of these ions. Therefore, we have extended our theory by incorporating these ions. The results show an influence to the equilibrium value of Ca^{++} due to ionic strength and common ion effects and ion pairs, c.f. Picknett et al. (1976). The α-values, however, remain practically unchanged. We have verified these results experimentally (Buhmann and Dreybrodt, to be published).

From all these data we conclude that our theory has a sound basis and can well be used to predict dissolution rates even for natural situations in karst areas. All experiments described here have been performed at Ca^{++} concentrations with $[Ca^{++}] \leq 0.9\ [Ca^{++}]_{eq}$. At Ca^{++} concentrations very close to equilibrium it might be possible that a different reaction path becomes dominant and rates may decrease sharply in comparison to our theoretical predictions. There is some experimental evidence, although not conclusive, that this might happen (Herman, 1982; Plummer and Wigley, 1976). We regard our theory as reliable in all cases of undersaturated waters up to $0.9\ [Ca^{++}]_{eq}$.

IMPORTANT CONCEPTS IN KARSTIFICATION

As we have seen in the previous section calcite dissolution rates depend on the chemical reactions at the calcite surface and in the bulk volume. They also depend, however, on transport by diffusion. The last is determined by geometrical dimensions of the water film and also by flow conditions. It is this combination of solution chemistry and transport conditions, which lead to the dependence of the kinetic factor α, c.f. eq. (5), on chemical composition, geometric dimensions of the water film, and hydrodynamic flow conditions, and which determines dissolution rates in real karst systems.

The Concept of Penetration Distance

Since the length scale of caves is determined by the length of path that aggressive water can flow until it reaches equilibrium and no longer can dissolve calcite, this length also called penetration distance or saturation length is of upmost importance in understanding karstification (Weyl, 1958; White, 1977; Dreybrodt, 1981a, 1981b).

Water flowing on a rock with velocity has travelled a distance x after time $t = x/v$. Inserting this into eq. (10) yields the Ca^{++}-concentration as a function of x

$$[Ca^{++}](x) = [Ca^{++}]_{eq} \bullet (1 - \exp(-\frac{X}{L_S})),\ L_S = v \bullet \tau \qquad (11)$$

Thus, after travelling the penetration distance L_S, the solution has reached 63.2% of saturation, and correspondingly because of dissolution kinetics reflected by eq. 5, the dissolution rate has dropped to 36.8% of its inital value. In general τ is given by

$$\tau = \frac{V}{S \bullet \alpha}, \qquad (12)$$

where V is the volume of water and S the surface of calcite being in contact with this volume. Thus, for flow under closed system conditions in joints or partings of width d we obtain $\tau_j = \frac{d}{2\alpha}$ for flow in circular tubes of radius r, we have $\tau_c = \frac{r}{2\alpha}$. For flow of water films of thickness d° in contact with the atmosphere (open system) $\tau_o = \frac{d^\circ}{\alpha}$.

To calculate the saturation length, we have to know the flow velocities. For laminar flow the velocity is given by the Hagen-Poiseuille law

$$v_j = \frac{d_j^2}{72\eta} \bullet \frac{\Delta p}{l_j} = \frac{d_j^2 \sigma g}{12\eta} h_j , \; v_c = \frac{r^2 \sigma g}{8\eta} \bullet h_c \quad (13)$$

v_j is the velocity of flow between two parallel planes with distance d_j, l_j the length of the conduit, v_c the flow velocity in a circular tube with radius r. σ is the density of the flowing medium and η its viscosity. g is the earth acceleration constant, Δp is the pressure head, and h the hydraulic gradient.

For turbulent flow in circular tubes Dreybrodt (1981b) has derived the expression.

$$v_{tub} = 5.86 \bullet t^{0.655} \bullet (h \bullet g)^{0.555} \bullet (\sigma/\eta)^{0.11} \quad (14)$$

With these expressions we have calculated the saturation length L_S as a function of r for flow in circular tubes for a solution under closed system conditions with initial $P_{CO_2} = 5 \bullet 10^{-2}$ atm, i.e. $\alpha = 2.5 \times 10^{-5}$ cms. Figure 12 shows the results.

The hydraulic gradients are listed on the curves. For flow in joints the saturation lengths are differing only by a geometrical factor in the order of 1 and therefore the results also hold for this case.

For flow in narrow joints with $d \leq 0.01$ cm even at the extreme hydraulic gradient of $h = 1$ the lengths are below 1 m. At joint widths of $d > 0.1$ cm the saturation length increases to about 1 m for $h = 10^{-3}$ and to 1 km for $h = 1$. At still higher joint widths turbulent flow sets in at a Reynold number of 2000. This reduces the saturation length by about a factor of 10, since onset of turbulence reduces the flow velocity and increases the dissolution rate. At channel widths larger than 1 cm the saturation lengths are all above 1 km increasing steeply with channel widths. In a mature cave with channels of 1 m diameter at a low hydraulic gradient of 10^{-3} the penetration distance amounts to 100 km. In this case of conduit flow the waters remain solutionally aggressive and they are still highly undersaturated at the outlets. In the case of diffuse flow through narrow joints, however, where the saturation lengths are small, the cave waters become saturated. This is in accordance to the observations of Shuster and White (1971), who observed highly undersaturated water at wells fed by conduit systems, whereas diffuse flow springs exhibit waters very close to saturation.

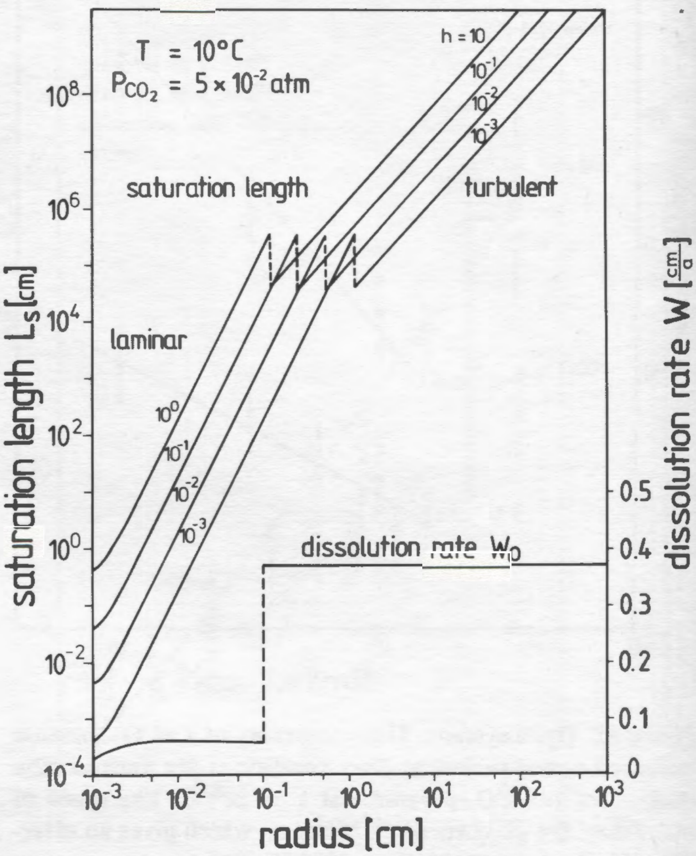

***Figure 12.* Saturation lengths in the closed system in dependence on the radius r of the solutional channel for different hydraulic gradients. The transition from laminar to turbulent flow is indicated by the dotted line. The lower curve represents the characteristic dissolution rate W_o, scaled into retreat of rockwall in cm/a. It shows clearly the hydraulic jump on the onset of turbulence.**

In Figure 12 we have also represented a characteristic dissolution rate W_O, scaled to the retreat of the rock wall by dissolution. This characteristic rate is given by

$$W_O = \alpha \bullet [Ca^{++}]_{eq} \bullet 1.174 \bullet 10^6 \frac{cm}{a} \quad (15)$$

and corresponds to the extrapolation of eq (5) for waters with no Ca^{++} already dissolved. The actual rate for waters with concentration $[Ca^{++}]$, can then be calculated by

$$W = W_O \bullet \left(1 - \frac{[Ca^{++}]}{[Ca^{++}]_{eq}}\right) \quad (16)$$

At the onset of turbulent flow the hydraulic jump increases the rate drastically. For waters with $[Ca^{++}]/[Ca^{++}]_{eq} = 0.95$ the value of W amounts to about $2 \bullet 10^{-3}$ cm/a in the case of laminar flow and to $2 \bullet 10^{-2}$ cm/a for turbulent flow. These values determine the time scale of cave development from its initial state to the mature cave state.

The Concept of a Simple Flow Net

To obtain the values for saturation lengths, one has to know how the hydraulic gradients are distributed in the aquifer. We assume an idealized system, where the bedding planes are practically horizontal. They are fed by water through joints. The whole system is covered by a highly permeable caprock, acting as a water reservoir, feeding the joints by diffuse insurgence, Figure 13a. In the initial state of karstification we assume that the joint widths d, and the widths of the partings between the bedding planes, D, are all approximately equal.

1 is the distance between the covering caprock and the bedding plane into which the final resurgence develops. We assume that all the beds above remain practically impermeable. L is the average distance between joints, reaching down to the bedding plane. We also assume lower bedding planes to be practically impermeable. This is a very simple model of development of karstification in the shallow phreatic zone. Its assumptions are justified by the results of Beddinger (1966) who simulated comparable situations on an analogous resistor network. His findings show that most of the waterflow develops in the shallow phreatic zone.

The pressure head driving the flow of water is given by

$$p = \sigma \bullet g \bullet l \qquad (17)$$

The flow densities in the joints and partings are q, and Q respectively.

$$q_k = \frac{d^3}{12\eta} \bullet \frac{\Delta P_k}{l} = \frac{d^3 \sigma g}{12\eta} \bullet h_k \,;\, Q_k = \frac{D^3 \sigma \bullet g}{12\eta} H_k \qquad (18)$$

Δp_k is the corresponding pressure head acting on the particular joint, or on the parting between points K and K + 1, ref. Figure 13a. h_k, H_k are the corresponding hydraulic gradients in the joints and bedding planes. They determine the flow velocities at point K. To calculate these numbers, and to ultimately obtain the saturation lengths L_S at point K in the joints and corresponding beddings, we transform the flow net into a resistor network represented by Figure 13b.

In this case the currents I_k correspond to the flow density Q_k in the corresponding section of the bedding plane. The flow density q_k in the corresponding joint is related to the currents by

$$q_k = \tau_k - \tau_{k-1} \,;\, Q_k = \tau_k \qquad (19)$$

The resistances of the resistors R and r are related to the flow resistances.

$$R = \frac{12\eta L}{D^3 \sigma \bullet g} \,;\, r = \frac{12\eta L}{d^3 \sigma g} \qquad (20)$$

R corresponds to flow resistance in the bedding plane partings, and r to that in the joints. The voltage drops across the resistors are Δu_k and ΔU_k

$$\Delta u_k = U_k - U \,;\, \Delta U_k = U_k - U_{k-1} \qquad (21)$$

where U is the driving voltage and U_k is the voltage at point K. The voltage U is related to 1 by

$$U = l \qquad (22)$$

From the knowledge of the currents I_k, we have

$$\Delta u_k = r(\tau_k - \tau_{k-1}) \,;\, \Delta U_k = R \bullet \tau_k \qquad (23)$$

The hydraulic heads in the flow system of Figure 13a are then given by

$$H_k = \frac{\Delta U_k}{L} \,;\, h_k = \frac{\Delta U_k}{l} \qquad (24)$$

where h refers to the joints and H to the bedding planes. From these numbers and the widths d, D respectively, one can obtain the corresponding saturation lengths by use of eqs. (11) to (13). Note that this only refers to the case of laminar flow, since turbulent flow is not related to the pressure head in a linear way. Thus, our simulation is only valid for the case of cave initiation, where widths of joints and partings are sufficiently small and only laminar flow results.

The currents in the network of Figure 13b and correspondingly, Q_k, q_k, can be calculated by electric network theory. Here we only give the results.

We define the numbers

$$s = \frac{R + 2r}{r} \,,\, E_1 = \frac{L}{l} \,,\, E_2 = \frac{D}{d} \,,\, \gamma = \frac{r}{2} + \sqrt{\frac{s^2}{4} - 1} \qquad (25)$$

Then we find for the flow densities and the hydraulic gradients

$$Q_k = \gamma \bullet Q_{k-1} \,,\, H_k = \gamma \bullet H_{k-1} \,,\, q_k = Q_k \bullet (1 - 1/\gamma) \qquad (26)$$

$$h_k = H_k \bullet E_2^3 \bullet (1 - 1/\gamma) \,,\, h_k = \gamma \bullet h_{k-1}$$

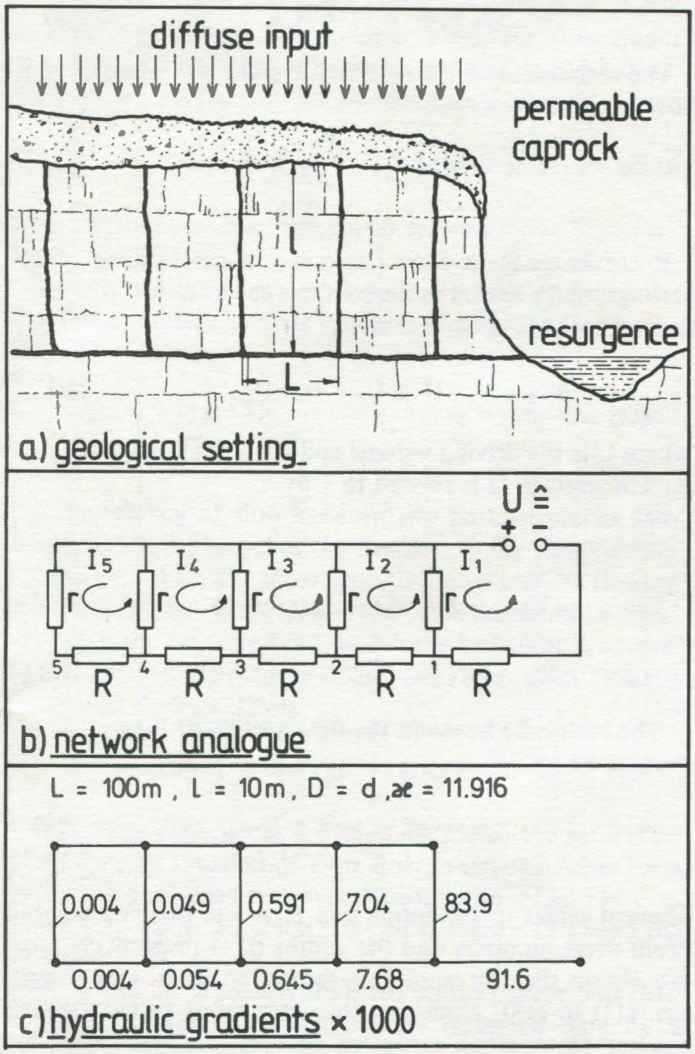

Figure 13. **Electric network analogue (b) of the geological setting shown in (a). (c) gives the hydraulic gradients multiplied with a factor 1000 in the joints and the partings of the bedding planes.**

The flow Q_1 and the hydraulic gradient H_1 at the outlet have to be calculated numerically. It should be noted that the results are depending only on the ratios d/D and l/L. Thus, the values in Table 3 can be scaled into any scale.

Table 3a and Figure 12 give the results for l = 1.000 cm and d = D for various values of L. Table 3b gives similar results for d = 2D. All have been calculated for networks with M = 20 joints. An increase in the number of joints does not change the results for the last 10 joints nearest to the resurgence. The most important result is that the currents and the hydraulic gradients decrease in a geometrical progression, when going from the outlet into the interior of the networks. For $s \geq 10$ practically 90% of the flow is transported through the joint nearest to the resurgence. In the case of $s = 3$ only the 4 joints nearest to the outlet carry 99% of the flow. The flow in the fifth joint is only about 1% of the total flow and there is practically no flow in joints with $K \geq 5$. This means that most of the solutional activity takes place near to the resurgence. Once these first joints and partings have become sufficiently large to represent only small resistances to flow, they may lose contact to the water supply in the caprock. The diffuse input will then mainly be transported by the next joints not yet enlarged. This just means that the electrical network has lost one mesh and the process repeats. Thus, the cave will grow into the interior of the mountain, in accordance to statements of Beddinger (1966) and Ewers (1978).

Table 3. Hydraulic gradients H_1 and h_1 for $\epsilon_2 = 1$ (a) and $\epsilon_2 = ½$ (b) and for $l = 10^3$ cm for various values of L. The values H_K and h_K can be calculated for all K = 2, 3, . . . from these numbers by use of eq. (26). The values q_K and Q_K can be then obtained from eq. (18).

3a) l = 1000 cm, $\epsilon_2 = 1$

L[cm]	s	ϑ	H_1	h_1
10000	12	11.916	0.0916	0.0839
5000	7	6.854	0.171	0.146
2000	4	3.732	0.366	0.268
1000	3	2.618	0.618	0.382
500	2.5	2	1.000	0.500
200	2.2	1.558	1.791	0.642
100	2.1	1.370	2.701	0.730
50	2.05	1.25	4.000	0.8

3b) l = 1000 cm, $\epsilon_2 = ½$

L[cm]	s	ϑ	H_1	h_1
10000	82	81.99	0.099	0.0122
5000	42	41.98	0.195	0.0238
2000	18	17.94	0.472	0.0557
1000	10	9.9	0.899	0.101
500	6	5.828	1.657	0.1716
200	3.6	3.297	3.483	0.303
100	2.8	2.38	5.798	0.420
50	2.4	1.863	9.267	0.537

The situation of $D \leq d \leq 2D$ and $10 \text{ m} \leq L \leq 100$ m, l = 10 m may well simulate a situation like that of Mammoth-Flint-Cave. Inspection of Table 3 shows that in all these cases the hydraulic gradients are well below 1 in the joints. This corresponds to saturation lengths of less than 1 m, if one assumes d = 0.01 cm. Thus aggressive water, when reaching the bedding parting, has lost its solutional aggressiveness completely. It is difficult, therefore, to understand how cave initiation can result.

It should be noted here that although this network simulation of flow in karst areas appears to be rather simplified, it should give at least the right order of magnitude of the hydraulic gradients. Its advantage lies in its mathematical

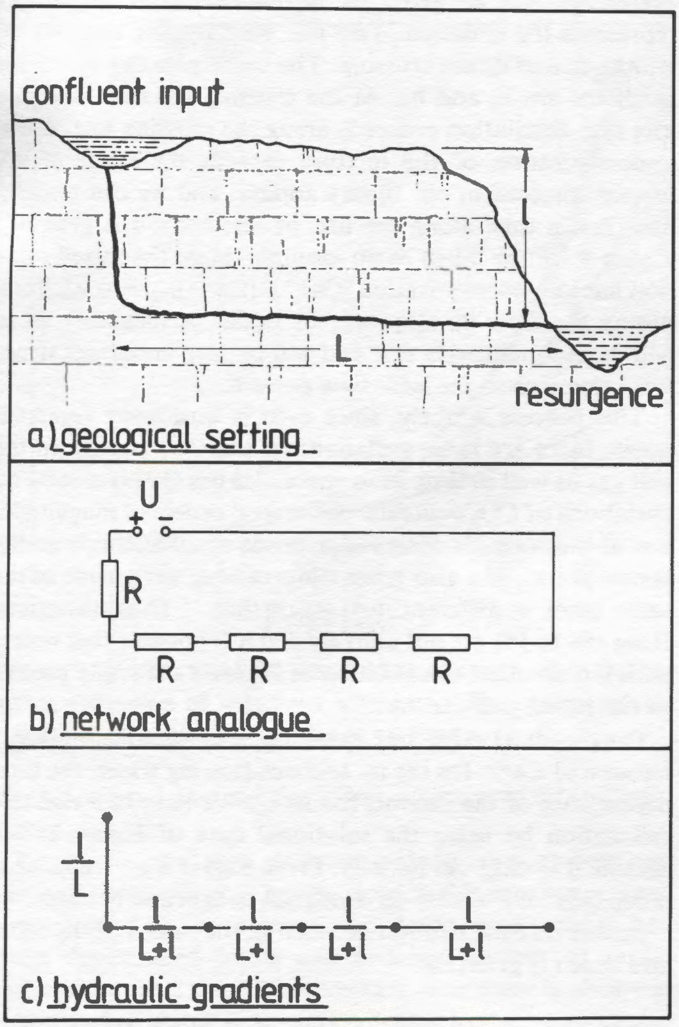

***Figure 14.*Electric network analogue (b) of the geological setting (a). (c) The hydraulic gradients are evenly distributed in the flow path.**

simplicity, in contrast to complicated networks, which have been simulated by Beddinger (1966). Its most important result is the finding that high hydraulic gradients are feasible in geological situations as described by Figure 13.

There are different geological situations of course, which cannot be simulated by the network in Figure 13. If, for instance, insurgence is confluent and enters the system at an elevated point as is shown in Figure 14, the appropriate network is most simply simulated by a number of equal resistors in series. In this case the hydraulic gradients are evenly distributed along the resistors and will be $1/(1+L)$. Thus, hydraulic gradients of 0.1 seem feasible. The saturation lengths again can be read from Figure 12. Assuming an hydraulic gradient of 0.1 and D, the width of the bedding of 0.01 cm one obtains $L_S \approx 10$ cm. Such a situation is encountered in Onesquethaw Cave described by Palmer (1972).

Karstification From Its Initiation to Maturity

Cave Initiation

If one assumes that in the initial state the widths of joints and partings are in the order of $5 \cdot 10^{-3}$ cm (Davis, 1966), and the hydraulic gradients are between 0.1 to 1, the maximal penetration distances are in the order of 1 m (Fig. 12). Any solutional activity of the water entering thus would be confined to a distance of a few meters from the surface and no dissolution of the rock below that zone can occur. Karst erosion should start from the surface and no underground drainage system should evolve.

One possible way out of this dilemma is White's (1977) suggestion, that close to equillibrium, at $[Ca^{++}]/[Ca^{++}]_{eq} > 0.95$ dissolution becomes inhibited and a new surface controlled reaction regime sets in. This has been observed by Plummer and Wigley (1976) and by Hermann (1982) for open system conditions at $P_{CO_2} = 1$ atm. In our laboratory we also have observed some evidence for this effect. We have conducted dissolution experiments under open system conditions in a turbently stirred solution on several natural marble and limestone samples by monitoring conductivity. In the first stage of dissolution we clearly observe an exponential approach to equillibrium as predicted by the theory. Close to saturation, however, a small, approximately linear increase in conductivity of the solution is observed for times up to $t = 50\tau$. These findings show that a regime of low reaction rates close to saturation is existing with dissolution rates lower by a factor of 10^{-2} to 10^{-3} than our theory would predict.

We therefore can simulate the situation of inhibited dissolution by assuming for $[Ca^{++}]/[Ca^{++}]_{eq} > 0.95$, to be a factor of 1,000 lower. According to eq. (5) this also lowers the corresponding dissolution rates by a factor of 1000 to the order of $5 \cdot 10^{-6}$ cm/a, scaled to annual retreat of bedrock. The saturation lengths, however, increase by a factor of 1,000. Thus it takes about 10^4 years, to widen the joints and partings to $5 \cdot 10^{-2}$ cm in a length of about 100 m and to produce significant permeability.

Once this fissure permeability has been established, saturation lengths do not any longer represent a problem, since dissolution can now proceed in the uninhibited regime, and saturation lengths are in the order of 100 m. In this regime our theoretical results can be applied, and conclusions, drawn to karst development, have a sound theoretical and experimental basis.

Intermediate State of Cave Evolution

Once fissure permeability to joint widths of $5 \cdot 10^{-2}$ cm has been established by inhibited solution, this type of dissolution is no longer of importance, since saturation lengths are now sufficiently large to keep the solution in the uninhibited regime. This trigger effect, called kinetic trigger (White, 1977), determines the further evolution of karstification.

The first pathways of water, having reached sufficient dimensions for the kinetic trigger to take place, will now experience a highly increased dissolution rate in the order of $10^{-9}\ \frac{\text{mmole}}{\text{cm}^2\text{s}}$, corresponding to retreat of bedrock of 10^{-3} cm/a. Thus, these pathways will develop quickly at the expense of the others, enlarging to diameters in the order of 1 cm in about 1000 years, determining the future structure of the cave.

If insurgence is confluent entering a bedding plane parting at one or several points (c.f. Fig. 14), pathways will be accidential, all being oriented more or less in the dip direction. Cave passages developing from these will show no significant joint control, as is the case in Onesquethaw Cave (Palmer, 1972).

If insurgence, however, is mainly diffuse along joints, as is illustrated in Figure 13, joint controlled caves can originate where the majority of passages are aligned along joints. In this case a close relation in the directional distribution of the joint pattern and the directional distribution of cave passages exists (Powell, 1977; Jakucs, 1977; and Deike, 1969).

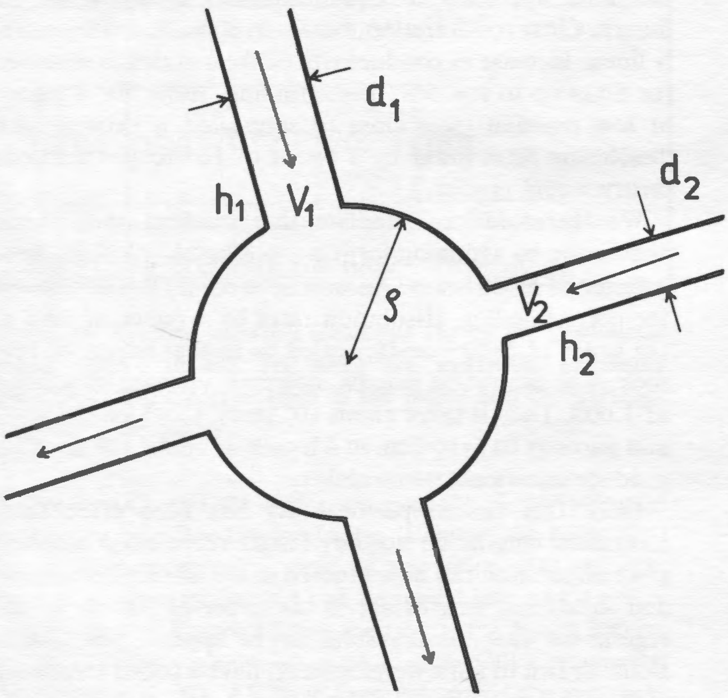

Figure 15. **Evolution of a solution channel by mixing corrosion at the crossing of two joints with widths d_1 and d_2. The hydraulic gradients in the joints are h_1 and h_2.**

Often dissolution takes place preferentially at intersections of joints and bedding planes. An explanation of this preference can be given by mixing-corrosion. Figure 15 represents the situation. Two flat waterleading conduits of widths d_1 and d_2 are crossing. The corresponding hydraulic gradients are h_1 and h_2. At the crossing the two solutions mix and dissolution proceeds along the crossing line. If the undersaturation of the mixture exceeds the range of inhibited dissolution our theory applies, and we can predict, how fast a tube along the line of intersection is growing. Figure 8 will be taken as an example. Here the mixed solution has an undersaturation $[Ca^{++}]/[Ca^{++}]_{eq} = 0.92$. Thus during the slow development of initial permeability tubes will develop relatively fast and will impose important structural elements to the later flow pattern.

This process is likely, since even in uniformly vegetated areas, there are large variations of the CO_2 content in the soil gas as well in time as in space. Jakucs (1977) reports on variations of CO_2 contents "by several orders of magnitude, not only as regards observation made simultaneously at different points, but also when observations were made at the same point at different instants of time." Thus, variations from 1% to 5% are not unlikely and it is possible that waters with the chemical composition of Figure 8 are really present in the joints and partings.

Dreybrodt (1981a) has calculated, by considering mass balance of Ca^{++} for the in- and out-flowing water, the time dependence of the channel radius s_t. We have repeated this calculation by using the solutional data of Figure 8. We assume d = 0.01 cm initially. From Figure 8 we realize that α depends only weakly on d and can be taken to be constant.

In this case the relation between s_t, the radius of the tube, and time t is given by

$$t = \frac{1}{\epsilon\,([Ca^{++}]_{eq} - [Ca^{++}]_m)} \bullet \left(\frac{s_t - s_i}{\alpha} + \frac{\pi\,(s_t - s_i)^2}{V_f} \right) \qquad (27)$$

$\epsilon = 1.174 \bullet 10^6$ is a factor converting the dissolution rates from mmole/cm²s into annual retreat of bedrock in cm/a. s_i is the initial radius of the tube at the crossing; ($s_i = \delta/2$). V_f is the volume of water flowing per second across one centimeter length of the tube. $[Ca^{++}]_m$ is the concentration immediately after mixing.

Figure 16 shows the increase of radius s_t in time for a mixture represented in Figure 8. $d_1 = d_2 = 10^{-1}$ cm. The hydraulic gradients $h_1 = h_2$ are listed on the curves. From this it becomes feasible, that in very short times tubes with diameters of several mm can develop. Although, at first these tubes remain unconnected with each other, they will be important structural elements for the flow of water, once the permeability of the fractures has developed to a sufficient amount. Then these tubes can be important "short circuits" of water flow, and they determine the further flow pattern.

Especially in caves developing in flat strata with dips of a

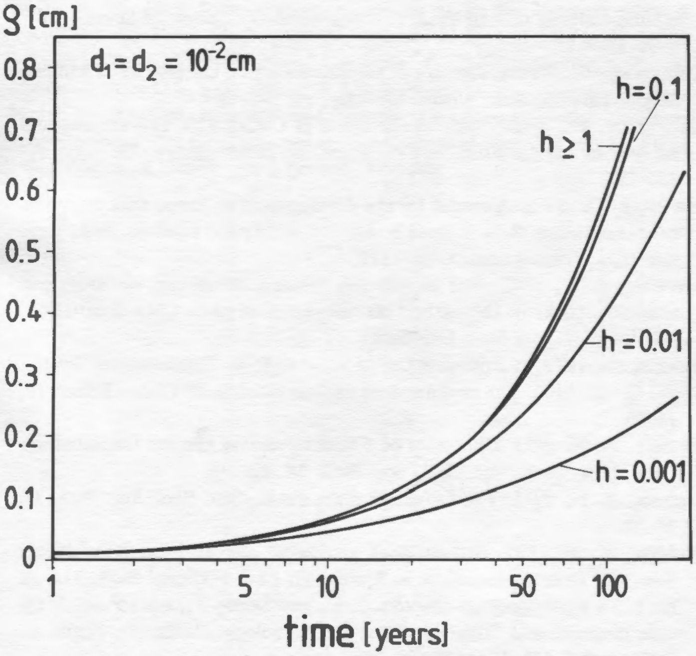

Figure 16. **Radius st of the dissolution channel, evolving by mixing corrosion of solutions with initial P_{CO_2}-pressures of 0.01 and 0.05 atm, in dependence on time.**

few meters per kilometer this effect can become most dominant.

Tubes will grow with preference along crossing between beds and strike-oriented joints, since in this case water flow perpendicular to the intersection is large. Intersections between dip-oriented joints and beddings cannot so easily evolve into tubes, since it is necessary, that there is always a component of water flow perpendicular to the intersection. This is not so likely for flow oriented crudely along the dip.

Anyway, once these tubes have developed, they can accept water flowing along the bedding planes. Particularly the strike-oriented tubes can accept water, entering from the dip direction, and will develop into turbular cave passages. Since the permeability of fractures has simultaneously developed almost evenly in the region of low dissolution at the stage of initiation, these passages eventually will concentrate the flow down dip and create dip-oriented passages. These later will be preferred paths of vadose flow, and dip-oriented canyons can result in a dentritic pattern. Once all these features have developed to cross sectional dimensions of about 1 cm, turbulent flow may occur and the first pathways exhibiting turbulent flow conditions will enlarge by about a factor of ten faster than the others, evolving the cave into its mature state. This may explain the origin of caves such as Mammoth-Flint-Cave System, which is almost entirely structured by strike-oriented tubes and dip-oriented canyons, Palmer (1984, 1981a, 1977).

In cases with diffuse insurgence and where also resurgence is low due to porous, insoluble caprocks covering the resurgence areas, in the initial state permeability of the fractures develops evenly over large areas. Furthermore, turbulent flow will not likely occur. Therefore, all the structural elements will grow with equal rates and networks or maze caves will be the result, as is the case of Clark's Cave, Virginia (Palmer, 1975).

Mature State of Caves

Once waterleading pathways with cross sectional dimensions of a few mm have evolved turbulent flow sets in, and the dissolution rates increase by about a factor of twenty for two reasons; first from the increased dissolution rates due to the hydraulic jump, and secondly from the fact, that since penetration distances are now in the order of 1 km the solutions remain largely undersaturated. Thus, dissolution rates of 10^{-2} cm/year result, in agreement with dissolution rates we have calculated for the chemical composition of undersaturated karst springs, as described by Shuster and White (1971). With dissolution rates that high, 10,000 years are needed to enlarge cave conduits to diameters of 2 m.

In the case of vadose flow at CO_2-pressures between $3 \cdot 10^{-4}$ to $5 \cdot 10^{-3}$ atm the entrenchment rate of canyons, developing in that situation, are between $8 \cdot 10^{-3}$ to $2 \cdot 10^{-2}$ cm/a (c.f. Fig. 2 and 4).

Therefore, the time scale from the intermediate state to the mature state is in the order of 10^4 years. The time to create the first permeability in the initial state may be in the same order.

The time scale of several 10^4 years is in accordance to observations at caves in the Helderberg Karst Plateau, New York, which have been initiated 10–15 thousand years ago (White, 1977) and to estimations of other authors (Bakalowicz, 1982). The length scale is related to the saturation lengths and also follows from our kinetic theory. For mature caves it is in the order of 100 km even at lowest hydraulic gradients of 10^{-3} (c.f. Fig. 12).

Thus the kinetic theory explains well the dimension of karstification in time and length and can be used as a framework in the interpretation of karstification.

It should be noted finally that the theory can also be applied to other processes in karstification, as karst denudation, the formation of dolines, and to all kinds of precipitation processes, i.e., the formation of speleothems and sinter.

Only one application should be mentioned. In mature karst, where the vadose zone reaches deep into the rock formation, Jakucs (1977), has described an upper level of infiltration restricted to about 10 m (b-zone) below the surface. In this zone most of surfacial karst erosion takes place. The depth of this zone can be well explained by our theory. Assuming an average width of the fissures of about $2 \cdot 10^{-2}$ cm and hydraulic gradients of 1, as are feasible in a joint in the vadose zone, the saturation length predicted from Figure 12 is about 10 m, which is the correct order of magnitude.

PERSPECTIVES TO FUTURE RESEARCH

Our theory presents a first comprehensive proposal, how to understand karstification from a chemical and hydrological basis, applied to different geological situations. It needs, however, to really understand the initiation phase of karstification, more reliable data of dissolution kinetics close to equillibrium are necessary. Very careful experiments have to be performed on pure calcite and natural limestones under experimental conditions as close to nature as possible.

Application of our theoretical framework to real karst system needs both, knowledge of what is possible from the physics and chemical kinetics in such a system, and with equal importance knowledge on geological settings and knowledge on what is possible geologically. Therefore, interdisciplinary cooperation is required to a better understanding of the complicated processes occurring in karstification.

ACKNOWLEDGEMENTS

I thank Dr. D. Buhmann for many valuable and stimulating discussions and C. Niemeyer for typing the manuscript. The authors acknowledge the financial support of the Deutsche Forschungsgemeinschaft (SSP: Hydrogeochemische Vorgänge im Wasserkreislauf der ungesättigten und gesättigten Zone).

REFERENCES

Bakalowicz, M., 1982. La genèse de l'aquifer karstique vue par un geochimiste. Reunion Monografica sobre el Karst, Larra 82, 159–174.

Baumann, J., Buhmann, D., Dreybrodt, W. and Schulz, H. D. 1985. Calcite dissolution kinetics in porous media. Chem. Geol.

Beddinger, M. S. 1966. Electric-analog study of cave formation Natl. Speleol. Soc. Bull. *28*, 127–132.

Bird, R. B., Stewart, W. E., Lightfoot, E. N., 1960. Transport Phenomena. John Wiley & Sons. New York.

Bögli, A. 1964. Corrosion par mélange des eaux. Int. J. Speleol. *1*, 11–23.

Bögli, A. 1980. Karst hydrology and physical speleology, Springer-Verlag, Berlin.

Buhmann, D. 1984. Ein neues kinetisches Modell zur Berechnung der Lösung von Kalk bei Verkarstungsprozessen und seine experimentelle Bestätigung. Dissertation, Dr. rer. nat., Universität Bremen.

Buhmann, D. und Dreybrodt, W., 1985a. The kinetics of calcite dissolution and precipitation in geologically relevant situations of karst areas. Part 1: open system. Chem. Geol., *48*, 189–211.

Buhmann, D. und Dreybrodt, W., 1985b. The kinetics of calcite dissolution and precipitation in geologically relevant situations of karst areas. Part 2. closed system. Chem. Geology.

Davis, S. N., 1968. Initiation of groundwater flow in jointed limestone. Bull. Natl. Speleol. Soc., 28, 111–117.

Deike, R. G. 1969. Relations of jointing to orientation of solution cavities in limestones of central Pennsylvania. American Journ. of Science, 267, 1230–1248.

Dreybrodt, W., 1981a. Kinetics of the dissolution of calcite and its application to karstification. Chem. Geology, *31*, 245–269.

Dreybrodt, W., 1981b. Mixing corrosion in $CaCO_3$-CO_2-H_20 systems and its role in the karstification of limestone areas. Chem. Geology, *32*, 221–236.

Ewers, R. O., 1978. A model for the development of broad scale networks of groundwater flow in steeply dipping carbonate aquifers. Brit. Cave Res. Ass. Transactions *5*, 121–125.

Herman, J. S., 1982. The dissolution kinetics of calcite, dolomite and dolomitic rocks in the carbon dioxide-water system. PhD dissertation. The Pennsylvania State University.

Jakucs, D., 1977. Morphogenetics of karst regions. Adam Hilger, Bristol.

Kern, D. M. 1960. The hydration of carbon dioxide. J. Chem. Educ., *37*, 14–23.

Palmer, A. N. 1972. Dynamics of a sinking stream system: Onesquethaw Cave, New York. Nat. Spel. Soc. Bull. 34, 89–110.

Palmer, A. N. 1975. The Origin of maze caves. Nat. Spel. Soc. Bull. 37, 56–76.

Palmer, A. N. 1977. Influence of geological structure on groundwater flow and cave development in Mammoth Cave National Park, U.S.A. In: Karst Hydrogeology (Tolson, J. S., and Doyle, F., eds.) Proc. of the 12th International Congress, Karst Hydrogeology, Huntsville, Alabama, U.S.A., 405–432. UAH Press.

Palmer, A. N., 1981a. A geological guide to Mammoth Cave National Park. Zephyrus Press, Teaneck, New Jersey.

Palmer, A. N., 1984. Geomorphic interpretation of karst features In: Groundwater as a geomorphic agent. La Fleur, R. G. (ed.), Allen and Unwin. Inc., London, 173–209.

Picknett, R. G., Bray, L. G. and Stenner, R. D., 1976. The chemistry of cave waters. In: T. D. Ford and C. H. D. Cullingford (eds.), The Science of Speleology. Academic Press, London, 213–266.

Plummer, L. N., Parkhurst, D. L. and Wigley, T. M. L., 1979. Critical review of the kinetics of calcite dissolution and precipitation. In: E. A. Jeune (ed.), Chemical Modelling in Aqueous Systems. Am. Chem. Soc., Symp. Ser. 93, 537–572.

Powell, R. L., 1977. Joint patterns and solution channel evaluation in Indiana. In: Karst Hydrogeology. Tolson, J. S. and Doyle, F. (eds.) Proc. of the 12th International Congress, Karst Hydrogeology, Huntsville, Alabama, U.S.A., 255–269, UAH Press.

Plummer, L. N. and Wigley, T. M. L., 1976. The dissolution of calcite in CO_2 saturated solutions at 25° C and 1 atmosphere total pressure. Geochim. Cosmochim. Acta, 40: 191.

Plummer, L. N., Wigley, T. M. L. and Parkhurst, D. L., 1978. The kinetics of calcite dissolution in CO_2-water systems at 5 to 60° C and 0.0 to 1.0 atm CO_2. Am. J. Sci., 278, 179.

Rauch, H. W. and White, W. B., 1977. Dissolution kinetics of carbonate rocks, 1. Effects of lithology on dissolution rate. Water Resour. Res., 13, 381–393.

Shuster, E. T., and White, W. B., 1971. Seasonal fluctuations in the chemistry on limestone springs: A possible means for characterizing carbonate aquifers. Jour. Hydrol. 14, 93–128.

Skelland, A. H. P., 1974. Diffusional Mass Transport. Wiley, New York, New York.

Tien, C. L., 1959. On the eddy diffusivities for momentum and heat. Appl. Sci. Res., Section A, *8*, 345–348.

Thrailkill, J., 1968. Chemical and hydrologic factors in the excavation of limestone caves. Geol. Soc. Am. Bull., *79*, 19–46.

Usdowski, E., 1982. Reactions and equilibria in the systems CO_2-H_20 and $CaCO_3$-CO_2-H_2O (0°-50° C). A review. N. Jb. Miner. Abh. *144*, 148–171.

Weyl, P. K., 1958. Solution kinetics of calcite. J. Geology, *58*, 163–176.

White, W. B., 1977. Role of solution kinetics in the development of karst aquifers. In: Karst Hydrogeology. Tolson, J. S. and Doyle, F. (eds.) Proc. of the 12th International Congress, Karst Hydrogeology, Huntsville, Alabama, U.S.A., 503–517, UAH Press.

White, W. B., 1984. Rate processes: chemical kinetics and karst landform development. In: Groundwater as a geomorphic agent. R. G. La Fleur (ed.). Allen & Unwin, Inc., Boston, 227–248.

White, W. B., 1979. Water balance, mass balance, and time scales for cave system development. Nat. Spel. Soc. Bull. *41*, 115.

White, W. B. and Longyear, J., 1962. Some limitations on speleogenetic speculation imposed by the hydraulics of ground water flow in limestone. Nittany Grotto Newsl., *10*, 155–167.

Wigley, T. M. L., and Plummer, L. N., 1976. Mixing of carbonate waters. Geochim. Cosmochim. Acta, 40, 989.

Palmer, Arthur N.—Cave Levels and Their Interpretation: *NSS Bulletin* **49: 50-66.**

CAVE LEVELS AND THEIR INTERPRETATION

Arthur N. Palmer
Department of Earth Sciences
State University of New York
College at Oneonta, NY 13820

The concentration of passages at common levels in a solution cave can be used to interpret the evolution of the cave in relation to its regional setting. It is usually assumed that cave levels of this type are controlled by fluvial base level, although stratigraphic influence must also be considered. High-precision vertical surveys that show past vadose/phreatic transition points (piezometric limits), rather than relative passage size alone, are needed for proper identification of levels. Stratigraphic perching can cause a false interpretation, but base-level control, where present, can be recognized even where the strata have a great influence. Although the largest passages in a cave owe their origin to increasing discharge rates, their ultimate size depends primarily on the length of time they have been active.

Sharply defined cave levels with narrow vertical ranges, such as those in Mammoth Cave, Kentucky, appear to have formed in response to intermittent episodes of rapid valley entrenchment, probably by headward erosion, followed by a lengthy period of virtually static base level. Piezometric limits are adjusted to base-flow conditions and do not reflect short-term variation in river level or groundwater discharge. Most cave levels are not so distinct, owing to erratic or slow lowering of base level, or to large fluctuations in groundwater flow. Some levels in caves formed by short-lived deep-seated processes may not represent static base levels.

The Concept of Cave Levels

Nearly every cave contains passages at a variety of elevations, and even the casual visitor tends to group them mentally into different "levels." Serious investigators usually restrict this term to large low-gradient passages that appear to represent distinct stages of cave development. This idea assumes that the cave-forming process has concentrated at a particular elevation because of favorable geologic or geomorphic conditions, and that elsewhere in the same cave, or in nearby caves, a similar concentration of passages should exist at the same elevation.

Passage levels can be used to interpret the evolution of caves with relation to the surrounding landscape. This technique is used less frequently than might be expected, because of limited field data of sufficient accuracy, combined with uncertainty as to what constitutes a true cave level. The issue is confused further by the fact that there are several different types of levels, with many passages having a composite origin. The vertical position and relative size of cave passages are controlled by the following factors:

(1) Base level: When entrenched rivers experience a long period of rather static base level, cave springs along the river banks tend to remain stable throughout that time without shifting elevation. Base-level passages remain active long enough for them to grow by solution to a relatively large size. On the other hand, rapid valley deepening causes frequent diversion of groundwater to lower elevations. Passages at or near river level are quickly abandoned by their water or acquire entrenched canyons in their floors, so growth of the original water-filled sections is arrested. This is the standard interpretation of cave levels and the primary subject of this paper.

(2) Stratigraphic control: Where water is perched above surface rivers by insoluble or impermeable beds, preferential enlargement of passages takes place at that zone. Selective enlargement of phreatic cave passages can also occur within relatively soluble or highly fractured beds, or at the base of a poorly soluble bed where groundwater is rising toward an outlet.

(3) Sequential diversion of vadose water to lower levels: Vadose entrenchment of a canyon passage is often accompanied by periodic diversion of water from the original path. A common example is where the passage direction is influenced by prominent bedding-plane partings that conduct water in the down-dip direction. Each parting usually possesses a slightly different dip direction, especially in low-dip areas. As progressively lower bedding planes are encountered, the vadose water may divert to a new direction. This is an example of stratigraphic control on a very fine scale. These "vadose levels" are not true levels in the geomorphic sense and have no regional significance.

(4) Variations in discharge: The cross-sectional area of a passage is usually proportional to the discharge of the water that formed it. Whether passages with high discharge en-

large faster or simply represent a longer time of development is a topic discussed in a later section.

(5) Chemical zonation: Cave development may concentrate at the boundaries between groundwater zones of different chemical character, where the solutional capacity of the mixture may be greater than that of either source.

Several of these influences may combine to varied degrees in the same passage, and identifying a single dominant process is sometimes difficult. This paper offers suggestions for distinguishing base-level control of passage levels and for interpreting their vertical layout.

PREVIOUS WORK

Most European and American karst researchers early in this century recognized the control of valley deepening on the evolution of caves. The largely American controversy over the relationship of cave origin to the position of the water table during the 1930s was a distraction that probably set back the interpretation of cave levels several decades. At that time the ideas of Swinnerton (1932) most easily explained cave levels, as he favored cave origin at or near the water table, and therefore at the level of entrenched rivers. Only after many more caves were mapped was the correlation between cave levels, base level, and fluvial terraces firmly established to nearly everyone's satisfaction. Pertinent work includes that of Sweeting (1950), Davies (1957), White (1960), Ek (1961), Wolfe (1964), Ford (1965), Droppa (1966), Bögli (1968), Powell (1970), Miotke and Palmer (1972), White and White (1974), and Wilson (1985).

The influence of geologic setting on cave levels has received less attention. Gardner (1935) attributed them to the establishment of down-dip water circulation through favorable strata as they are exposed by erosional deepening of nearby valleys. Waltham (1970) showed that certain caves formerly thought to show base-level control were stratigraphically perched. Passages in certain Indiana caves have formed preferentially in highly fractured beds (Powell, 1976) and in oolitic limestones (Wilson, 1985).

FIELD DATA AND ANALYSIS

The interpretation of cave levels requires precise vertical surveying. Ideally, continuous profiles are made showing the relationship of the cave to the surrounding geology. All passages should be included where feasible, to distinguish those that constitute levels from those that do not. For the purpose of geomorphic interpretation a horizontal error of several percent can be tolerated in a cave survey, but the vertical error must be much smaller. This is particularly true for caves in low-dip, low-relief areas, where passage inclinations, hydraulic gradients, and stratal dip are difficult to distinguish. Table 1 summarizes the types of equipment used for this study. Closure error differs widely among surveyors and also depends on proper instrument calibration, alternation of foresights and backsights to help cancel residual miscalibration, repetition of readings to avoid blunders, and indifference to harsh conditions.

This paper is based on about 60 km of geologic leveling surveys of caves in a variety of geologic settings: McFail's, Knox, Church, and Onesquethaw Caves, New York; Ludington Cave and part of McClung Cave, West Virginia; part of Clarks Cave, Virginia; Blue Spring Cave and parts of Popcorn Spring, Shiloh, and Sullivan Caves, Indiana; roughly 30 km in Mammoth, Long, and Great Onyx Caves, Kentucky; part of the Silvertip Cave System, Montana; parts of Wind and Jewel Caves, South Dakota; half of Big Brush Creek Cave, Utah; part of Groaning Cave, Colorado; Hicks Cave and part of Carlsbad Caverns, New Mexico; and most of the caves above sea level in Bermuda. All surveys were made with the help of Margaret V. Palmer. John E. Mylroie and J. Michael Queen assisted with several of them.

The recommended technique for conducting a geologic survey is as follows. A standard compass-and-tape survey is first made to determine the layout of the cave. Vertical angles are used mainly to obtain a true horizontal projection. Using this base map to mark locations, a detailed level survey is made using one or more of the techniques in Table

Table 1. Vertical survey methods used in preparing geologic profiles. Mean loop errors are calculated from all leveling surveys cited in this paper.

Survey Method	Mean Vertical Error in Loops	Best Suited For:	Limitations
Hand-held SUUNTO clinometer and tape	0.3%	High-gradient caves; rapid reconnaissance	Unacceptable for structural analysis in low-dip areas
Tripod-mounted Brunton compass and tape*	0.08%	Simultaneous cave mapping and vertical measurements	"
Hand level and rods*	0.007%	General use in geologic mapping	Accuracy highly dependent on individual experience
Water tube**	0.003%	Spacious, low-gradient caves	Difficult to use in breakdown or crawlways
Tripod-mounted engineer's level and stadia rod	0.001%	Spacious, dry, low-gradient caves	Delicate equipment; requires stable footing and elbow room

*Alternate foresights and backsights.
**15-m flexible vinyl tube nearly filled with water, held in a wide "U"; water level in both ends is equal.

1. By conducting the detailed vertical survey independently, one can more easily concentrate on the geologic setting without distraction. At each leveling station the elevation of the following is obtained: solutional ceiling and floor, stratal contacts, major bedding planes, sediment levels, bedrock benches (as in a keyhole passage), past and present water levels, and solutional zones such as anastomoses. Details of passage character and relationships, geologic structures, and flow patterns are recorded.

Measurements should be spaced closely enough to distinguish the geologic control over the passage. For instance, the control of sinuosity by bedding structure in a passage can be determined only if the measurements are spaced no farther apart than about one quarter of the crest-to-crest length of the bends. Ordinarily this means that measurements should be made within sight of each other, which unfortunately denies use of the water tube's ability to measure around corners.

Leveling information for this paper was plotted as continuous passage profiles and composite cross sections. Controlling beds or bedding-plane partings (if any) were identified, and in nearly flat-lying rocks the mean dip direction and inclination of each bed were calculated by planar regression, from which broad relationships between passage trends and the mean dip of controlling beds could be determined. Analysis of individual passage segments was made by comparing their gradients and trends to the local structure (see, for example, A. N. Palmer, 1974, and M. V. Palmer, 1976). Most details of the structural analysis lie beyond the scope of this paper.

HYDROLOGIC CONTROL OF PASSAGE PROFILES

The Piezometric Limit

In distinguishing former base levels it is not sufficient merely to cite the elevation of large tubular cave passages. Much of their development may have taken place below the contemporary base level, and such passages can also be formed above base level by vadose flow perched on resistant beds.

When forming, a typical cave passage that is fed by recharge from the surface contains a vadose upstream section and a phreatic downstream section. The most foolproof method for determining past base levels is to determine the elevation of the former vadose-phreatic transition point, where gravitational flow changed to flow influenced by hydrostatic pressure. Several distinct changes take place there: (1) from a consistently downward profile to one that is either nearly horizontal or has undulations with sections that rise in the downstream direction; (2) from the steepest available path (for instance, directly down the dip of a bedding-plane parting) to a path that has no consistent relationship to the dip of the guiding structure; and (3) in most cases, from passages with little or no upward solution of the ceiling (e.g., canyons and shafts) to passages with prominent upward solution, such as tubes.

The point at which these changes take place has been called the "piezometric limit" by Palmer (1972), implying that it is the upstream limit for the effects of hydrostatic pressure on passage morphology. This term is applied to a single point (or, rather, a short zone) within a specific

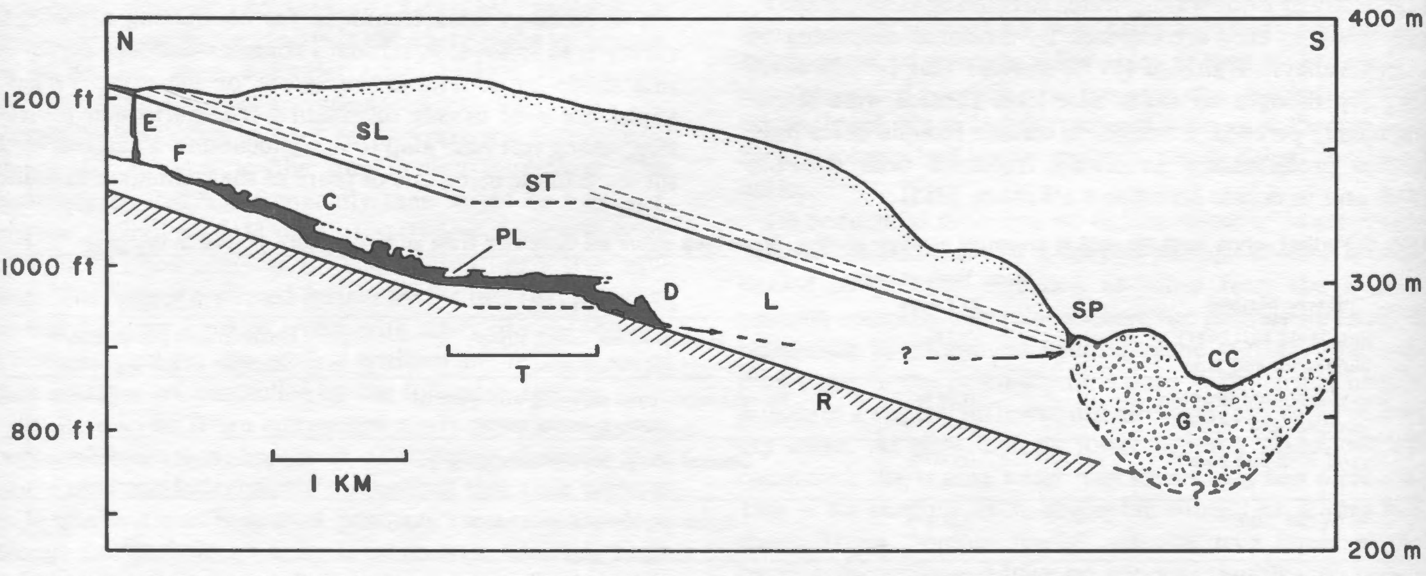

Figure 1. Profile through McFail's Cave, NY, showing piezometric limit at a former base level. PL = piezometric limit, E = northern entrance, F = fissure passages, C = down-dip canyon, T = tubular passages, D = diversion route, SP = spring, CC = Cobleskill Creek, G = glacial sediment, L = limestone (Coeymans and Manlius Formations), SL = shaly limestone (Kalkberg Formation), R = Rondout Dolomite, ST = strike-oriented break in profile.

passage, whether inactive or still forming, and does not imply the presence of a continuous piezometric surface. It is compatible with, but not equivalent to, the British term "rest level," which refers to the static level of an otherwise descending or fluctuating water table, usually deduced from cave levels. Knowing the piezometric limit eliminates the uncertainty of how "level" a passage must be to qualify as a true cave level.

An example can be seen in McFail's Cave, New York, located in gently dipping limestones of the Devonian Helderberg Group (Figs. 1 and 2). The main passage is a canyon that divides in places into two or three separate vadose levels, all trending relentlessly down the local dip, except for short sections controlled by prominent joints. All but the lowest level eventually terminate downstream in sediment fill. At one point the lowest level of the canyon becomes distinctly tubular, acquires a gentle gradient less than that of the dip, and eventually curves to a trend nearly parallel to the strike. The piezometric limit for that specific stage of cave development is located at the change from down-dip canyon to discordant tube. It is more common in other caves for the change in direction to occur right at the piezometric limit. The strike-oriented section in McFail's Cave is nearly concordant with the bedding, but it migrates up and down the dip with considerable sinuosity superimposed on the roughly linear trend. From the piezometric limit, the solutional ceiling drops only half a meter over the 640 m distance to the junction with a major tributary tube. Most passages beyond are also tubes nearly parallel to the strike, implying a phreatic origin, although they still contain streams perched as much as 10 m above the water table.

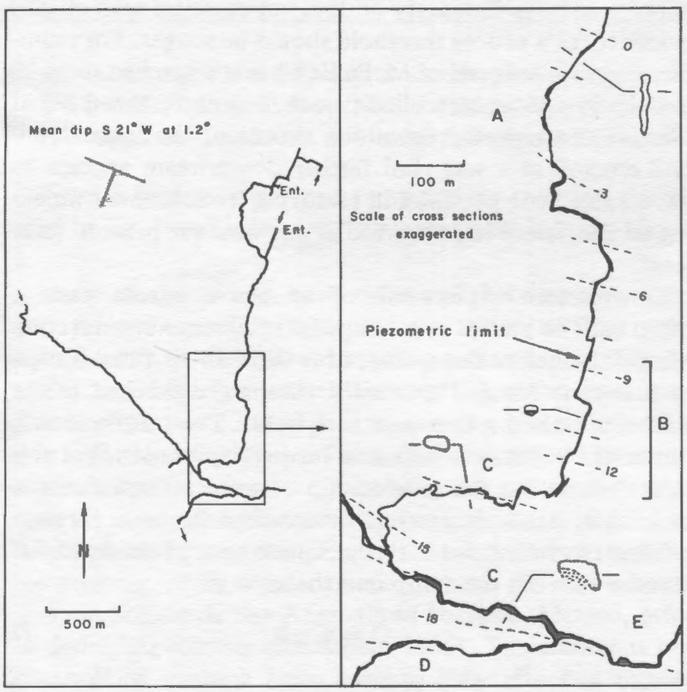

Figure 2. **Map of McFail's Cave, showing structural contours in the vicinity of the piezometric limit (arbitrary structural datum, contour interval 1.5 m). A = down-dip canyon, B = dip-oriented tube with low gradient cutting upward across strata, C = tubes of mainly strike orientation, D = diversion route cutting downward across strata, E = abandoned continuation of main passage.**

This example is pertinent to the interpretation of local pre-glacial history, because virtually all surface clues have been effaced by Wisconsinan glacial erosion and deposition. The cave is pre-Wisconsinan, as shown by till plugs and varved clays within it, as well as by a passage pattern adjusted to pre-Wisconsinan topography (Palmer, 1976). The cave level described here lies 303 m above sea level, approximately 100 m above the bedrock floor of the nearby entrenched valley and 50–80 m above the present river, which is now superimposed on glacial till and outwash. No interpretation is offered here on the basis of this single point; but it is obvious that cave levels can retain very precise evidence about erosional history that may be lacking or obscure at the surface.

Elevation of the Piezometric Limit

The piezometric limit of an actively forming passage must lie slightly higher than the spring outlet, because some head is required to drive the water through the phreatic section. Under ideal conditions this elevation difference can be estimated from the Darcy-Weisbach flow equation:

$$\Delta h = 8\,\frac{Q^2\,fL}{\pi^2\,d^5\,g} \qquad (1)$$

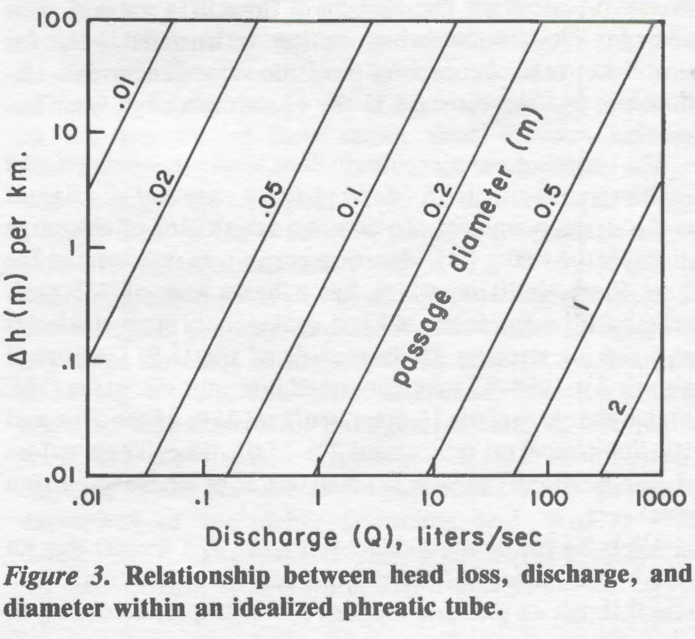

Figure 3. **Relationship between head loss, discharge, and diameter within an idealized phreatic tube.**

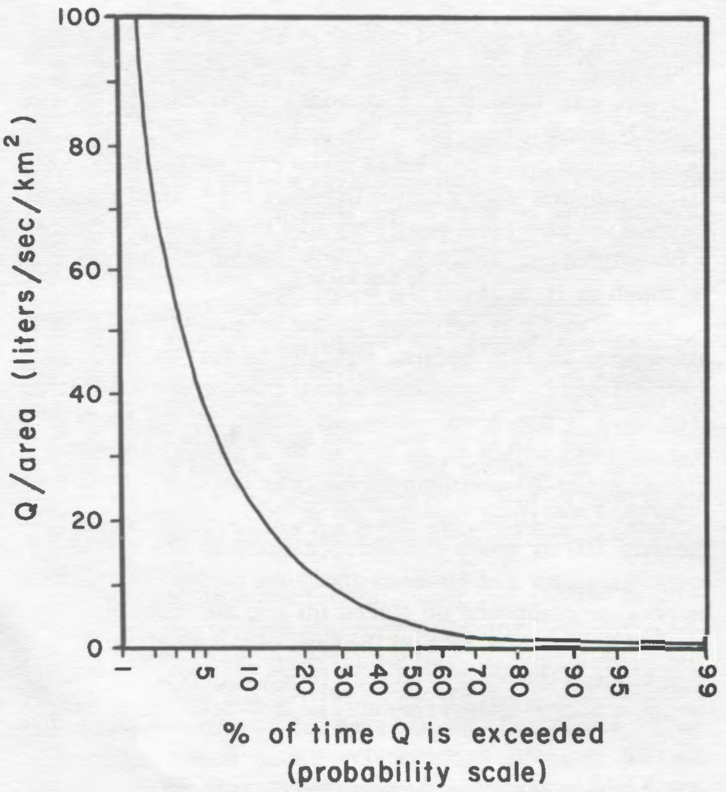

Figure 4. **Flow duration graph for the Lost River basin, Indiana (1969–72).**

where Δh = head difference between two points in the flow (in this case, essentially the vertical distance between the piezometric limit and the spring outlet), Q = discharge, L = flow distance between the two points, d = passage diameter, g = gravitational field strength, and f = friction factor (about 0.05 for turbulent flow in a typical cave passage). A circular cross section is assumed here for simplicity; other geometries have the same functional relationship, but the constant in the equation is slightly different.

The height of the piezometric limit above the spring outlet is shown graphically in Figure 3 for a range of discharges and passage diameters. To obtain a rough idea of discharge in typical caves, a flow-duration graph was constructed for Lost River, Indiana, which has a basin area of 735 km^2, most of it having internal karst drainage through sinkholes and sinking streams. Daily records of the U.S. Geological Survey for 1969–72 were converted into unit discharge (Fig. 4). Discharge exceeds 10 liters/sec/km^2 25% of the time and 100 liters/sec/km^2 only about 2% of the time. These values should be slightly greater in small basins or where soil is thin or absent.

Applying the discharge data to Figure 3, it is clear that an active cave passage of traversable size has only a small head loss through its phreatic section. For example, according to the Indiana data, a passage one meter in diameter draining a square kilometer would average a one-meter rise in water level per kilometer of passage length only about one day each year. Conditions are not so stable in passages fed by large sinking streams or partly blocked with debris. There are several other complications: the discharge increases in an unpredictable way as a cave passage grows; the stage of the controlling surface river fluctuates a great deal during the year; and the aggressiveness of cave water often increases with discharge when a greater proportion of direct, high-velocity infiltration routes are utilized during floods. With so many variables, no conclusions can be made about the height of the piezometric limit until field examples are considered.

Vadose Thresholds

Structural basins or downward-tightening fractures may create perched phreatic zones where descending water is ponded and spills over a vadose threshold (Fig. 5). The leveling data suggest that most of these zones are drained by solutional downcutting before false piezometric limits can affect the passage shape significantly, except where the threshold consists of resistant rock. Where a passage level appears to be rudimentary or does not correlate with others, evidence for a vadose threshold should be sought. For example, the upstream end of McFail's Cave is a perched sump 10 m deep in a joint-controlled fissure. A lengthy threshold of massive, unfractured limestone maintains the water level, and erosion at a waterfall farther downstream appears to have made little headway in removing it. Solutional widening of the fissure has occurred at and near the present water level.

Downstream exploration of an active stream passage often ends or pauses at a sump. Is the passage beyond completely flooded to the spring, or is there an air-filled section in between? Many "terminal" sumps are perched in the vadose zone and spill over at thresholds. This information is important not only in planning further exploration, but also in understanding the relationship between active caves and base level. According to Eq. 1, turbulent discharge through a filled conduit varies with the square root of the head difference between the sump and the spring:

$$Q = C\sqrt{h} \quad (2)$$

where C varies with passage cross section, friction, and length. C can be considered an expression of hydraulic efficiency. Internally consistent units (e.g., ft and cfs) are needed in Eq. 2 only if an evaluation of C is desired. If the discharge were to diminish to zero, the head difference would also be zero in a completely water-filled conduit (or in an air-filled passage floored with ponded water). At zero flow, a perched sump would stand above the spring at a height equal to that of the vadose threshold (z). The head

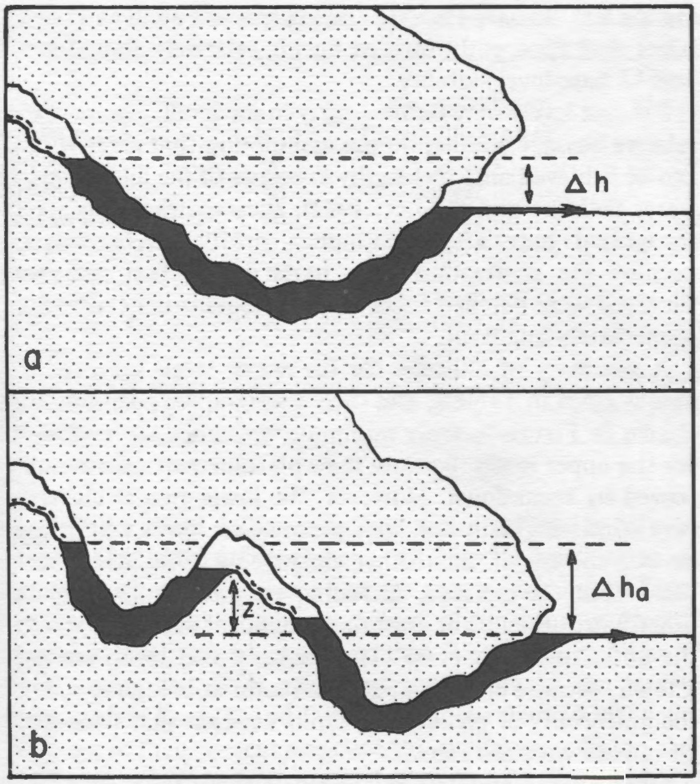

Figure 5. **Comparison between a simple phreatic loop (a) and a perched phreatic loop with a vadose threshold (b). Δh_a = apparent head loss, z = height of vadose threshold.**

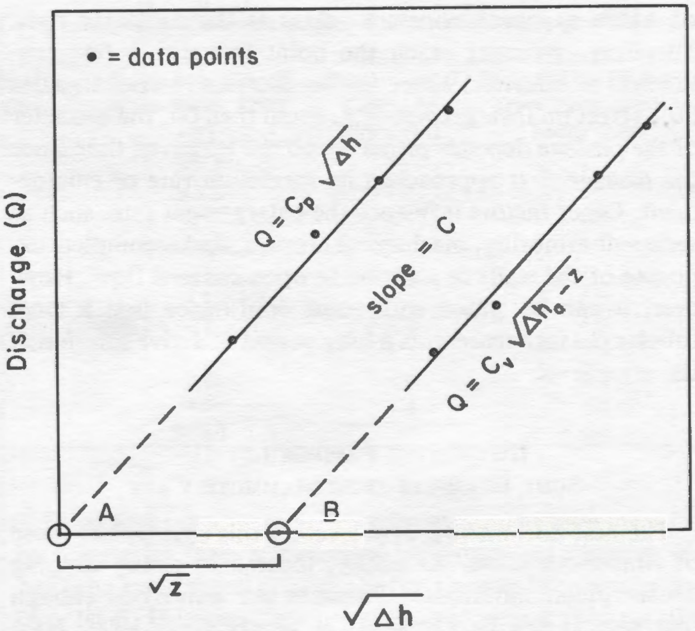

Figure 6. **Determination of the height of a vadose threshold (z). A line drawn through the data points will show the presence (intercept B) or absence (intercept A) of a vadose threshold. Height of threshold = B^2.**

difference between a perched sump and the outlet cannot be used in Eq. 1 and is labeled "apparent Δh" (Δh_a) in Figure 5.

If the discharge and head difference between the sump and spring are carefully measured at a variety of flow rates, a graph of Q vs $\sqrt{\Delta h}$ should produce a straight line (Fig. 6). The slope of the line is the efficiency (C), either of a completely phreatic section (C_p) or a perched vadose sump (C_v). Extrapolation of this line to zero discharge should give zero head if there is no vadose threshold. An intercept greater than zero indicates the presence of a vadose threshold of height z above the spring. This approach was used to verify the presence of air-filled passages beyond the downstream sump in Sotano de San Augustin in Huautla, Mexico, prior to diving expeditions (see Stone, 1983). The answer is obvious in a passage that accepts large fluctuations in discharge with little change in head; but an inefficient debris-choked passage with high discharge may require the full analysis.

Effect of Discharge on Passage Size

In general, the largest discharges occur in the largest passages, those most likely to constitute levels in a cave. Is passage size controlled by the amount of flow, or does the flow adjust to the size of the passage?

Discharge through a cave depends mainly on the amount of available recharge and on the catchment area that feeds it. However, the specific route followed by the water depends greatly on hydraulic efficiency. Early in the development of a limestone cave, when laminar flow begins to enlarge the pre-solutional openings, both the recharge rate and the efficiency are greatest in the widest fractures, provided they offer an uninterrupted network. At that stage, virtually all outflow emerges close to carbonate saturation, so the rate at which any route enlarges depends on the amount of flow rather than solution kinetics. Discharge patterns shift with time as differential enlargement changes the efficiency of flow routes (Ewers, 1982).

Regardless of the exact flow pattern, no passage can increase its enlargement rate unless it is able to increase its discharge, either by drawing water from its neighbors or by increasing its primary catchment area (Palmer, 1984). As discharge increases within a growing passage, water begins to emerge while still far from saturation. Solution kinetics begin to take control of enlargement rate. At the pH of water in a growing cave (typically 7 to 8), the solution rate depends on the reaction at the cave walls, but is almost independent of turbulence (Plummer and Wigley, 1976; White, 1977). The reaction rate is determined by carbon dioxide content, temperature, and degree of saturation, all of which approach constant values as the discharge rises. Therefore, passages reach the point (roughly a few centimeters in diameter) where further increase in discharge has little effect on their growth rate. From then on, the diameter of the passage depends primarily on the length of time since the passage first approached its maximum rate of enlargement. Other factors influence the enlargement rate, such as sediment armoring, mechanical erosion, and incomplete exposure of the walls to solution in open-channel flow. However, it can be stated with some confidence that a large tubular passage represents a long period of active solution at the same level.

Identifying Passage Levels: Some Examples from Mammoth Cave

The best-documented cave levels in this country are those of Mammoth Cave, Kentucky, located in gently dipping Mississippian limestones. Passages are numerous enough that several can be identified at nearly every level. Four main levels at altitudes of 210, 180, 168, and 152 m, plus a few minor ones, have been described in detail elsewhere (Palmer, 1981). In brief, the upper two are mainly wide canyons partly filled with detrital sediment, which are thought to correlate with slow valley deepening and aggradation during the late Tertiary Period. The lower levels are Quaternary tubes that apparently formed during relatively short intervals of base-level stability.

Passage levels were defined early in the leveling project by relative passage widths, on the assumption that great width can be achieved only by lengthy exposure of the limestone to water (Miotke and Palmer, 1972). Piezometric limits were recognized only after continuous profiles were drawn, because the upstream vadose parts of the first passages surveyed were perched tubes whose vadose origins were not immediately apparent.

A summary of altitudes for the major levels surveyed to date is given in Table 2, and their stratigraphic positions are shown in Figure 7. Only minimum estimates are available for the upper levels, because their piezometric limits are obscured by breakdown. However, the lower two levels have very consistent altitudes, with piezometric limits within one or two meters of each other throughout Flint Ridge and Mammoth Cave Ridge, including an area of 30 km². In other words they lie at essentially identical altitudes, within the limits of survey error. The former outlet levels are not known, because each passage terminates at breakdown, but the uniformity of piezometric limits suggests that the outlet elevations were the same.

Only a very static base level could account for such sharp-

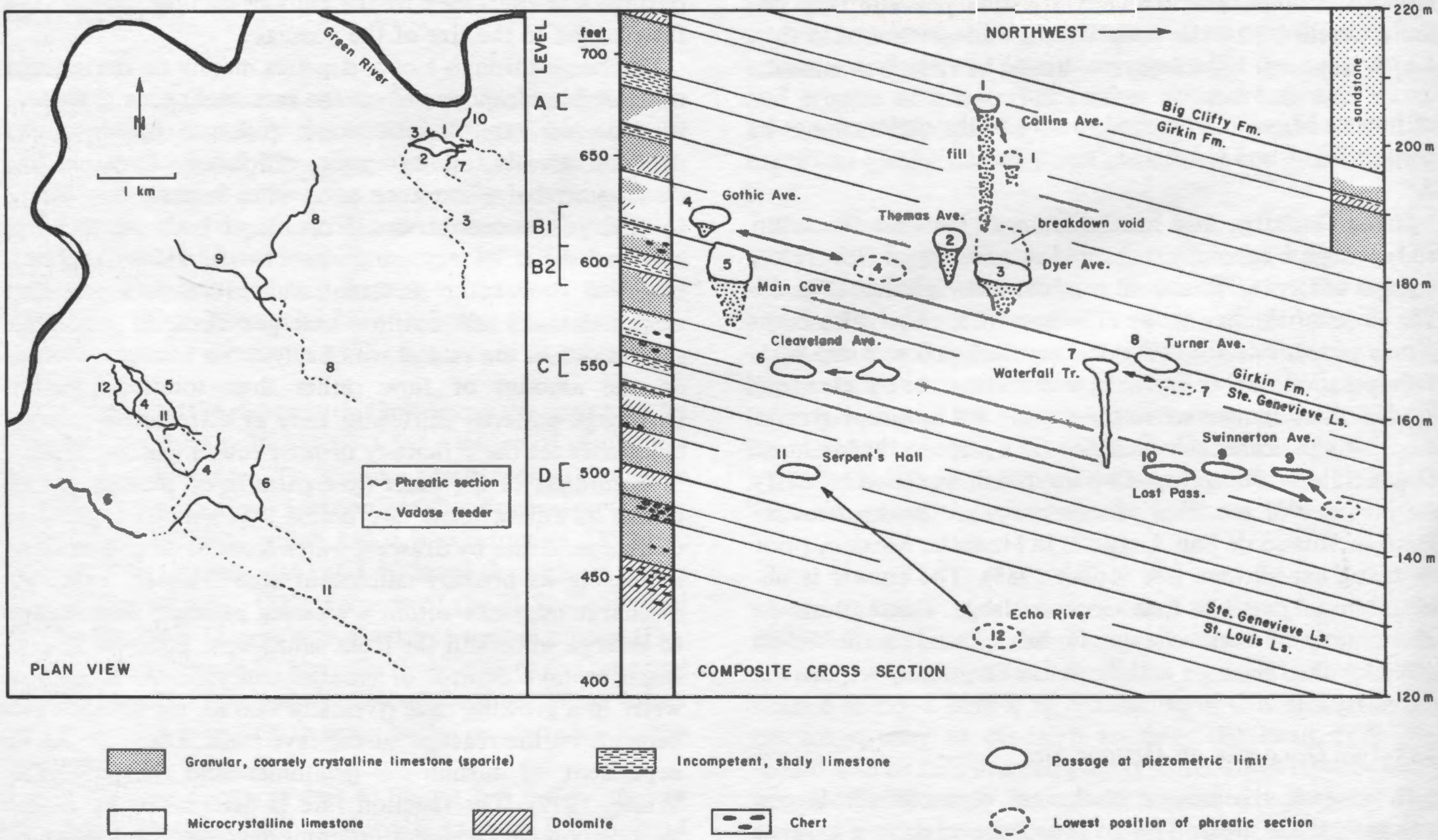

Figure 7. **Relative altitude and stratigraphic position of major levels in Mammoth Cave, KY. Interconnecting passages are omitted from map.**

Table 2. Characteristics of major passage levels surveyed to date in Mammoth Cave, Kentucky. Altitudes are subject to minor adjustment as calibration between surveys is improved.

Passage	Level	Alt. of Ceiling at Piezometric Limit (M)	Min. Altitude of Phreatic Solution (M)	Max. Ceiling Depth Below Piezo. Limit (M)	Discordance of Ceiling to Strata (M)	Straight-Line Distance From Piezo. Limit to Valley (KM)*
Collins Ave.	A	≥207.5	198.4	≥7.3	7	1
Thomas Ave.	B1	≥187	181.7	≥1.5	1.5	3
Gothic Ave.	B1	≥193	180 ±2	≥9	<1?	2.5
Upper Salts	B2	≥183	175 ±2	obscured	?	1
Main Cave	B2	186 ±2	obscured	1–3	<1?	2
Waterfall Tr.	C	168 ±0.5	164 ±0.5	2.7	<1	0.8
Cleaveland Ave.	C	169 ±0.5	166 ±0.5	<1	<1	6.5
Turner Ave.	C	167 ±1	165 ±1	1–2	<1	1.5
Lost Passage	D	152 ±0.5	149 ±0.5	0.6	<1	0.4
Swinnerton Ave.	D	153 ±1	147 ±1	4.0	6	3.2
Echo River	D	153 ±1	128 ±1	21 ±1	19	≥1

*Extrapolated along trend of phreatic section.

ly defined levels. Needless to say, this condition is rare. A simple slowing of entrenchment or a reversal from entrenchment to aggradation would blur the piezometric limits. Most levels are not so clearly developed. By measuring present water chemistry and assuming that it is representative of past conditions, it is estimated that some of the largest passages on levels C and D required more than 50,000 years to grow to their present size once the maximum solution rate had been approximately reached (Palmer, 1984). Probably it took at least that long for the passage to evolve from the slow initial solution to the approximate maximum rate.

Each passage within a given level is located in different beds, which encompass a great variety of rock types, so the levels are apparently not stratigraphically controlled. Some phreatic passages are located at the tops of relatively insoluble beds: Collins Avenue, Waterfall Trail, Turner Avenue, and parts of the Echo River system. Although the vadose sections may have been perched on these beds, the phreatic sections only appear to be so. In the prominently bedded limestones of the region, passages tend to complete the vadose-phreatic transition without changing stratigraphic horizon. Downstream from their piezometric limits Collins Avenue and Echo River cut discordantly across the beds, showing that the phreatic sections are not perched.

The major passages show little discordance to the bedding over their surveyed lengths (Table 2). However, even those with less than a meter of discordance have slightly undulant profiles because their sinuosity contains up-dip and down-dip components along single stratigraphic horizons (e.g., Waterfall Trail) or because they follow irregularly dipping beds that originally conducted flow to varied depths below the water table (e.g., Gothic Avenue). Other passages show abrupt local jumps from one bed to another that interrupt long concordant sections. In Swinnerton Avenue the stratigraphic discordance is even greater than the vertical solutional relief, owing to stratal dip, a situation more clearly displayed in structurally deformed regions.

Echo River is a large active tube at present base level fed by tributaries from a variety of elevations. In the past this has been interpreted as evidence for a major late-Pleistocene cave level. However, when traced upstream it changes to a dip-oriented canyon at level D, 23 m higher. This is an example of how the lower parts of a phreatic loop can remain active long after its contemporary passages were abandoned, and it serves as a reminder not to define levels simply from the elevation of large tubes.

No evidence has been found in Mammoth Cave for base-level control at elevations between the levels described above. Although the wide Tertiary canyons appear to have kept pace with valley deepening, levels C and D represent the only times that downward cave development was able to overtake the more rapid entrenchment during the early and middle Pleistocene. Valley deepening during the Pleistocene probably took place by headward erosion, with rapids migrating upstream, so that at any fixed point the drops in river level were rather sudden from the standpoint of cave development. The few scattered levels observed below level D may indicate diminishing rates of entrenchment or more frequent fluctuations in river level.

The clarity and narrow vertical range of levels C and D in Mammoth Cave are remarkable, especially in view of the great fluctuations now seen in the Green River. According to data of the U.S. Geological Survey the mean-annual flood level of the Green River is about 9 m. Surface runoff may be flashier today than during most of the geologic past because of deforestation and agriculture, but it is doubtful that the river ever maintained an elevation as uniform as the cave levels. The conclusion can only be that well-defined cave levels develop in adjustment with base-flow conditions.

Passage Orientation and Depth

The change from dip orientation to a direction nearly parallel to the local strike at the piezometric limit has been documented so frequently (e.g., A. N. Palmer, 1972, 1981;

Kastning, 1975; M. V. Palmer, 1976; Mylroie, 1977) that it is sometimes erroneously considered a hard and fast rule. However, others offer evidence that phreatic passages, at least initially, favor the dip (e.g., Ford and Ewers, 1978). However, there is enough variety in passage profiles, even in the nearly undisturbed low-dip setting of Mammoth Cave, to dispel any thought that phreatic passages must have a consistent structural relationship. Nevertheless, certain patterns tend to dominate within certain geologic settings.

It might seem that water in the phreatic zone should follow the steepest and most direct route to the nearest outlet. However, the true flow direction is determined much more by variations in passage width or diameter. In laminar flow, during the early stages of cave development, the discharge along a given fracture depends on the third power of the fracture width, but only the first power of the hydraulic gradient (Palmer, 1984). The paths of greatest flow are those with the widest effective fracture widths throughout their length. These are the ones that enlarge into caves. Phreatic flow can afford to sacrifice considerable directness to achieve even a slight gain in fracture width, which explains the seemingly devious routes of some phreatic passages.

Fractures diminish in number and width downward, so it is usually more efficient for phreatic water in bedrock to follow shallow paths, rather than deep, looping ones. Deep passages occur mainly where faulting or folding disrupts the tendency for the shallow fractures to be widest, as shown by caves in the Sierra de El Abra of Mexico (Fish, 1978), or where water follows relatively soluble beds at depth (Ash, 1984). These include the "bathyphreatic" caves of Ford and Ewers (1978). Ford (1971) considers the depth of phreatic loops to decrease with the frequency of fissures (i.e., fractures and partings), which correlates roughly with average fracture width. Fissure frequency and width should increase with time of exposure above base level; however, the depth of phreatic loops shown in Table 2 does not decrease systematically with time. The relatively deep phreatic loops in the Echo River system may have been influenced by relatively rapid valley entrenchment, which would not allow much time for fracture widening.

Where bedding is prominent or the limestone is partitioned by insoluble beds, water tends to follow the same stratigraphic horizon in the phreatic zone that it did immediately upstream in the vadose section. However, in most situations this horizon extends beneath the local river level in the down-dip direction and may not crop out in that direction for many tens of kilometers. Upward flow across the strata is not favored in such rocks, so the most efficient flow remains shallow, along the widest openings, emerging where the controlling horizon crops out more or less along the strike. Of the two possible strike directions available to the incoming vadose flow, groundwater normally follows the shorter distance to the entrenched river. Where the dip is away from the valley, as at Onesquethaw Cave, New York (Palmer, 1972), phreatic water is forced to follow a non-dip direction (usually along the strike) to the valley.

The prominent bedding of the Mammoth Cave area is responsible for its many strike-oriented tubes. For example, the water in Cleaveland Avenue followed the strike for a straight-line distance of more than 6 km. By flowing upward across the strata it could have reached the river in little more than half that distance. However, some discordant passages follow a trend far from that of the strike, although not at all parallel to the dip. Even in such deformed areas as the Appalachian Mountains, prominent bedding and interbedded insoluble rocks cause strike passages to be very common (Davies, 1960). Deviation from the strike is greatest in massive, uniform, highly deformed rocks, as in many alpine karst areas. This is especially true where the limestones are better exposed in the dip direction than in either of the strike directions, as in the central Mendips of England (Ford, 1965).

Regional Correlation

Perhaps the ultimate goal in the study of cave levels is to correlate them on a regional scale (e.g., Powell, 1970; Miotke and Palmer, 1972; White and White, 1974; Wilson, 1985). However, correlation of caves with the nearby land surface is usually not as rewarding as expected. Precise indicators of past base level at the surface are quickly destroyed by mass wasting and erosion, so usually only the most recent erosional benches and alluvial terraces are clearly defined. Bedrock benches tend to be irregular and influenced by stratigraphy.

Cave levels can usually provide a great deal of information about the local erosional and depositional history. However, a regional interpretation of that history can only be accomplished with the aid of surface data. On a topographic map or from an overland survey, breaks in slope can be identified in the walls of almost any large valley. Whether these represent terraces correlative with cave levels is usually debatable. More information is needed to verify the presence of a former floodplain, such as the distribution of sediment types (e.g., Miotke and Palmer, 1972).

The following example shows some of the goals as well as some of the problems of regional correlation of cave levels.

Quaternary glaciation caused major changes in drainage patterns in the east-central United States. One of the greatest was the channeling of water from northern routes into the Ohio River, at least doubling its drainage area, leaving the northerly routes almost completely buried by glacial till (Thornbury, 1965). The rate of valley entrenchment of the Ohio and its tributaries increased markedly, accounting for the change in passage character between the upper and lower levels of Mammoth Cave described earlier.

Every major passage above 180 m in the Mammoth Cave area contains thick detrital sediment, except where it has subsided into lower passages or been removed by streams. In places the sediment fills passages to the ceiling. It consists mainly of interbedded sand and gravel up to 25 m thick capped with silt and clay. Cut-and-fill structures in the sediment indicate that at least some of this material was deposited by open-channel flow (James Currens, Lexington, Kentucky, personal communication, 1982). The passages are canyons and tubes as much as 30 m wide and high, each of which is among the largest in the cave. Most of them (level B in Table 2 and Fig. 7) lie at essentially the same altitude as the rather flat Pennyroyal Plateau surface and apparently formed contemporaneously with it in the late Tertiary or early Quaternary.

Levels A, B1, and B2 show various stages of passage development alternating with sediment filling. The unusually great passage widths and the episodic nature of the sediment fill in the upper levels of Mammoth Cave indicate slow fluvial entrenchment alternating with aggradation, with base-level changes of 20–30 m. Climatic changes were probably responsible, causing alternate entrenchment and aggradation either by variations in runoff or by worldwide sea-level changes. There is some evidence for the latter idea, because the widespread Quaternary glaciation was preceded by periodic glaciation at high latitudes as early as Miocene (about 30 million years B. P.), spanning the time in which the Pennyroyal surface and upper-level cave passages formed.

A possible correlative of the cave sediment is an overburden of more than 20 meters in parts of the Pennyroyal Plateau and its northern extension into Indiana, the Mitchell Plain. It has often been regarded as weathering residuum, but close inspection shows it to consist also of river, lake, and colluvial deposits (Powell, 1964). Although local areas of the Pennyroyal surface are influenced by differential resistance of strata (Howard, 1968; Quinlan, 1970; Woodson, 1981), the uniformity and distinctive character of the upper levels of Mammoth Cave suggests that the overall control of the surface was a slowly fluctuating base level. This is an example of how cave information can give clues about regional history.

These levels can be extrapolated to other areas. However, only a few caves in the region have detailed vertical surveys, and the caves are confined to such a narrow vertical range that correlating by elevations alone is troublesome. A tentative correlation of Mammoth Cave with Wyandotte and Blue Spring Caves in Indiana is given here only to show the potential and some of the problems of the regional approach.

The vertical layout of the caves is shown in Figure 8, along with pertinent surface data. The Wyandotte levels are those of Powell (1968). The low-relief Pennyroyal / Mitchell Plain surface provides a continuous geomorphic datum and is shown here at the contact between the Ste. Genevieve and St. Louis Limestones to minimize the effect of stratigraphic variation. Its surface elevation is lowest in the vicinity of major rivers, as expected, but higher at the Ohio River than at the Green River or East Fork of White River. The short, pre-glacial upstream reach of the Ohio was apparently higher and geomorphically less significant than some of its downstream tributaries. However, glacial diversion of northerly streams into the Ohio increased its rate of deepening, and now its channel is lowest of any in the region.

The contact between the top of the cavernous limestone and the overlying insoluble rocks is lower in Indiana than in Kentucky, so the prominent upper levels correlative with the Pennyroyal at Mammoth Cave are poorly developed in the northern caves. The largest passages in the Indiana caves are roughly contemporaneous with the two lowest levels in Mammoth, although it is not certain that their piezometric limits correlate exactly. The lowest in each cave matches the elevation of terraces in nearby valleys. Higher-level terraces must have existed at one time, but valley widening has left only ambiguous traces. The upper level of Wyandotte Cave is a large keyhole-shaped passage partly filled with thick sediment, similar in character to levels A or B in Mammoth, but it is lower than the nearby Mitchell Plain. The lower level of Wyandotte lies below any of the major levels in Mammoth or Blue Spring. Levels in Blue Spring are less clear than those in the other caves because it lies directly beneath the Mitchell Plain and is subject to intense flooding from overlying sinkholes and sinking streams.

Solid conclusions cannot be drawn from such scanty data, so the following is offered only as a guide to future studies. The upper levels of the Indiana caves may correlate with level C in Mammoth, as all three lie at virtually identical altitudes. Those at Mammoth and Blue Spring lie about 15–25 m below the Pennyroyal / Mitchell Plain surface, but the one at Wyandotte is about 30–40 m below it. Either the base level at Wyandotte had less relationship to that of the Mitchell Plain than at the other caves, or the Ohio and its nearby tributaries had already begun their rapid entrenchment when this level formed. It is not clear why the sediment fill in this passage should resemble that of the higher (or older?) levels in Mammoth.

By the time the lowest level formed, valley deepening had apparently progressed farther at Wyandotte than elsewhere. The Wyandotte level is not only 5–15 m lower than those of the other caves, but the vertical separation between it and

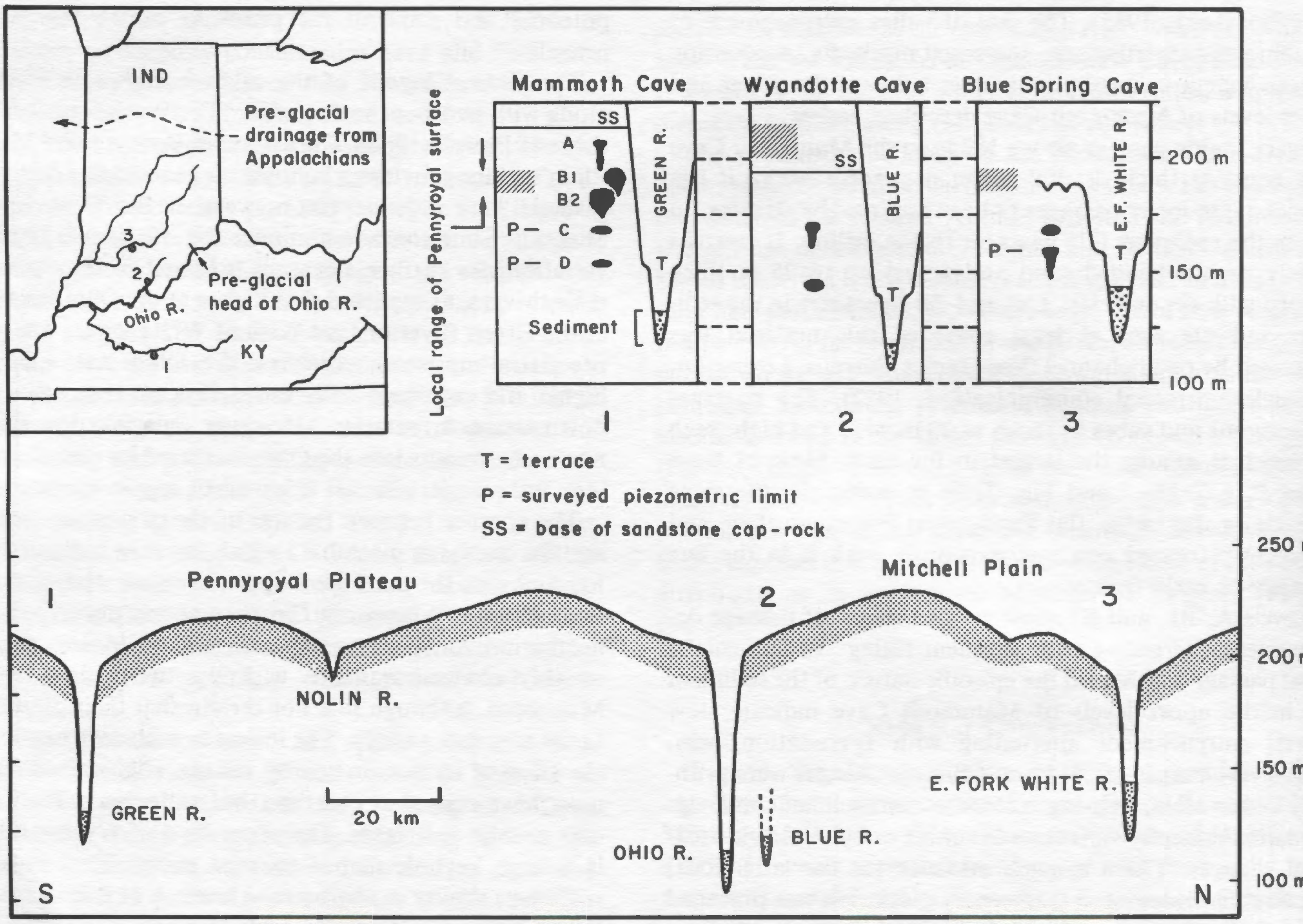

***Figure 8.* Tentative correlation of levels between Mammoth, Wyandotte, and Blue Spring Caves, and their relationship to surface features. The Pennyroyal / Mitchell Plain erosion surface is drawn below at the Ste. Genevieve / St. Louis contact, with depth of Quaternary entrenchment and alluviation shown.**

the overlying level is greatest. Alluvial valley fill is thickest at Blue Spring, probably because of greater proximity to isostatic effects and outwash from continental glaciers, and the separation between levels is less. In this way, cave levels may indicate differential rates of valley deepening and therefore clarify the regional drainage history.

It is humbling to see months of field work reduced to a few dots on a cross section, especially because such simplified data will always appear to correlate even if there is no true relationship. For more convincing results the caves should be closely spaced and their deposits dated, for example by paleontology (Droppa, 1966), radiometric methods (Harmon and others, 1975) and paleomagnetism (Schmidt, 1982).

Processes That Obscure Cave Levels

Cave levels are indistinct where hydrologic conditions do not favor low-gradient passages or the preservation of piezometric limits. The major disruptive factors are outlined below.

Floodwater Recharge

Figures 3 and 4 show that passages fed by large recharge areas can be subject to severe flooding to heights considerably above base level. They do not have the sharply defined transition from vadose to phreatic that is seen in passages with limited recharge, such as McFail's Cave and Mammoth Cave. For example, Hölloch, in Switzerland, is fed by a large plateau of bare karst in which rain and snowmelt are transmitted underground so rapidly that water levels often rise more than 100 m. Even though several levels have been identified in the cave (Bögli, 1968), exact piezometric limits cannot be determined. It can also be difficult to interpret the origin of individual passages in caves fed by sinking streams, such as Friar's Hole Cave in West Virginia, where floodwater solution obscures many of the vadose features (Worthington, 1984).

Paragenesis

Downward phreatic loops tend to accumulate insoluble sediment transported by cave streams, especially during floods. Where the floor and lower walls of a passage are shielded by sediment, bedrock solution is concentrated upward in a process known as paragenesis (Renault, 1967). As the passage grows, more sediment is deposited, so the flow velocity is kept roughly at the threshold for sediment transport. In extreme cases a high canyon may be produced entirely in the phreatic zone, with upward solution terminating only at the water table (Ford and Ewers, 1978).

Paragenetic canyons can easily be mistaken for vadose canyons that have been filled by later aggradation. The upper levels of Mammoth Cave provide a good case study, as they are canyons and tubes partly or completely filled with stratified sand and gravel as much as 25 m deep. If they are paragenetic, the idea that they formed during slow fluvial entrenchment alternating with periods of aggradation is entirely wrong.

The following criteria were used to support vadose entrenchment and aggradation in Mammoth Cave: (1) many passages are filled to the ceiling with sediment; (2) cut-and-fill structures and sinuous channels in the sediment suggest open-channel flow; (3) the ceilings of all but Collins Avenue are exactly concordant with the strata, implying a vadose origin; (4) breakdown blocks, identified stratigraphically, have been found in the sediment as much as 7 m below their point of origin, indicating rather large minimum passage heights at the time of breakdown; (5) some sediment-filled passages on level B1 are wide tubes rather than canyons. In some passages, particularly Collins Avenue, the evidence is inconclusive. A valid criterion for paragenesis is the upward propagation of meanders in the downstream direction, rather than downward as in an entrenching canyon (Ewers, 1985), but exposures were not sufficient to make this distinction. Finally, it seems unlikely that *all* passages on levels A and B should contain thick fill without some regional significance; and it is doubtful that each one should originate deep within the phreatic zone, which would require an amount of discordance to the strata that is rare in the nearly flat, well-bedded limestone. Similar criteria can be used in other caves to distinguish whether paragenesis has affected passage elevations.

Deep-Seated Cave Origin

Some caves are not formed by water descending from the nearby land surface, but by rising fluids or by local aggressiveness in zones of mixing between waters of different chemistry. Passage levels formed in this way represent conditions somewhat different from those described previously.

Rising water often contains hydrogen sulfide, which usually forms sulfuric acid where it oxidizes at the water table or comes in contact with water from a shallow source. Gaseous hydrogen sulfide can also rise on its own, even without upward water flow, producing a similar result. Levels in such caves can be fairly distinct if the oxidation is concentrated at the water table. Caves of the Guadalupe Mountains are good examples (Egemeier, 1981; Davis, 1980; Hill, 1981), many of which contain distinct levels (Fig. 9). Identification of levels must rely mainly on clustering of large passages and rooms at similar elevations (e.g., Jagnow, 1979), as there are no vadose feeder passages to create piezometric limits.

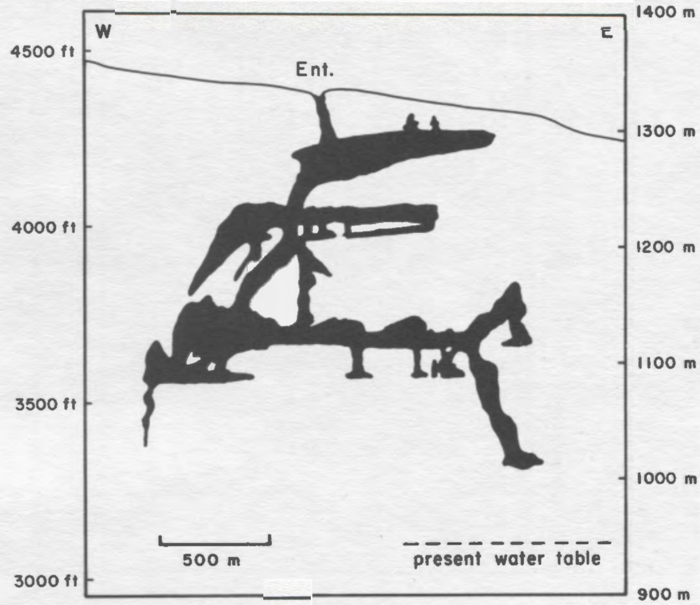

Figure 9. **Levels in Carlsbad Caverns, formed by local production of sulfuric acid at past positions of the water table (modified from Jagnow, 1979).**

The presence of rising water or gas is commonly episodic and short-lived by geologic standards. The resulting cave levels may not represent static base level, but only the contemporary position of the water table during an episode of rising hydrogen sulfide. It is necessary to compare them with fluvial landforms to see whether they relate to tectonic or geomorphic events.

Local aggressiveness can be produced by the mixing of two carbonate-saturated waters having different concentrations of carbon dioxide, hydrogen sulfide, or salinity. This process was first applied to cave development by Bögli (1964). Cave levels are known to form in porous limestones along the seacoast, such as Bermuda and the Yucatan Peninsula, where saturated, high-CO_2, low-salinity water mixes with brackish water of low CO_2 at sea level (Fig. 10). Aggressiveness increases with increasing CO_2 and decreasing salinity, which in turn correlates with infiltration rate

Figure 10. **Shark Hole, Bermuda, formed in poorly consolidated Quaternary limestone at the zone of mixing between fresh and saline water. Scattered openings are located at and near present sea level, with a concentration 5 m higher, representing a former sea-level stand, but most Bermuda caves are formed by collapse into lower openings.**

(Plummer, 1975; Palmer and others, 1977; Back and others, 1984). Levels in such caves can be used to interpret past stands of sea level or of vertical tectonic movements.

STRATIGRAPHIC PERCHING

Tubular passages can form in the vadose zone where water is perched on relatively insoluble or resistant beds. They may resemble tubes formed in the phreatic zone, except for their consistent downward slope. The resistance of the underlying bed is also a clue to vadose perching, but, as seen earlier, this is common in phreatic tubes as well. Most perching is caused by chert, shale, shaly or sandy limestone beds, or dolomite. In any study of cave levels, the possibility of stratigraphic perching must be confronted.

Waterfall Trail in Mammoth Cave is a particularly good example of perching of aggressive vadose water on rock that superficially seems to offer little resistance to solution or erosion. This passage consists of a down-dip vadose tube that changes to a phreatic tube at 168 m altitude. Vadose entrenchment and diversion have taken place throughout the phreatic section, leaving it dry (Fig. 11). However, most of the vadose section still contains the original stream (Fig. 12), which now lies 38 m above present base level. Paleomagnetic data from sediment in other passages at this level indicate an age of more than 700,000 years (Schmidt, 1982). Although the vadose tube has been active that entire time, it averages only a meter in height. Its stream is perched at the top of the Aux Vases Member of the Ste. Genevieve Limestone, which is dolomitic and is 15–30% silt and clay. The bedrock weathers to a punky dolomitic mud with an insoluble content as high as 75%. It is highly resistant to solution but offers little resistance to erosion. The stream has a modest gradient of 9 m / km (about half a degree) and does not carry much sediment load, so mechanical erosion is limited. The

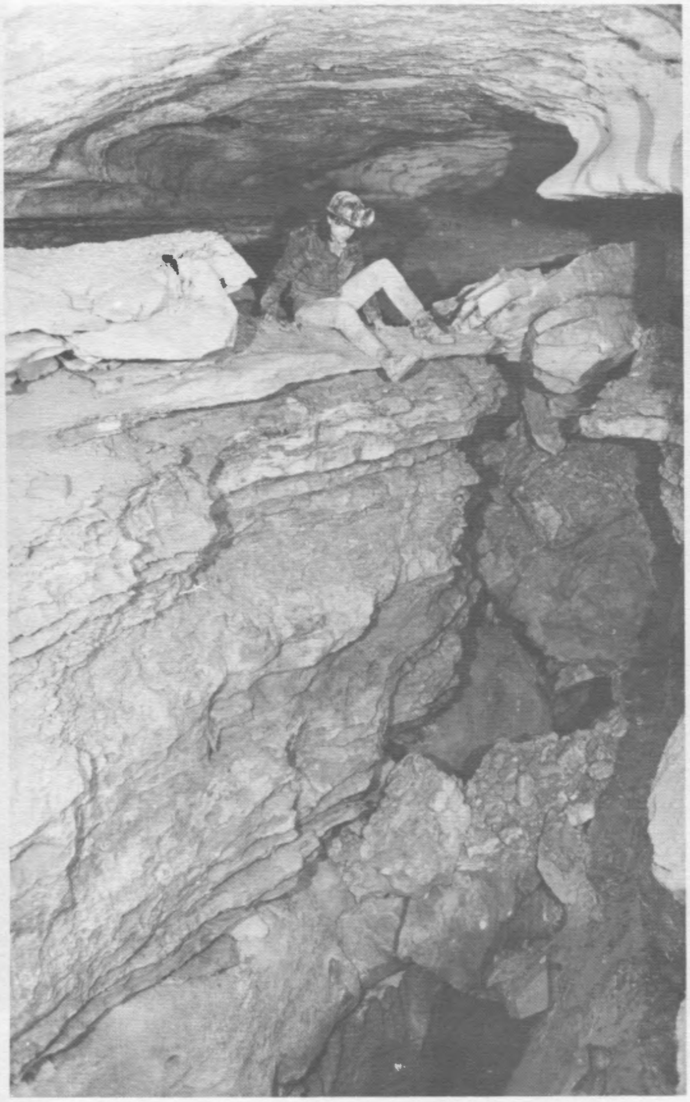

Figure 11. **Downstream section of Waterfall Trail, Mammoth Cave, KY, a phreatic tube with later vadose entrenchment. The top of the structurally incompetent but solutionally resistant Aux Vases Member (Ste. Genevieve Limestone), on which the upstream section is perched, lies at the person's right foot.**

Figure 12. **Upstream section of Waterfall Trail, with water still perched on the shaly, dolomitic Aux Vases Member after several hundred thousand years.**

stream is fed by recharge from a karst valley and runs through more than 2 km of passages before it cuts downward through the dolomite. Even at that point the water is highly aggressive year round, with mean saturation indices of -1.15 for calcite and -1.7 for dolomite, lower than in any other stream yet measured in the cave.

The main passage of the Silvertip Cave System of Montana is an example of a perched vadose tube modified by periodic flooding. The passage is located along the axis of a broad syncline having virtually no plunge. It is floored by insoluble shale of the Maywood Formation and emerges at a

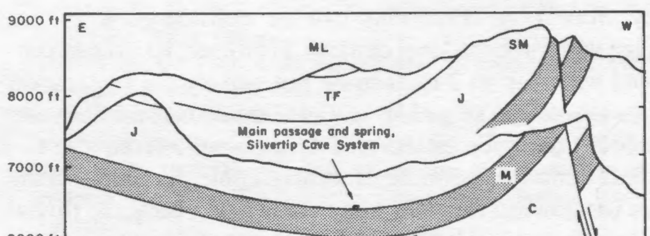

Figure 13. **Structural cross section showing the perched main passage of the Silvertip Cave System, Montana. SM = Silvertip Mt., ML = Mississippian limestone, TF = Devonian Three Forks Fm., J = Devonian Jefferson Ls., M = Devonian Maywood Fm. (mainly shale), C = Cambrian formations.**

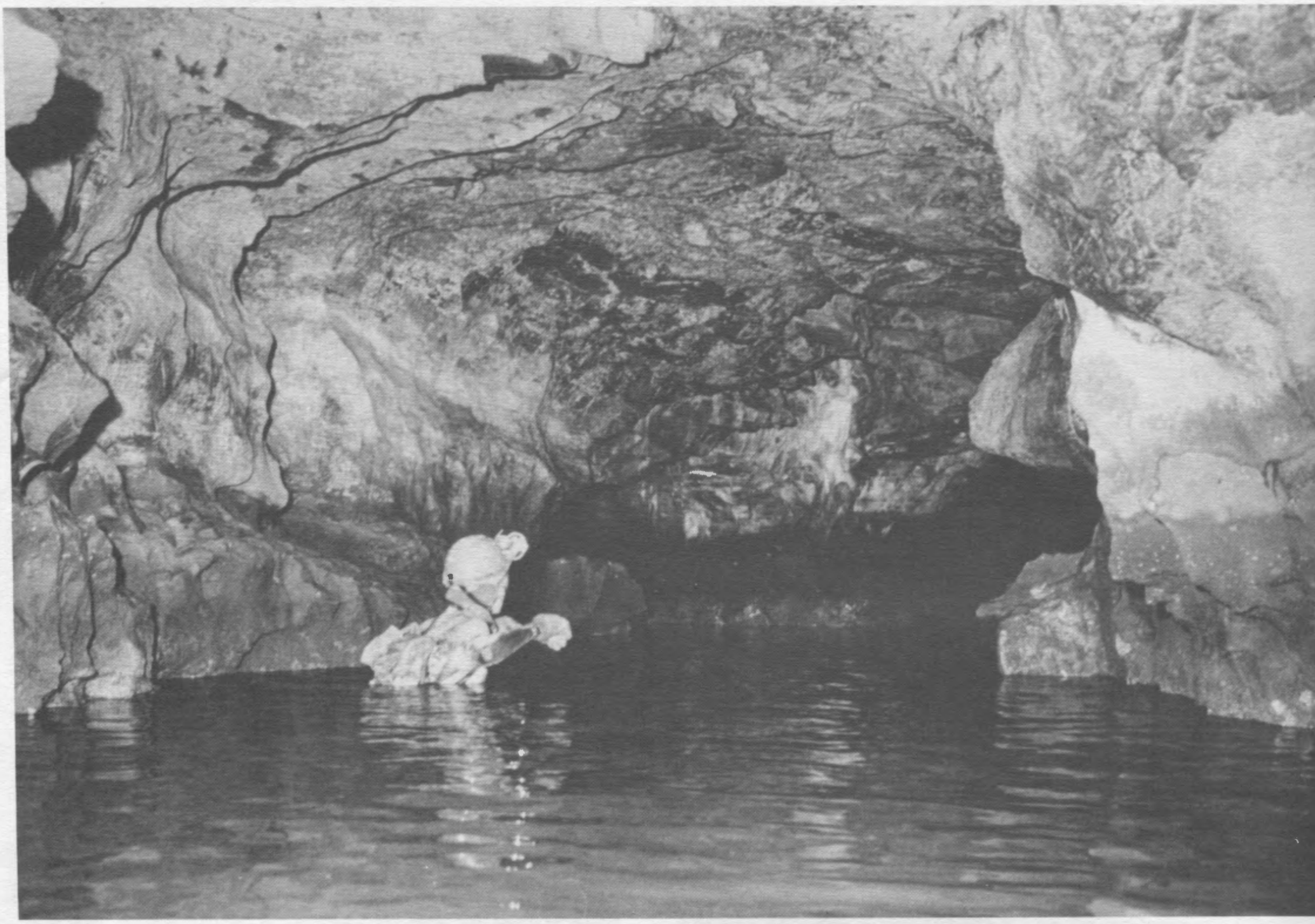

Figure 14. **Although the main passage of the Silvertip Cave System appears to be a phreatic tube, it is actually perched on shale. Upward enlargement has been caused by floodwaters ponded by breakdown.**

perched breakdown-choked spring 200 m above the main valley floor (Fig. 13). This can be considered a vadose passage with no base-level control. However, its arched ceiling and water up to 2 m deep do not convey the impression of a vadose origin (Fig. 14). Without the structural data this tube could easily be interpreted as a phreatic level.

A less common example of stratigraphic perching occurs where the downstream end of a cave is held above the fluvial base level by an insoluble bed dipping away from the valley. The water table may represent the top of the true phreatic zone and yet be held at an unusually high elevation by the low-permeability barrier. Cave levels adjusted to the water table can contain phreatic loops and well-defined piezometric limits but still have no relationship to base level. This is apparently the case in some karst areas along the Allegheny Escarpment. For example, cave streams flowing into the Cloverlick Valley in West Virginia are graded toward points where impure limestone beds crop out in the valley walls (Werner, 1973).

CONCLUSIONS

Even under the closest scrutiny the concept of base-level control of cave levels has passed every test so far devised. In the clearest examples, base level indeed seems to have remained static for long time periods interrupted by episodes of downcutting. A well-defined piezometric limit lies very close to the former outlet level, and measurement of one should give a close approximation of the other. Most levels appear to have developed under less favorable conditions, such as unstable river levels and floodwater recharge, but they do not invalidate the basic concept. Stratigraphic perching is easily accounted for by conducting precise vertical surveys that relate passage profiles and orientations to the local geologic structure. With no reason to test the hypothesis of base-level control any further, future studies should concentrate on regional correlation and on interpreting the history of base-level changes, past climates, erosion and deposition, and paleohydrology.

REFERENCES

Ash, D. W. 1984. Evidence for deep-seated groundwater movement in Middle Mississippian carbonate lithologies of south-central Indiana [abs]: Proc. Natl. Speleol. Soc. ann. conv., Sheridan, Wyoming, p. 28.

Back, W., Hanshaw, B. B., and Van Driel, J. N. 1984. Role of groundwater in shaping the eastern coastline of the Yucatan Peninsula, Mexico *in* LaFleur, R. G., ed., Groundwater as a geomorphic agent: Boston, Allen and Unwin, 281–293.

Bögli, A. 1964. Mischungskorrosion, ein Beitrag zum Verkarstungsproblem: Erdkunde; 18(2):83–92.

________ 1968. Höhlenniveaus und Höllochniveaus: Proc. 4th Internatl. Congr. Speleol., Ljubljana, 23–27.

Davies, W. E. 1960. Origin of caves in folded limestone: Natl. Speleol. Soc. Bull. 22(1):5–18.

Davis, D. G. 1980. Cave development in the Guadalupe Mountains, a critical review of recent hypotheses: Natl. Speleol. Soc. Bull. 42(3):42–48.

Droppa, A. 1966. Untersuchungen der Parallelität von Flussterrassen mit horizontalen Höhlen: Proc. 3rd Internatl. Congr. Speleol., Vienna, 5:79–81.

Egemeier, S. J. 1981. Cavern development by thermal waters: Natl. Speleol. Soc. Bull. 43(2):31–51.

Ek, C. 1961. Conduits souterrains en relation avec les terrasses fluviales: Annales Soc. Géol. de Belgique, v. 84, 28 p.

Ewers, R. O. 1982. Cavern development in the dimensions of length and breadth: Ph.D. thesis, McMaster Univ., 398 p.

________ 1985. Patterns of cavern development along the Cumberland Escarpment *in* Dougherty, P. H., Caves and karst of Kentucky: Ky. Geol. Survey, Special Publ. 12, Ser. 11, 63–77.

Fish, J. E. 1978. Karst hydrology of the Sierra de El Abra, Mexico: Ph.D. thesis, McMaster Univ., 620 p.

Ford, D. C. 1965. The origin of limestone caverns: a model from the central Mendip Hills, England: Natl. Speleol. Soc. Bull. 22(1):109–132.

________ 1971. Geologic structure and a new explanation of limestone cavern genesis: Trans. Cave Res. Group Gt. Britain, 13(2):81–94.

________, and Ewers, R. O. 1978. The development of limestone cave systems in the dimensions of length and depth: Canadian Jour. Earth Sci., 15:1783–1798.

Gardner, J. H. 1935. Origin and development of limestone caverns: Geol. Soc. America Bull. 46(8):1255–1274.

Harmon, R. S., Thompson, P., Schwarcz, H. P., and Ford, D. C. 1975. Uranium-series dating of speleothems: Natl. Speleol. Soc. Bull. 37(2):21–33.

Howard, A. D. 1968. Stratigraphic and structural controls on landform development in the central Kentucky karst: Natl. Speleol. Soc. Bull., 30(4):95–114.

Jagnow, D. H. 1979. Cavern development in the Guadalupe Mountains: Columbus, Ohio, Cave Research Foundation, 55 p.

Kastning, E. H. 1975. Cavern development in the Helderberg Plateau, east-central New York: M. A. thesis, Univ. of Conn., 194 p.

Miotke, F.-D., and Palmer, A. N. 1972. Genetic relationship between caves and landforms in the Mammoth Cave National Park area: Wurtzburg, Böhler Verlag, 69 p.

Mylroie, J. E. 1977. Speleogenesis and karst geomorphology of the Helderberg Plateau, Schoharie County, New York: Ph.D. thesis, Rensselaer Polytechnic Inst., 336 p.

Palmer, A. N. 1972. Dynamics of a sinking stream system, Onesquethaw Cave, N.Y.: Natl. Speleol. Soc. Bull. 34(3):89–110.

________ 1974. Geologic influence upon cave-passage orientation in Ludington Cave, Greenbrier County, West Virginia: Proc. 4th Conf. on Karst Geol. and Hydrogeol., W. Va. Geol. and Econ. Survey, 33–40.

________ 1981. A geological guide to Mammoth Cave National Park: Teaneck, N.J., Zephyrus Press, 210 p.

________ 1984. Geomorphic interpretation of karst features *in* LaFleur, R. G., ed., Groundwater as a geomorphic agent: Boston, Allen and Unwin, 173–209.

________, Palmer, M. V., and Queen, J. M. 1977. Geology and origin of the caves of Bermuda: Proc. 7th Int. Congr. Speleol., Sheffield, England, 336–339.

Palmer, M. V. 1976. Groundwater flow paths in limestone solution conduits: M. A. thesis, State Univ. of N.Y., Oneonta, 150 p.

Plummer, L. N. 1975. Mixing of seawater with calcium carbonate groundwater: quantitative studies in the geological sciences: Geol. Soc. Amer. Memoir 142:219–236.

________, and Wigley, T. M. L. 1976. The dissolution of calcite in CO_2-saturated solutions at 25° C and 1 atmosphere total pressure: Geochim. et Cosmochim. Acta, 40:191–202.

Powell, R. L. 1964. Origin of the Mitchell Plain in south-central Indiana: Indiana Acad. Sci. Proc., 73:177–182.

________ 1968. The geology and geomorphology of Wyandotte Cave: Proc. Indiana Acad. Sci., 77:236–244.

________ 1970. Base-level, lithologic, and climatic controls of karst groundwater zones in south-central Indiana: Proc. Indiana Acad. Sci., 79:281–291.

________ 1976. Some geomorphic and hydrologic implications of jointing in carbonate strata of Mississippian age in south-central Indiana: Ph.D. thesis, Purdue Univ., 169 p.

Quinlan, J. F. 1970. Central Kentucky karst, *in* Actes de la Réunion Internationale karstologie en Languedoc-Province, Mediterranée, Etudes et Traveaux, 7:235–253.

Renault, P. 1967. Le problème de las spéléogenèse: Annales de Spéléol., 22:5–21, 179–216.

Schmidt, V. A. 1982. Magnetostratigraphy of sediments in Mammoth Cave, Kentucky: Science, 217:827–829.

Stone, B. 1983. A breakthrough at the Huautla resurgence: Natl. Speleol. Soc. News, 41(6):169–180.

Sweeting, M. M. 1950. Erosion cycles and limestone caverns in the Ingleborough District of Yorkshire: Geogr. Jour., 124:63–78.

Swinnerton, A. C. 1932. Origin of limestone caverns: Geol. Soc. Amer. Bull. 43:662–693.

Thornbury, W. D. 1965. Regional Geomorphology of the United States: New York, Wiley, 609 p.

Waltham, A. C. 1970. Cave development in limestone of the Ingleborough District: Geog. Jour., 136:19–46.

Werner, E. 1973. Control of vertical position of cave levels by perched groundwater bodies [abs.]: Natl. Speleol. Soc. Bull. 35(1):26–27.

White, W. B. 1960. Terminations of passages in Appalachian caves as evidence for a shallow phreatic origin: Natl. Speleol. Soc. Bull. 22(1):43–53.

________ 1977. Role of solution kinetics in the development of karst aquifers *in* Tolson, J. S., and Doyle, F. L., eds., Karst Hydrogeology: Huntsville, Ala., Univ. of Alabama Press, 503–517.

________, and White, E. L. 1974. Base-level control of underground drainage in the Potomac River basin: Proc. 4th Conf. on Karst Geol. and Hydrogeol. W. Va. Geol. and Econ. Survey, 41–53.

Wilson, W. L. 1985. Evolution of groundwater flow paths in the Garrison Chapel karst valley, Indiana [abs.]: Program for 1985 Natl. Speleol. Soc. ann. conv., Frankfort, Ky., 45–46.

Wolfe, T. E. 1964. Cavern development in the Greenbrier Series, West Virginia: Natl. Speleol. Soc. Bull. 26(2):37–60.
Woodson, F. J. 1981. Lithologic and structural controls on karst landforms of the Mitchell Plain, Indiana, and Pennyroyal Plateau, Kentucky: M.A. thesis, Indiana State Univ., 132 p.
Worthington, S. R. H. 1984. The paleodrainage of an Appalachian fluviokarst: Friar's Hole, West Virginia: M.S. thesis, McMaster Univ., 216 p.

FIELD EVIDENCE OF THE MINIMUM TIME FOR SPELEOGENESIS

JOHN E. MYLROIE
Department of Geology and Geography
Mississippi State University
Mississippi State, MS 39762

JAMES L. CAREW
Department of Geology
The College of Charleston
Charleston, SC 29424

INTRODUCTION

A critical factor in the study of speleogenesis is the amount of time required for solution conduits to develop. In most areas of the world, caves are developed in rocks many tens or hundreds of millions of years in age. In that case it is difficult to be certain that a cave system currently being studied did not have its origin far in the past under conditions vastly different from today. Even caves that are in apparent equilibrium with the present surficial environment may have begun their genesis long ago under another hydrologic setting.

Recent work by investigators such as A. N. Palmer (1984) and White (1978, 1985) has produced equations, developed mostly from laboratory experiments, that demonstrate that solution conduits of humanly passable dimensions ($r \approx 1$ m) can develop in approximately 10,000 years (depending upon conditions). This work implies that currently active cave systems may have developed in concert with the existing landscape and hydrologic regime. A key assumption in applying the theoretical work to current field observations of caves in Paleozoic or Mesozoic rocks is that all of the conduit development has occurred in the immediate geologic past, and not earlier in the history of the host rock. White (1985) has discussed the importance of the time involved in the initial enlargement of the original fracture or opening in the host rock. Caves that are in apparent equilibrium with the surficial environment may have completed their macroscopic enlargement relatively recently, as their geomorphic setting suggests, but the initiation of their development could be more proportional to the age of the enclosing rock.

To provide conclusive proof of the speleogenetic chronology proposed by A. N. Palmer (1984) and White (1978, 1985), among others, has been an interesting challenge. Cave systems, when explored, often give a subjective feeling of great antiquity. Caves most certainly can be very old, as paleontologic and radiometric data have amply shown. If it can be demonstrated that cave systems may form rapidly ($\approx$ 10,000 years), then cave scientists will be in the pleasant situation of having, in the study of solution conduits, a data base that persists through time while being sensitive to local and transient changes of environmental conditions during that time span. Complex cave systems may well represent a long-duration, high-resolution indicator of past surficial conditions.

GLACIAL FIELD DATA

To provide a field demonstration of the laboratory and theoretical work, investigators have examined cave systems where the geomorphic setting makes it likely that the cave systems developed in the recent geologic past. One of the better sets of field examples comes from glaciated areas, where landscapes emerged from ice cover in the last 10,000 to 15,000 years. Cave systems found in these localities often appear perfectly adjusted to the recently deranged surficial landscape and hydrologic regime. This strongly suggests that the caves developed in the post-glacial time frame. Examples are common from around the world, and A. N. Palmer (1972), Mylroie (1977), Lauritzen (1981), and others have provided documented case histories. Figure 1 illustrates a typical example of this evidence. Glaciation both scours and mantles the pre-existing landscape, and upon retreat a deranged drainage can occur. Drumlins break up valleys, swamps and ponds develop in depressions, and streams wander across planar till sheets. If a cave system consisting entirely of small, active passages can be found beneath such a landscape, with the cave's tributary passages arranged so as to collect water efficiently from the land-

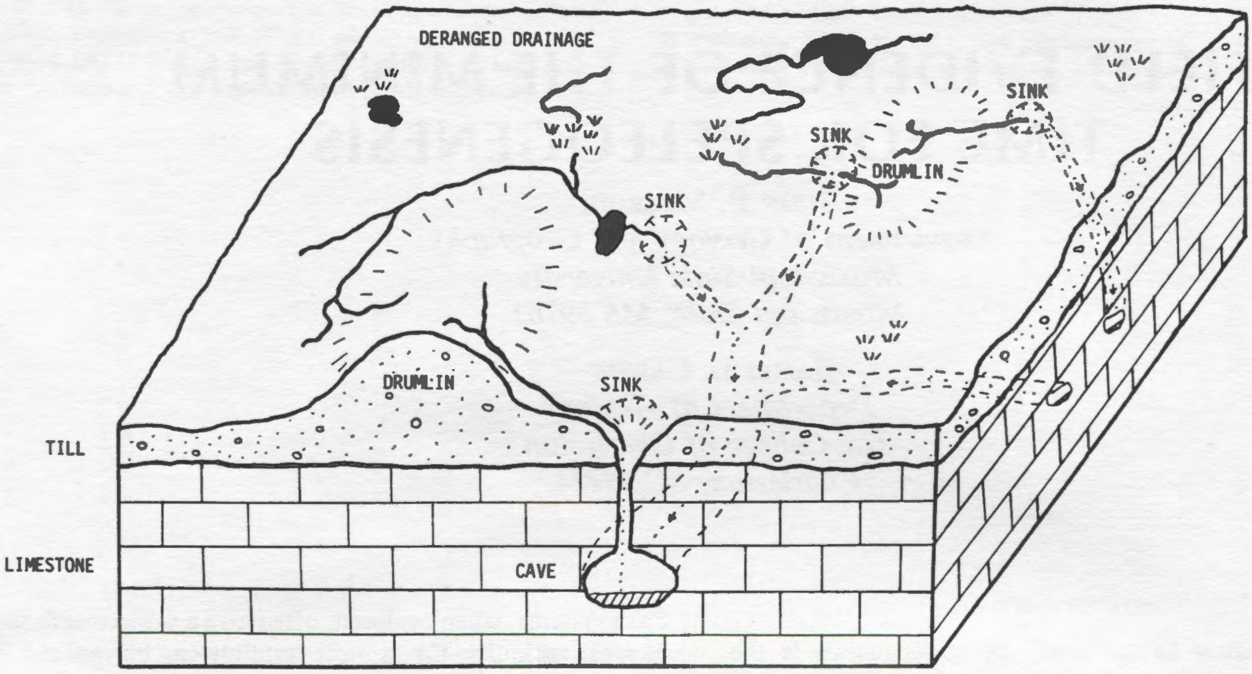

Figure 1. **The placement of small, active cave passages so that they efficiently collect surface water from a glacially deranged landscape suggests the cave passages are younger than the landscape.**

scape, then the argument that the cave development is post-glacial is compelling. Despite this evidence, it can be argued that the initial fracture or flow path enlargement took place before or during glaciation. Data from the present (Ford et al., 1983) and the Late Pleistocene (Lauritzen, 1981) show that caves can be active beneath glaciers. Active caves beneath glaciers could control aspects of the ice/ground contact and help control the final nature of the surficial derangement after ice withdrawal. Circulation of water between the sole of the glacier and the limestone bedrock beneath could influence the nature of sediment deposition. After ice withdrawal the resulting concordance of the solution conduits and the overlying deranged landscape could then be seen as indicating the prior existence of conduits.

BAHAMIAN FIELD DATA

The data available in the Bahama Islands regarding the time necessary for speleogenesis are unique. The limestone is young, providing an upper limit on the age of any enclosed solution conduit. The host rock and deposits within the solution conduits can be dated quantitatively, thus providing a time window during which the cave must have formed. The data presented here were collected from San Salvador Island, Bahamas, which lies approximately 600 km east-southeast of the Florida Peninsula (Fig. 2). The island consists almost entirely of Late Pleistocene and Holocene carbonate rocks (Carew and Mylroie, 1985), and it has a well developed karst topography that has been in part controlled by the glacially induced eustatic sea level fluctuations of the Pleistocene.

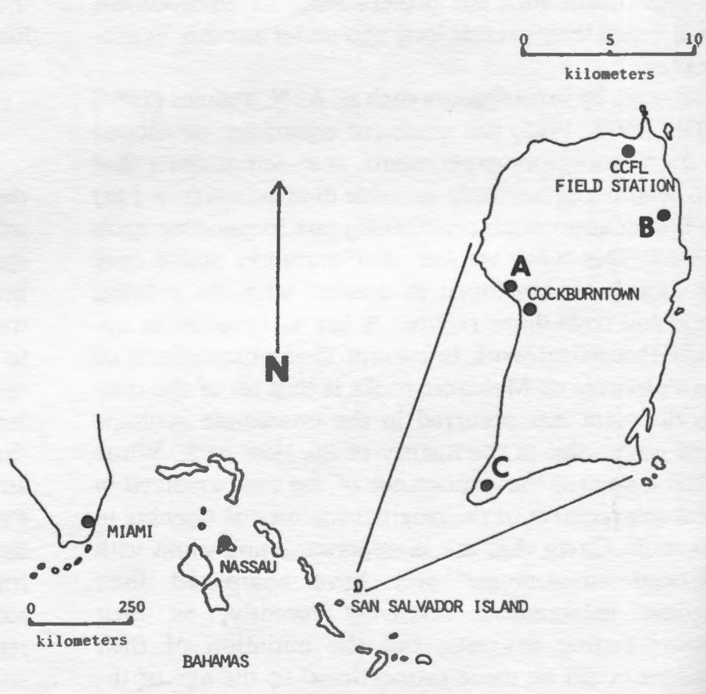

Figure 2. **Location of San Salvador Island, Bahamas; map of the island; and location of major features discussed in the text. A, Cockburn Town fossil reef; B, Lighthouse Cave; C, Sandy Point Pits.**

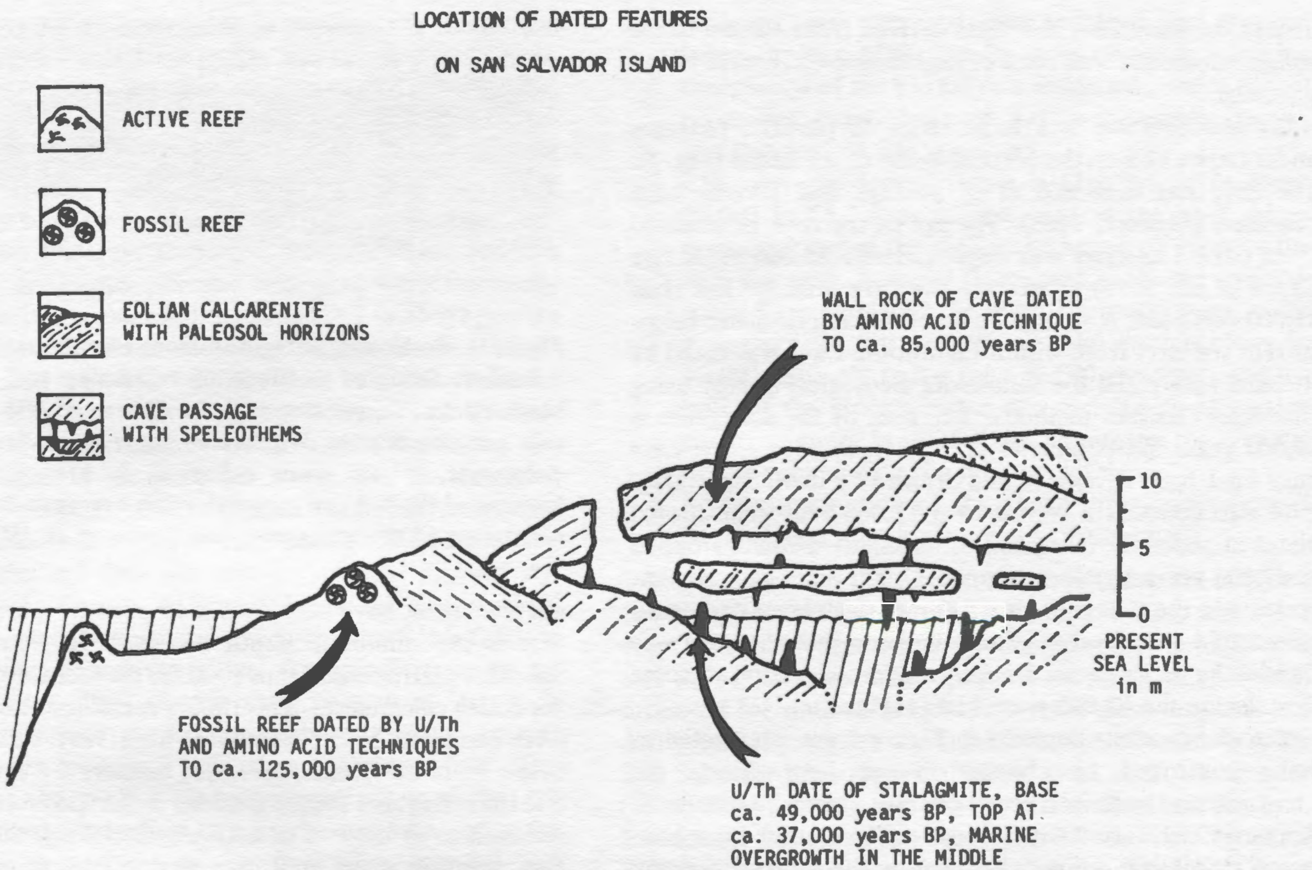

Figure 3. **Diagramatic representation of the Late Pleistocene chronology of San Salvador Island. See text for discussion.**

The data are summarized in Figure 3, a diagrammatic representation of the key features used to date the development of Lighthouse Cave, a major cave on the island. The initial data are from a fossil reef in Cockburn Town, on the west side of San Salvador. The reef contains fossil corals in growth position, and extends up to 4 m above current sea level. Because the island, like the rest of the Bahamas (Mullins and Lynts, 1977), is considered to be tectonically stable, and is undergoing only slow isostatic subsidence, the fossil reef must represent an earlier, high stand of sea level. Corals dated at Lamont-Doherty Geological Observatory by Uranium/Thorium method yield an age of approximately 125,000 years before present (Carew et al., 1984). Specimens of the bivalve *Chione cancellata* recovered from the reef matrix were dated at approximately that same age by John Wehmiller at the University of Delaware using amino acid racemization techniques. The 125,000 year age in conjunction with the reef's +4 m elevation, indicate that the reef developed during the Oxygen isotope substage 5 e high sea level (Broecker and VanDonk, 1970; Emiliani, 1972). The age determination also provided the basis for calibrating the amino acid racemization kinetics of the terrestrial gastropod *Cerion* found in interior eolian calcarenites (carbonate

Figure 4. **Speleogens produced by phreatic (water filled) conditions, Lighthouse Cave, San Salvador. The steeply dipping foreset beds of the eolian calcarenite can be seen, dipping from right to left.**

dunes). In particular, the dates derived from *Cerion* in the eolian calcarenite wall rock of Lighthouse Cave were of importance.

Lighthouse Cave is a large series of phreatic passages under Dixon Hill on the northeast side of the island (Fig. 4). The cave has over 800 m of passage and several large chambers (Mylroie, 1983). The age of the rock determined from *Cerion* analysis was approximately 85,000 years (see Carew et al., 1984). Therefore the cave must be less than 85,000 years old. A stalagmite recovered at one meter below current sea level from within Lighthouse Cave was dated by Richard Lively and the Minnesota Geological Survey using Uranium/Thorium methods. The base of the stalagmite is 49,000 years old (Carew et al., 1984), therefore, the cave must have been developed and drained by then. The stalagmite also contains a record of a 12,000 year depositional hiatus at about the mid point of its length. Growth stopped at 49,000 years ago and resumed 37,000 years ago. At that position in the stalagmite is a 2–3 mm thick layer composed of serpulid worm tubes. These indicate that the cave was flooded by a rise in sea level to modern elevation at some time during the 12,000 years hiatus (Fig. 5).

The observations depicted in Figure 3 are interpreted as being controlled by changes in sea level during the Pleistocene. Those interpretations are shown in Figure 6. Approximately 125,000 years ago sea level must have been in the vicinity of +6 m, as shown by the Cockburn Town fossil reef data. At about 85,000 years ago, sea level was at least 2 m below present elevation, as the steeply dipping foreset beds of the eolian calcarenites that enclose Lighthouse Cave can be followed to at least that depth. However, sea level must have been within 10 m of its present level as that is the minimum depth necessary to flood the San Salvador platform and thus produce the sediment source for the eolian calcarenites. This timing coincides with a high sea level proposed by Boardman et al. (1983). Sea level was below –1 m at 49,000 years ago, because the cave was dry and the stalagmite started growing at that position. Sea level returned to at least –1 m between 49,000 and 37,000 years ago, then again fell until its return to present levels about 5,000 years ago.

The above interpretation of the data leaves a time window of not more than 36,000 years for the cave to form (between 85,000 and 49,000 years ago). This time window is already

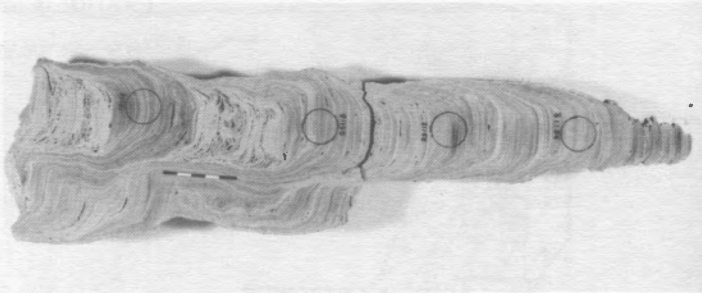

Figure 5. **Sectioned stalagmite from Lighthouse Cave, San Salvador. Sampled portions of remaining half shown by black circles. Lower two samples date to 49,000 BP; upper two samples date to 37,000 BP. Scale in centimeters. The stalagmite, whole when collected, is broken along the horizon of the 2–3 mm serpulid worm overgrowth. For a full discussion of the stalagmite, see Carew et al. (1984).**

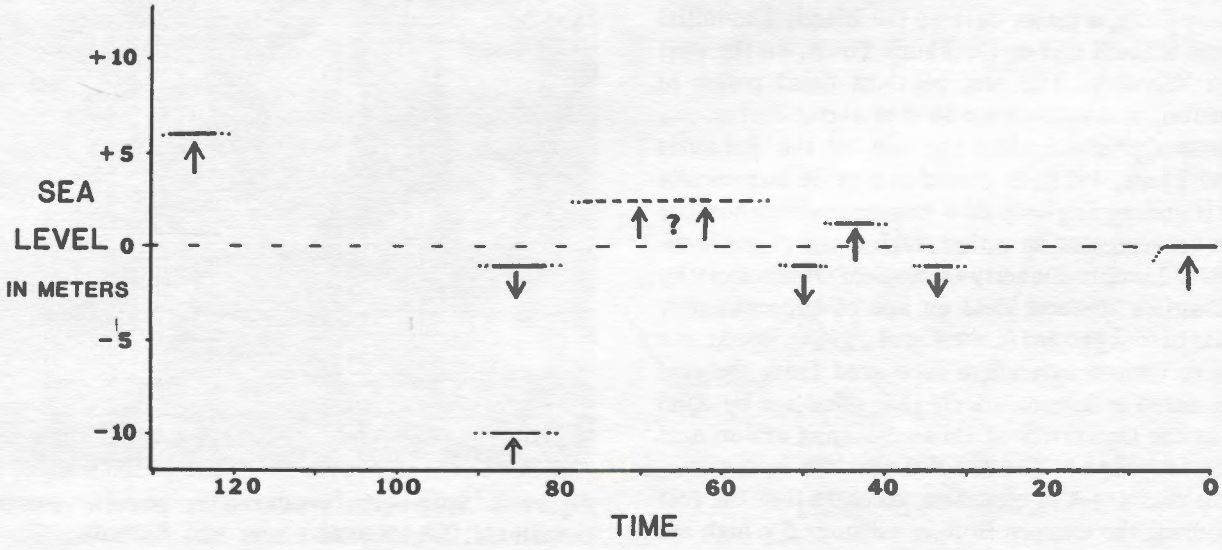

Figure 6. **High sea level positions for the Late Pleistocene, based on the data of Figure 3. Horizontal lines show position of sea level at various times: arrows pointing up indicate sea level at least that high, arrows pointing down indicate sea level somewhere below the elevation shown. Late Pleistocene low sea level elevations omitted.**

the proper order of magnitude to support the theoretical equations of A. N. Palmer (1984) and White (1985); however, the time window can be further narrowed significantly. The cave extends, as currently explored, from -2 m to +7 m with respect to present sea level. The cave has limited breakdown development, and all surfaces within the -2 m to +7 m range have well developed phreatic (water filled conduit) solution features. Therefore, the cave developed in a brackish or freshwater phreatic zone that was solutionally aggressive and that extended to at least +7 m above present sea level. Work by Back and others (1984), A. N. Palmer and others (1977) and R. Palmer (1985) have demonstrated that solution in coastal limestone environments such as San Salvador may preferentially occur at the halocline, the boundary between intruding sea water and the overlying non-marine water. Even if both the sea water and the overlying non-marine waters are saturated with respect to calcite, mixing at the halocline will provide renewed aggressivity. While the halocline can be near or below sea level, formed by a fresh or brackish water Ghyben-Herzberg lens floating on underlying, denser sea water, the halocline cannot be above sea level. The solution surfaces seen at +7 m in numerous locations throughout Lighthouse Cave suggest that either sea level was high enough at some time after 85,000 years ago to place the halocline at +7 m, or that the cave developed somewhere in a freshwater lens above the halocline. The position of the freshwater lens on San Salvador is a function of rain fall, infiltration rate, permeability of the limestone, and the position of sea level. The data indicate that the island currently supports a Ghyben-Herzberg lens under portions of the island. The position of Lighthouse Cave in eolianites within a kilometer of the platform margin of San Salvador would support the argument that the elevation of the conduit is an approximate measure of sea level at the time of conduit formation (within 5 m or so), as a Ghyben-Herzberg lens would thin and pinch-out at sea level at the platform margin. Lighthouse Cave could not develop with phreatic solution features at +7 m unless sea level were at least at or near its present elevation during development. The time window for the development of Lighthouse Cave is therefore limited to the duration of a high sea level at or near its present elevation between 85,000 and 49,000 years ago.

There are four options that can be considered:

1. The sea level rise of 85,000 years ago, that flooded the San Salvador platform and so produced the eolian calcarenite that contains Lighthouse Cave, could have continued to rise, allowing a freshwater lens to form in the newly developed eolian calcarenite and syngenetically produce the cave.
2. Sea level rose to the necessary elevation near present sea level, then dropped, as a separate event. This separate event occurred after sea level had dropped below the level of the San Salvador platform following completion of the 85,000 year eolian calcarenite (dune) producing event, but well before stalagmite growth was initiated 49,000 years ago.
3. The cave developed during a high sea level about 50,000 to 55,000 years ago, and as sea level subsequently dropped the stalagmite began to grow in the then dry cave. A minor fluctuation in the sea level fall could have emplaced the marine serpulid layer in the stalagmite. In this case the serpulid layer is closer to 49,000 years old rather than 37,000 years old, and the bulk of the growth hiatus can perhaps be accounted for by changes in rainfall accompanying the climatic events surrounding the high sea level.
4. Some combination of the above three options could have yielded a multiple genesis of the cave.

Examination of the known sea level data (Boardman, 1984) implies that option one, involving the dune producing event at 85,000 years ago, is the most likely scenario. In that case the cave was produced syngenetically as Jennings (1968) proposed for similar rocks in Australia. Assuming that the dating techniques used are at least moderately accurate, the San Salvador data suggest that the work of A. N. Palmer (1984), White (1985), and others, is essentially correct. Late Pleistocene eolian calcarenites are not exact analogues of Paleozoic or Mesozoic carbonates, but the data from the sea level curves would indicate that Lighthouse Cave, with its tubes, chambers, absence of breakdown, and sculptured walls, formed in only a few thousand years.

Further evidence of the speed with which karst processes can work is provided by the current relationship between Lighthouse Cave and the surficial environment. The cave has no apparent relationship with current topography, as it is located in a lobe of Dixon Hill, with entry gained by more recent vadose shafts. There is no apparent significant catchment for the cave, either laterally or vertically. Similar phenomena can be seen elsewhere on the island (e.g., Sandy Point Pits described in Mylroie, 1983), where surficial denudation has breached phreatic tubes and left large vadose shafts with no source of recharge at the crest of hills. This evidence argues for a rapid denudation, and therefore evolution, of the surficial landscape as well.

Cave development on San Salvador provides another useful piece of information bearing on the relationship of the "water table" to developing conduits. Because of the relationship of the water table or Ghyben-Herzberg lens, to sea level, caves such as Lighthouse Cave developed in the vicinity of sea level. As sea level is not known to have been more than a few meters above its present elevation during the last 85,000 years, the water table also must have been reasonably close to present ocean elevation (within +7 m) as the cave formed. Therefore, features seen in Lighthouse Cave such as sponge work, solution pillars, spans, pendants, and undulating tubes can develop under what are clearly shallow fresh or brackish water conditions, and a deep phreatic environment is not a prerequisite.

CONCLUSIONS

The data available strongly suggest that macroscopic solution conduits ($r \approx 1$ m) can develop in limestones in the time span of about 10,000 years. The theoretical equations, the laboratory experiments, and the field evidence are consistent. The field evidence is particularly critical, as it is the real-world representation rather than a theoretical model. The data from glaciated areas although compelling, was not conclusive. The Bahamian data is conclusive with regard to the time needed for conduit development and has implications about conduit relationship to the water table and overall karst denudation rates.

ACKNOWLEDGEMENTS

The authors wish to thank the College Center of the Finger Lakes Bahamian Field Station, Dr. Donald T. Gerace, Director, for logistical and financial support. Richard Lively, Minnesota Geological Survey did the stalagmite Uranium/Thorium analyses; John Wehmiller, University of Delaware, did the amino acid racemization analyses; and Lamont-Doherty Geological Observatory did the coral Uranium/Thorium analyses. The College of Charleston and Murray State University provided additional support. Bill Back reviewed the manuscript and supplied helpful suggestions. Nancie Upchurch and the Department of Geology and Geography, Mississippi State University, processed the manuscript. Finally, the hospitality of the Bahamian landowners, and the work of our numerous student field assistants, is greatly appreciated.

REFERENCES

Back, W., Hanshaw, B. B., and Van Driel, J. N., 1984, Role of Groundwater in Shaping the Eastern Coastline of the Yucatan Peninsula, Mexico, *in* LaFleur, R. G., ed., Groundwater as a Geomorphic Agent, The Binghampton Symposia in Geomorphology, No. 13, Boston: Allan and Unwin, p. 281-293.

Boardman, M. R., Dulin, L. A., and Kenter, R. J., 1983. High Stands of Sea Level: Rhythmic Deposition of Bank Derived Carbonate Sediment in the Deep Periplatform Environment: Geol. Soc. America, Abstr. Prog. 15 (6): 528.

Boardman, M. R., Dulin, L. A., Kenter, R. I., and Neumann, A. C., 1984. Episodes of Banktop Growth Recorded in Periplatform Sediments and the Chronology of Late Quaternary Fluctuations in Sea Level, in J. Teeter (ed.), Proceedings of the 2nd Symposium on the Geology of the Bahamas. C. C. F. L. Bahamian Field Station, San Salvador, Bahamas, p. 129-152.

Broecker, W. S. and VanDonk, J., 1970. Insolation Changes, Ice Volumes, and the ^{18}O Record in Deep Sea Cores: Reviews of Geophysics and Space Physics, v. 18, p. 169-198.

Carew, J. L., Mylroie, J. E. Wehmiller, J. F., and Lively, R. S. 1984. Estimates of Late Pleistocene Sea Level Stands from San Salvador, Bahamas, *in* J. Teeter (ed.), Proceedings of the 2nd Symposium on the Geology of the Bahamas. C. C. F. L. Bahamian Field Station, San Salvador, Bahamas, p. 153-175.

Carew, J. L. and Mylroie, J. E., 1985. Pleistocene and Holocene Stratigraphy of San Salvador Island, Bahamas, with Reference to Marine and Terrestrial Lithofacies at French Bay, *in* Curran, H. A., ed., Pleistocene and Holocene Carbonate Environments on San Salvador Island, Bahamas—Guidebook for Geological Society of America, Orlando annual meeting field trip: Ft. Lauderdale, Florida, CCFL Bahamian Field Station, p. 11-62.

Emiliani, C. E., 1972. Quaternary paleotemperatures and the duration of the high-temperature intervals: Science, v. 178, p. 398-401.

Ford, D. C., Smart, P. L., and Ewers, R. O., 1983. The physiography and speleogenesis of Castleguard Cave, Columbia Icefields, Alberta, Canada. Arctic and Alpine Research, 15: 437-450.

Jennings, J. N., 1968. Syngenetic Karst in Australia: Dept. of Geography Publication G/5, National University, Canberra, p. 41-110.

Lauritzen, S. E., 1981. Glaciated Karst in Norway: Proc. 8th Intl. Cong. Speleol., p. 410-411.

Mullins, H. T. and Lynts, G. W., 1977. Origin of the Northwestern Bahama Platform: Review and Reinterpretation: Geol. Soc. Amer. Bull., v. 88, p. 1447-1461.

Mylroie, J. E., 1977. Speologenesis and Karst Geomorphology of the Helderberg Plateau, Schoharie County, NY: Bulletin II of the NY Cave Survey, 336 p.

Mylroie, J. E., 1983. Caves and Karst of San Salvador, *in* Gerace, D. T. (ed.), Field Guide to the Geology of San Salvador Island, C. C. F. L. Bahamian Field Station, San Salvador, Bahamas, p. 67-96.

Palmer, A. N., 1972. Dynamics of a Sinking Stream System, Onesquethaw Cave, NY: Nat. Speleol. Soc. Bull., 34, 89-110.

Palmer, A. N., Palmer, M. V., and Queen, J. M., 1977. Geology and the Origin of the Caves of Bermuda, Proc. of the 7th Int'l Speleological Congress, Sheffield, England, p. 336-341.

Palmer, A. N., 1984. Geomorphic Interpretation of Karst Features. *In* R. A. LaFleur (ed.), Groundwater as a Geomorphic Agent, Boston: Allen and Unwin, p. 173-209.

Palmer, R., 1985. The Blue Holes of the Bahamas, Jonathan Cape Ltd., London, 184 pages.

White, W. B., 1978. Water Balance, Mass Balance, and Time Scales for Cave System Development: Nat. Speleol. Soc. Am. Abstr. Prog., p. 36.

White, W. B., 1985. Speleogenesis: A Geochemical-Mass Transport Model: Program of the 1985 National Speleological Society Annual Convention, Frankfort, KY, p. 45.

Egemeier, Stephen J.—A Theory for the Origin of Carlsbad Caverns: *NSS Bulletin* **49**: 73-76.

A THEORY FOR THE ORIGIN OF CARLSBAD CAVERNS

STEPHEN J. EGEMEIER*
(Deceased)
34 Pine St., Tillson, NY 12486

INTRODUCTION

The origin of Carlsbad Caverns has long been an enigma. The caverns do not easily fit the general model for cavern development in humid karst areas. The 1973 National Park Service flyer for Carlsbad Caverns' visitors states this model quite succinctly. "Rainwater, converted to a weak carbonic acid by adsorption of carbon dioxide in the soil and decaying matter above, seeped into the cracks and worked its way down to the permanently saturated zone—water table. It then slowly dissolved the rock to create the immense galleries."

Caves formed by carbonic acid are underground river systems in karst areas. Carlsbad does not resemble a river system, nor is the region karst. Also, the cave has substantial gypsum beds that are difficult to fit into a carbonate solution model.

A different model is required. As the processes that formed Carlsbad are no longer operating, that model cannot be developed readily without looking at similar caves in another area that are still actively growing. Thus, it is necessary to discuss the development of some caves in the Big Horn Basin in Wyoming, as it appears these caves are a key to understanding Carlsbad. Only then can a general model for the origin of Carlsbad Caverns be developed that explains the origins and major features of the caverns.

THE MODEL

Figure 1 is a diagrammatic cross section of an actively growing Wyoming cave. The cave is Lower Kane Cave in Little Sheep Mountain in the Big Horn Basin. The diagram is explained by number below:

1. Water enters the cave from below through a narrow slot (under a meter wide) dissolved in the cave floor. Because the water is rising from considerable depths, in the Wyoming case the water is slightly thermal.

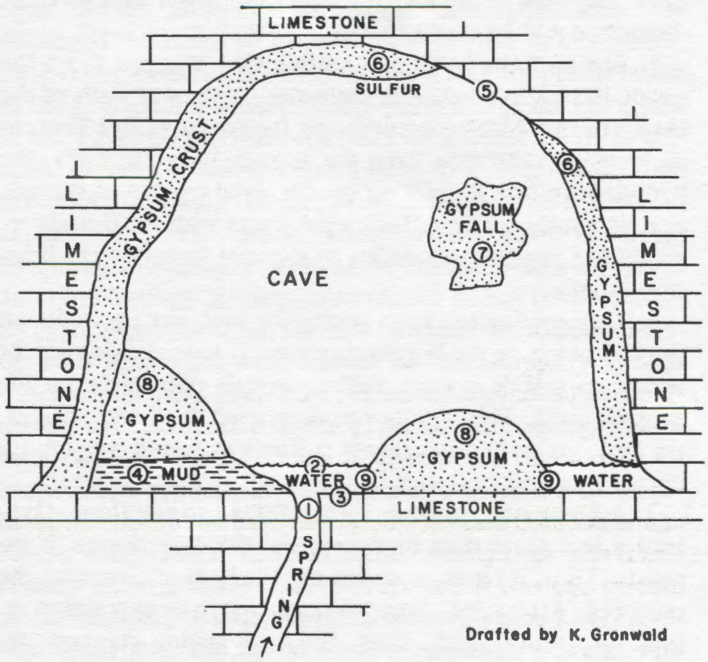

The entering spring water contains hydrogen sulfide. The hydrogen sulfide is formed apparently by bacteria using petroleum to reduce sulfate. The spring is found at the upstream termination of the cave, or at a considerable enlargement in the passage. Obviously, the spring is important in the cave-forming process.

2. Most of the hydrogen sulfide quickly escapes into the cave air (over 90 percent escapes after stream flow distances of less than 70 m). At the same time, oxygen enters the water.

3. Dissolved oxygen in the water oxidizes some hydrogen sulfide to sulfuric acid causing the stream to dissolve its bed. The amount of acid produced is small (stream pHs are nearly neutral [6.8 - 7.25]).

As the rate of reaeration or oxygen absorption by a stream depends on turbulence (and hence slope), more hydrogen sulfide will be oxidized in steeper stream reaches, causing these reaches to flatten, reducing reaeration. As a result, the cave streams can develop fairly low equillibrium gradients (a percent or so being typical). Also as a result, the

*Stephen J. Egemeier wrote the following paper shortly before his death in 1985 after a long illness. He submitted it for use in a proposed geologic guidebook on the Guadalupe Mountains, but its subject is appropriate for inclusion in this speleogenesis issue of the *Bulletin*. Dr. Egemeier was a pioneer in the subject of hydrogen sulfide speleogenesis, and despite the fact that his paper is somewhat dated, covering topics that have been carried further by other researchers, it is presented here virtually unchanged in view of its historical value.

Arthur N. Palmer

caves end up developed in levels that correspond to river terraces.

4. Small amounts of precipitate and fine muds can be deposited in and around the springs. The muds may contain heavy metals in minute amounts, apparently carried into the cave dissolved in petroleum (metals detected include: Ag, Co, Cr, Ar, Mn, Mo, Ni, Pb, Ti, Va, Zn, Zr). In the caves studied, the major metal deposited was iron sulfide. There are, however, many caves with economic mineral deposits that may have formed in a similar manner. The iron-rich clays in these caves oxidize red to hematite if exposed to air. Most clays are about a meter thick, but given enough time, deposits could be much thicker.

5. Some of the hydrogen sulfide that escaped from the spring in step 2 dissolves in the water on the wet walls of the cave. (In the Wyoming caves, air hydrogen sulfide content declines with distance from the springs.) On the walls, the hydrogen sulfide is oxidized by dissolved oxygen to sulfuric acid and sulfur. The sulfuric acid reacts with the limestone, producing gypsum. A coating of gypsum forms on the limestone, replacing it.

6. This coating thickens gradually, and was up to 50 cm thick in places in the Wyoming caves. If partial oxidation of hydrogen sulfide occurs, sulfur crystals may grow on the gypsum crust. This is only common near the active springs. (In fact, the only other places sulfur was found was on dry limestone at the entrance to one small cave.)

7. A block of gypsum is shown falling to the floor. Gypsum is less dense than limestone. As the crust forms, it expands. Thus, it tends to wedge off the bedrock, making the crust fall. After a fall, limestone may again be exposed to attack by sulfuric acid. Thus, the cave ceiling enlarges upward.

8. The fallen gypsum forms mounds on the cave floor, or piles up on the clays formed by the springs. Near the entrance, the gypsum may fall on alluvium deposited in the cave by backflooding of the outside river. The mounds may be from a meter to many meters thick. Some sulfur could be buried in a mound, but generally is not. Limestone usually is fully replaced and not found in the mounds.

9. The stream from the spring dissolves the gypsum and removes it from the cave. The process is quite rapid; blocks of gypsum placed in a stream dissolved in a week. Blocks of gypsum out of reach of the stream for one reason or another may be preserved. Those on silt or clay deposits would be most likely to be out of reach of the stream.

In short, the cave-forming process operates as follows: hydrogen sulfide entering a cave at springs is oxidized on the walls of the cave, where the limestone is replaced by gypsum. The gypsum forms a crust that thickens as more limestone is replaced, until it is so thick that it falls onto the cave floor due to its weight. There it is dissolved and removed by the cave stream. Thus, the process is called replacement-solution.

The basic chemical reactions are as follows:

1. $2H_2S + O_2 \rightleftharpoons 2S + 2H_2O$
(Oxidation of hydrogen sulfide to sulfur.)

2. $2H_2O + 2S + 3O_2 \rightleftharpoons 2HSO_4^- + 2H^+$
(Oxidation of sulfur to ionized sulfuric acid.)

3. $H^+ + HSO_4^- + CaCO_3 + H_2S \rightleftharpoons CaSO_4 \bullet 2H_2O$
(Replacement of limestone by gypsum.)

All reactions have negative free energy change as written, indicating they should proceed given enough time. Also, the reactions are known to proceed in laboratory experiments to the right in aqueous solution at conditions similar to those in caves. Detailed chemical studies verifying these processes are in Egemeier (1981) and not repeated here.

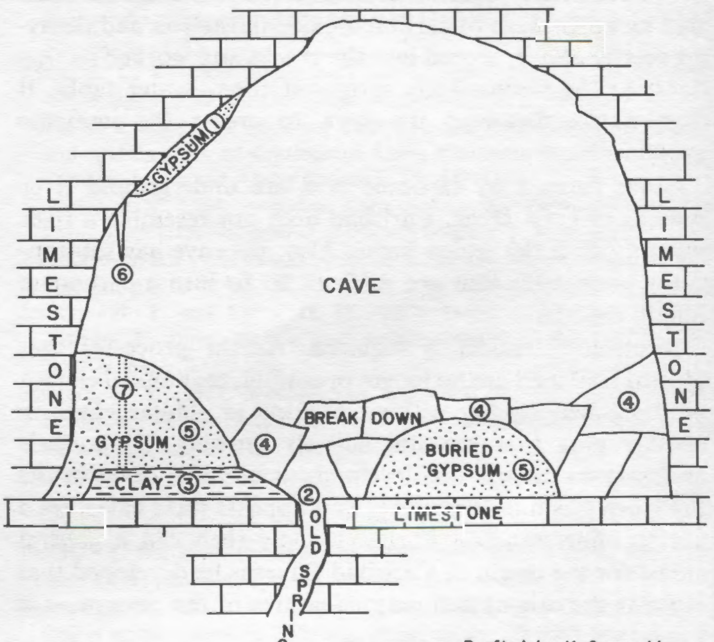

Drafted by K. Gronwald

After the springs dry up, much of what is seen in Figure 1 is lost. Figure 2 shows a typical dead cave. The diagram is explained by number below.

1. Some remnant gypsum crust remains where not removed by ceiling collapses or dissolved by seeping water. This crust is generally only a few millimeters thick. Because gypsum has a lower density than calcite (limestone), the crust expands when formed and is barely attached to the cave wall and it falls off easily. Remnants of the crust are often best preserved in breakdown at the edges of the main passage.

2. The spring slot is less than a meter wide and a few meters long, and is buried and hidden. A spring slot has yet to be found by this author in a dead cave.

3. The spring precipitates also cover a small area, but may be exposed as red clay beds in some cases. They also may be buried by gypsum or breakdown. Precipitates may be a meter or more in thickness.

4. Breakdown (fallen ceiling bedrock) covers the floor and may cover gypsum mounds, the spring, and the precipitate. Careful searching may be required to find evidence of a cave's origin, especially if collapse has been extensive.

5. Gypsum mounds, some buried and some exposed, may recrystallize depending on the moisture conditions in the cave. They may be like powder in dry caves, or solid blocks in caves with some moisture. In rare cases, sulfur may be preserved in the gypsum. The gypsum may be on the cave alluvium formed by backflooding near the cave mouth. The mounds can be quite large, covering extensive areas with gypsum several meters thick.

6. A calcite stalactite has formed and is dripping on a gypsum mound. The dripping water has drilled a hole in the mound known as a drip tube. (Other calcite speleothems could also form but are not shown, as they are not significant to this discussion.)

7. A drip tube dissolved in the gypsum block is shown, formed by dripping water from above. The presence of a drip tube shows that the ground water is undersaturated with respect to gypsum.

The passage is shown as a dome with a flat floor perhaps 10 to 30 m wide. This would be typical in flat-lying bedded limestone. If extensive, ceiling collapse could radically modify the appearance of the cave. (In dipping limestone, the original passages are enlarged down dip so the initial and final shapes would differ.)

The active caves discharge into rivers at river level, hence backflooding can occur in the lower ends of the caves, leaving an alluvial flood plain silt deposit in the cave. In these areas, gypsum generally would be washed away by the flood waters.

Evidence of Replacement-Solution in Carlsbad Caverns

The Big Room in Carlsbad Caverns has essentially all the features of a dead cave as shown in Figure 2. The room is fairly flat-floored, with an arched ceiling. On that flat floor red clays and gypsum are found.

The so-called "gypsum beds" are an impressive feature of the Big Room (in fact, they are not bedded). Over 7 m thick in places, they cover sizable areas of the floor. The "beds" often overlie red silts and clay beds that may be spring deposits. Hill (1981) reports sulfur admixed in gypsum at the Jumping Off Place in the Big Room. Here the cave ceiling is extraordinarily high and the upper and lower caves connect, a very likely place for a spring, as the caves are usually largest near the springs. Also, sulfur is usually only deposited near the springs. Gypsum wall crusts are rare, but some are preserved near the Pump Room and the Men's and Ladies' lavatories.

The main alternative explanation for the gypsum is that it is a precipitate. There are a number of problems with this idea. First, calcite would precipitate from a cave water. However, calcite layers are not present in the gypsum. The gypsum should be bedded; it is not. What rare layering there is at all dips and is not horizontal, which would be expected. One would expect rockfalls into the water and hence limestone blocks in the gypsum. In fact, limestone blocks are extremely rare in the gypsum. Sulfur in the gypsum is very difficult to explain. The gypsum may contain fossils, which are evidence of their replacement origin. There are possible relict ooliths and algal structures. Recrystallization has destroyed the detail so positive identification is impossible. Such relics would indicate replacement and not precipitation of the gypsum in the cave. The gypsum is at many elevations in the cave, rather than confined to a water level, as one might expect. All this evidence points to an origin other than precipitation. Using the precipitation theory, it is difficult to explain why the precipitation would have occurred. Evaporation is usually given as the reason. Hem (1970) says Jumping Springs (a gypsum-saturated spring in the Castile Gypsum near Carlsbad) has a total dissolved solids content of 2410 ppm. The evaporation of this Jumping Springs water would yield only 0.24 percent precipitate. After correcting for the density of the gypsum, evaporating 1 m of water will yield only 1 mm of precipitate. One meter of evaporation annually is reasonable in the desert outside the cave, but inside the cave that much evaporation could take many, many years, there being no sunlight to power the process underground. If cave evaporation was one percent of that outside, that would be optimistic. Thus, 1 m of gypsum could take 100,000 years to precipitate. It seems very unlikely the cave water levels would stay stable that long. One might also wonder why the gypsum crystals are sand size if they had so much time to grow larger. Evaporation does not seem to be a likely source for the gypsum found in Carlsbad.

Carlsbad Caverns is developed on several levels. The main ones are: the Bat Cave at 80 m, the Big Room at 230 m, and the Lower Cave at 260 m (m = meters below entrance). Interestingly, speleologists often state that levels are caused by water tables that control streams. The geomorphology literature states the reverse: that streams develop profiles of equillibrium and they control the water table. Because of the slope-sensitive nature of the reaeration, streams in replacement-solution caves form very gentle profiles, as are seen in Carlsbad. One lower level is reported to have silt banks along its sides which could be backflooded river silt from outside the cave. The cave, it seems, was graded to its various outlets, and therefore the passages are in levels.

The general pattern of passages in Carlsbad suggests it is not a usual carbonate solution cave. The passages do not look like a river system. They interconnect in mazes and have blind terminations. They have no stream flow features (vadose features) such as scallops or potholes. This is also true of replacement-solution caves.

In fact, there are other caves similar to Carlsbad in the region. Among them, Cottonwood Cave is reported to have sulfur (Davis, 1973). In addition, this cave has many other features including gypsum deposits that suggest it too is replacement-solution in origin. (As this author has visited Cottonwood, but not the other caves in the area, I am unable to comment on the origin of the other caves.)

CONCLUSIONS

It is proposed that Carlsbad Caverns was formed by ascending hydrogen sulfide waters that outgassed hydrogen sulfide into the cave air. The hydrogen sulfide redissolved on the cave walls and ceiling and was oxidized. The limestone was replaced as gypsum. When the gypsum crust formed, it became heavy and fell to the floor, where most was dissolved and removed by the same waters that brought in the hydrogen sulfide. Some sulfur formed by partial oxidation of hydrogen sulfide was trapped in the gypsum. The springs also deposited silts which lie on the cave floor. The valley outside the cave was cut lower and the process repeated at a new, lower elevation in the limestone, thus forming levels in the cave.

ACKNOWLEDGEMENTS

I would like to thank the Cave Research Foundation for use of the overnight facilities, the National Park Service for access to the cave, and my wife, Linda, for support and typing of the manuscript.

REFERENCES

Davis, D. G., 1973. Sulfur in Cottonwood Cave, Eddy Co., N.M.: Natl. Speleol. Soc. Bull., V. 35, No. 3, p. 22-23.

Egemeier, S. J., 1981. Cavern Development by Thermal Waters: Natl. Speleol. Soc. Bull., V. 43, No. 2, p. 31-51.

Hem, J. D., 1970. Study and Interpretation of the Chemical Characteristics of Natural Water, 2nd ed.: U.S. Geol. Surv. Water Supply Paper 1473, 363 pp.

Hill, C., 1981. Speleogenesis of Carlsbad Caverns and Other Caves of the Guadalupe Mountains: 8th Int. Cong. of Speleol., p. 143-144.

National Park Service, 1973. Carlsbad Caverns National Park, New Mexico, U.S. Dept. of Interior, (brochure).

Index to Volume 49 of the National Speleological Society Bulletin

Ira D. Sasowsky
Department of Geosciences
The Pennsylvania State University
University Park, PA 16802

This index contains references to all articles and other items of importance published in volume 49 parts 1 and 2.

The index consists of two parts. The first of these is a keyword index. Keywords include: unique words from the article title, cave names, geographic names, descriptive terms, and biologic names. The second part is an alphabetical author index. Articles with multiple authors are indexed under each author.

Citations are of the following form: names of all authors in the order which they appear in the journal; title of the article ; volume number and part number (separated by a colon); beginning and ending page (separated by a dash); and year of publication from the cover of the issue. Volume number and year are included in the citation so that their format will match that of the cumulative index of volumes 1 through 45. Within an index group, such as "Archaeology", the earliest article is cited first, followed by consecutive articles.

This index was prepared on an IBM 4341 computer running a VM/CMS operating system. Indexing was performed by the IBM KWIC/KWOC program. Formatting was accomplished using the SCRIPT text formatter, with camera-ready copy produced on a Xerox 2700 laser printer. Computer funds were provided by the College of Earth and Mineral Sciences, The Pennsylvania State University.

Keyword Index

Author Index

THE NSS BULLETIN

Volume 49 December, 1987 Number 2

CONTENTS

National Speleological Society
Cave Avenue
Huntsville, Alabama 35810